



UNIVERSITÀ  
DEGLI STUDI  
DI PADOVA

University of Padua  
Department of Surgery, Oncology and Gastroenterology

---

Ph.D. Course in Clinical and Experimental Oncology and Immunology  
XXX cycle

# **Genomic Analysis in Cutaneous Melanoma: a Tool for Predictive Biomarker Identification and Molecular Classification**

**Coordinator:** Prof. Paola Zanovello

**Supervisors:** Dr. Chiara Menin

Dr. Arcangela De Nicolo

**Ph.D. Student:** Camilla Stagni

*A Enrico, mamma e papà*

## INDEX

INDEX.....	3
ABSTRACT .....	5
Project 1. Identification of molecular signatures associated with response to MAPK inhibitors. ....	5
Project 2. Research of molecular biomarkers to classify acral melanoma. ....	6
INTRODUCTION .....	7
2.1 Clinical classification.....	7
2.2 Principals of staging: TNM classification.....	8
2.3 Epidemiology and risk factors in cutaneous melanoma .....	11
2.4 Key molecular pathways in melanoma .....	12
2.5 Progression from melanocyte to metastatic melanoma .....	17
2.6 Treatment options for melanoma .....	19
2.7 Resistance to MAPK inhibitors .....	21
2.8 TERT promoter gene mutations in melanoma.....	23
AIMS OF THE STUDY .....	25
AIM 1: Identification of molecular signatures associated with response to MAPK inhibitors. ....	26
AIM 2: Research of molecular biomarkers to classify acral melanoma.....	26
MATERIALS AND METHODS .....	27
4.1 Patient cohort .....	27
4.2 Tumor samples and DNA extraction and quantification .....	29
4.3 Real-time PCR .....	29
4.4 End-point PCR and Sanger sequencing .....	32
4.5 Copy Number Variation (CNV) analysis.....	33
4.6 Fluorescence <i>in situ</i> hybridization (FISH) analysis .....	34
4.7 Statistical analysis.....	35
RESULTS - PROJECT 1.....	36
5.1 Summary of the work reported in the submitted manuscript <i>BRAF gene copy number and mutant allele frequency correlate with melanoma patients' response to MAPK inhibitors</i> by Stagni C. et al. ....	36
5.2 Analysis of the PTEN gene.....	37
5.3 Analysis of TERT promoter status .....	39
5.4 Genome-wide CNV analysis.....	42

RESULTS - PROJECT 2.....	47
6.1 Genome-wide CNV analysis of acral lentiginous melanoma.....	47
DISCUSSION.....	51
REFERENCES .....	54
APPENDIX 1 .....	62

## ABSTRACT

### **Project 1. Identification of molecular signatures associated with response to MAPK inhibitors.**

BRAF V600-mutated melanoma benefits from MAPK inhibitors (MAPKi)-based therapy. Yet, the onset of resistance impacts long-term efficacy and can even be immediate. In this study, we examined the genetic alterations characterizing melanoma progression to identify predictive factors of response to MAPKi. Specifically, we evaluated BRAF copy number variation (CNV), BRAF mutant (BRAFMut) allele frequency, PTEN loss or mutations and TERT promoter mutations in pre-treatment melanoma specimens from MAPKi-treated patients (pts) and we analyzed their association with progression free survival (PFS). We also applied a comprehensive unbiased approach, using genome-wide CNV analysis, to identify additional genomic aberrations potentially associated with response to therapy.

We found that 65% pts displayed BRAF gains, often supported by chromosome 7 polysomy. In addition, we observed that 64% pts had a balanced BRAF mutant/wild-type allele ratio, while 14% and 23% pts had low and high BRAFMut allele frequency, respectively. Notably, a significantly higher risk of progression was observed in pts with a diploid BRAF status vs. those with BRAF gains (HR = 2.86; 95% CI 1.29–6.35;  $p = 0.01$ ) and in pts with low vs. those with a balanced BRAFMut allele percentage (HR = 4.54, 95% CI 1.33–15.53;  $p = 0.016$ ).

We identified PTEN gene mutations affecting the catalytic and C2 domains in 27% pts. Moreover, we observed a complete PTEN loss in 42% pts, partial loss in 35% pts and no loss in 23% pts. Of note, we found PTEN loss also in pre-treatment samples from pts with long PFS.

Sequencing of TERT promoter gene disclosed mutations in 78% pts. The -124C>T and the -146C>T mutations were equally frequent (36%) while the -138-139CC>TT was present only in 5% pts. Fifty-one % pts carried also the neighboring polymorphism rs2853669, which reportedly counteracts the activating effect of the above-mentioned mutations on TERT expression. Upon stratification of the TERT promoter mutant cohort based on presence/absence of the polymorphism, TERTmutant/SNPcarrier pts showed a trend toward better PFS (median PFS 11.5 mo., 95% CI 3.12–19.88) compared to TERTmutant/SNPnon-carrier pts (median PFS 7 mo., 95% CI 4.27–9.72). When stratifying based on mutation type, the -146C>T mutation correlated with shorter PFS (median PFS 5.45

mo., 95% CI 2.80–9.20) compared to the -124C>T one (median PFS 15.2 mo., 95% CI 5.57–).

Genome-wide CNV analysis pointed at chr3p24, chr3p21.2 and chr17p13.1, which are differently altered between pts with long and short time to disease progression, as regions of potential interest to identify new genes involved in therapeutic resistance.

Our data suggest that quantitative analysis of the BRAF gene and sequencing of the TERT promoter gene could be useful to select the melanoma pts who are most likely to benefit from MAPKi therapy. In addition, chromosome 3 and 17 could be regions that warrant further investigation. Conversely, because PTEN loss was present in pre-treatment samples from pts with both short and long PFS, the assessment of PTEN gene status does not seem to provide information about patient responsiveness to treatment.

## **Project 2. Research of molecular biomarkers to classify acral melanoma.**

Acral lentiginous melanoma (ALM) is a rare subtype of cutaneous melanoma with specific morphological, epidemiological, and genetic features. Since the genomic landscape of ALM is still incompletely described, we used whole genome CNV analysis to characterize ALM and detail the genomic signatures that differentiate ALM from non-acral melanoma (NAM).

We observed that the most strikingly different copy number aberrations were a higher frequency of losses of chromosome 16q24.2-16q24.3 in ALM than in NAM (64.7% vs. 10%) and a lower frequency of gains of chromosome 7q21.2-7q33 in ALM than in NAM (26.5% vs. 79.5%). We observed also that ALM more often (than NAM) harbored clusters of breakpoints and isochromosomes. Moreover, in ALM we identified focal amplification of TERT, CCND1, MDM2 and MITF. In NAM, instead, we found only two focal amplifications, involving BRAF and MITF. Focal homozygous copy losses affected especially the CDKN2A and PTEN genes, both in ALM and in NAM, even though they were more frequent in the latter group.

In keeping with previous observations that led to classify ALM as a distinct molecular subtype of melanoma, we observed a peculiar genomic landscape in ALM (vs. NAM). Our study provides insights into the molecular characteristics of ALM, which are key to full elucidation of its pathogenesis.

# INTRODUCTION

## 2.1 Clinical classification

Melanoma arises from the malignant transformation of melanocytes. These pigment-producing cells embryologically derive from the pluripotent neural crest stem cells that during fetal development migrate to and differentiate within the epidermis and to other extra-cutaneous pigment-containing sites including eyes, meninges, esophagus and mucous membranes. As a result, three subtypes of melanoma can be identified: cutaneous melanoma (the most common), which arises from melanocytes in the epidermis, mucosal melanoma from melanocytes residing in the mucous membranes, and uveal melanoma, from melanocytes residing in the ocular stroma<sup>1</sup>.

Cutaneous melanomas, the most common type in Caucasians, are classified based on the morphology of the early growth phase into superficial spreading, nodular, lentigo maligna, and acral lentiginous (Fig. 1)<sup>2</sup>. Superficial spreading melanoma is the most common subtype of cutaneous melanoma, accounting for 60–70% of all melanomas. It is related to intermittent sun exposure and may arise *de novo* or in association with a nevus. Nodular melanoma represents approximately 15–20% of all melanomas. It has a vertical growth phase, rapid growth and high rate of metastasis<sup>3</sup>. Lentigo maligna melanoma is a less common subtype, comprising approximately 9% of all cutaneous melanomas. Typically, lesions occur in older, chronically sun-damaged individuals and have a predilection for nose and cheeks in women, and for neck, scalp, and ears in men<sup>2</sup>. Acral lentiginous melanoma (ALM) is rare, accounting for 5% of melanomas in white people but it is the most common type of melanoma in Asian, Hispanic, and African pts. Typically, it occurs on the soles, but it can also commonly occur on the palms and in or around the nail apparatus. ALM is difficult to diagnose because it can look like a benign lesion (i.e. a plantar wart or hematoma), especially when it is amelanotic<sup>4,5</sup>.

Melanoma more rarely develops in non-cutaneous sites. Uveal melanoma is the most common form of intraocular malignancy. The median age at presentation is the 6th decade of life and there is no different rate between genders. Approximately 50% of pts with uveal melanoma will develop distant metastases, an incidence that is significantly higher than that of cutaneous melanoma. Mucosal melanoma accounts for less than 1.5% of all melanomas. Over half the cases originate in the head and neck region (oral, nasal, and sinus mucosa), while the other half involve the anal/genital mucosal surfaces<sup>2</sup>.

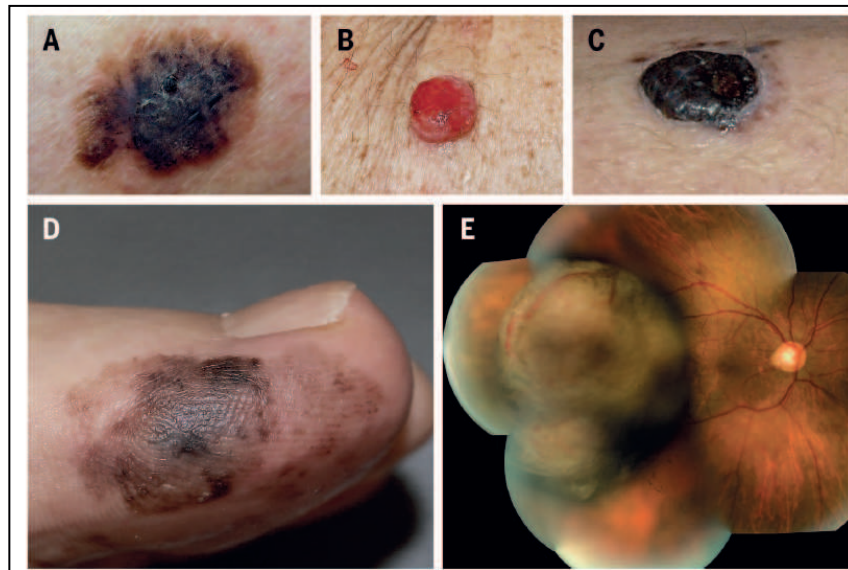


**Figure 1.** *Clinical images of melanomas.* Subtypes of melanoma include superficial spreading melanoma (A), amelanotic melanoma (B), nodular melanoma (C), acral lentiginous melanoma (D), and uveal melanoma (E).

*From Lo JA et al. The melanoma revolution: from UV carcinogenesis to a new era in therapeutics Science 2014*

## 2.2 Principals of staging: TNM classification

The eighth edition of the American Joint Committee on Cancer (AJCC) is the current melanoma staging system (Fig. 2)<sup>6</sup>. The staging is based on 3 categories: T (Tumor), N (Node) and M (Metastasis). The T category is classified primarily by measuring the thickness of the melanoma as defined by Alexander Breslow. Tumor thickness (Breslow) is measured from the top of the granular layer of the epidermis to the deepest invasive cell across the broad base of the tumor, in the dermis or subcutaneous. The second criterion for determining the T category is primary tumor ulceration. Ulcerated primary tumors are designated with a “b” suffix and non-ulcerated primary tumors with an “a” suffix.

The stratification of pts into the appropriate N category is primarily based upon the number of metastasis-containing regional lymph nodes, while the subclassification within the N grouping reflects the burden of disease, defined as either clinically occult (“a” suffix, clinical stages I-II) or clinically apparent (“b” suffix, clinical stage III). In case of microsatellites, satellites or in-transit metastases, the suffix “c” is assigned.

The M category refers to the presence of distant metastases. In the 8<sup>th</sup> edition of the AJCC manual, the “d” suffix was added for pts with central nervous system metastases, while



the (0)/(1) suffix was included to indicate not elevated/elevated lactate dehydrogenase (LDH) level, respectively.

Both clinical and pathological classifications are used in melanoma staging. Clinical staging consists of microstaging of the primary melanoma and clinical/radiologic/biopsy evaluation for metastases. Pathological staging includes all clinical staging information, along with any additional information derived from the excision of the primary tumor and lymph nodes.

## DEFINITIONS OF TNM

### Definition of Primary Tumor (T)

T Category	Thickness	Ulceration status
TX: primary tumor thickness cannot be assessed (e.g., diagnosis by curettage)	Not applicable	Not applicable
T0: no evidence of primary tumor (e.g., unknown primary or completely regressed melanoma)	Not applicable	Not applicable
Tis (melanoma <i>in situ</i> )	Not applicable	Not applicable
T1	≤1.0 mm	Unknown or unspecified
T1a	<0.8 mm	Without ulceration
T1b	<0.8 mm 0.8–1.0 mm	With ulceration With or without ulceration
T2	>1.0–2.0 mm	Unknown or unspecified
T2a	>1.0–2.0 mm	Without ulceration
T2b	>1.0–2.0 mm	With ulceration
T3	>2.0–4.0 mm	Unknown or unspecified
T3a	>2.0–4.0 mm	Without ulceration
T3b	>2.0–4.0 mm	With ulceration
T4	>4.0 mm	Unknown or unspecified
T4a	>4.0 mm	Without ulceration
T4b	>4.0 mm	With ulceration

### Definition of Regional Lymph Node (N)

Extent of regional lymph node and/or lymphatic metastasis		
N Category	Number of tumor-involved regional lymph node	Presence of in-transit, satellite, and/or microsatellite metastases
NX	Regional nodes not assessed (e.g., SLN biopsy not performed, regional nodes previously removed for another reason)	No
	<b>Exception:</b> pathological N category is not required for T1 melanomas, use cN.	
N0	No regional metastases detected	No
N1	One tumor-involved node or in-transit, satellite, and/or microsatellite metastases with no tumor-involved nodes	
N1a	One clinically occult (i.e., detected by SLN biopsy)	No
N1b	One clinically detected	No
N1c	No regional lymph node disease	Yes
N2	Two or three tumor-involved nodes or in-transit, satellite, and/or microsatellite metastases with one tumor-involved node	

Extent of regional lymph node and/or lymphatic metastasis		
N Category	Number of tumor-involved regional lymph node	Presence of in-transit, satellite, and/or microsatellite metastases
N2a	Two or three clinically occult (i.e., detected by SLN biopsy)	No
N2b	Two or three, at least one of which was clinically detected	No
N2c	One clinically occult or clinically detected	Yes
N3	Four or more tumor-involved nodes or in-transit, satellite, and/or microsatellite metastases with two or more tumor-involved nodes, or any number of matted nodes without or with in-transit, satellite, and/or microsatellite metastases	
N3a	Four or more clinically occult (i.e., detected by SLN biopsy)	No
N3b	Four or more, at least one of which was clinically detected, or presence of any number of matted nodes	No
N3c	Two or more clinically occult or clinically detected and/or presence of any number of matted nodes	Yes

### Definition of Distant Metastasis (M)

M Category	M Criteria	
	Anatomic site	LDH level
M0	No evidence of distant metastasis	Not applicable
M1	Evidence of distant metastasis	See below
M1a	Distant metastasis to skin, soft tissue including muscle, and/or nonregional lymph node	Not recorded or unspecified
M1a(0)		Not elevated
M1a(1)		Elevated
M1b	Distant metastasis to lung with or without M1a sites of disease	Not recorded or unspecified
M1b(0)		Not elevated
M1b(1)		Elevated
M1c	Distant metastasis to non-CNS visceral sites with or without M1a or M1b sites of disease	Not recorded or unspecified
M1c(0)		Not elevated
M1c(1)		Elevated
M1d	Distant metastasis to CNS with or without M1a, M1b, or M1c sites of disease	Not recorded or unspecified
M1d(0)		Normal
M1d(1)		Elevated

Suffixes for M category: (0) LDH not elevated, (1) LDH elevated. No suffix is used if LDH is not recorded or is unspecified.

Figure 2. The melanoma staging system as outlined by the 8<sup>th</sup> edition of the AJCC manual.

### **2.3 Epidemiology and risk factors in cutaneous melanoma**

Cutaneous melanoma is the most aggressive form of skin cancer. Its incidence continues to rise worldwide, although mortality rates stabilized since the early 90s in Australia, USA and some European countries, possibly reflecting the effects of early diagnosis. The highest recorded incidence of melanoma worldwide is in Queensland (Australia), where there is an incidence of  $55.8 \times 10^5$ /year for men and  $41.1 \times 10^5$ /year for women. Reported incidence rates vary within Europe, where Switzerland has the highest, and Greece the lowest rate. Unlike other solid tumors, melanoma mostly affects young and middle-aged people, and the median age at diagnosis is 57 years. The incidence of melanoma in Italy is 5-7 cases/100.000 inhabitant/year, although there appears to be a latitude gradient, with a higher incidence in northern Italy (Milan area), compared with that in the Naples area. The male/female ratio of melanoma varies among different countries. A male predominance has been recorded in countries with a high melanoma incidence, such as Australia and USA. In Europe, there is a different sex prevalence: most Western and Northern European countries report higher incidence rates in women, whereas in most Central, Eastern and Southern Europe melanoma predominates in men<sup>1, 7, 8</sup>.

Melanoma is considered a multifactorial disease arising from a combination of genetic susceptibility and environmental exposure. The most important environmental risk factor is the exposure to ultraviolet (UV) rays. Intermittent sun exposure and history of sunburns in childhood appear to be major determinants. The most important host risk factors are: number of melanocytic nevi, family history of melanoma, and genetic susceptibility. Melanocytic nevi are benign accumulations of melanocytes or nevus cells and may be congenital or acquired. Patients with more than 100 nevi, nevi larger than 5 mm, or presence of dysplastic nevi have increased risk of melanoma. A family history of melanoma constitutes a strong risk factor. It has been estimated that approximately 10% of melanomas are familial and 20-57% of familial cases have a mutation in the cyclin-dependent kinase inhibitor 2A (*CDKN2A*) gene, or, more rarely, in the cyclin-dependent kinase 4 (*CDK4*) gene. Additionally, certain phenotypic characteristics such as red hair, fair skin, numerous freckles, light eyes, sun sensitivity and inability to tan, raise the risk of developing melanoma by approximately 50%<sup>9</sup>.

## 2.4 Key molecular pathways in melanoma

The different types of melanoma appear to have distinct sets of relevant somatic alterations. Cutaneous non-acral melanoma is characterized by a high mutation rate with a predominant C>T nucleotide transition signature attributable to UV. On the other hand, non-UV-driven acral and mucosal melanomas lack this signature, have fewer point mutations and more structural variants such as deletions, duplications, clusters of breakpoints and rearrangements<sup>10, 11</sup>.

A key cell signaling pathway in cutaneous melanoma is the mitogen activated protein kinase (MAPK) pathway (Fig. 3). It is activated by mitogens binding to a receptor tyrosine kinase (RTK) at the cellular membrane, which leads to the recruitment of adaptor proteins that propagate the signal to intracellular effectors, including the small RAS GTPases. The RAS family consists of three isoforms (NRAS, ARAS and KRAS). Of them, NRAS is the most frequently involved in melanoma. Once activated, GTP-bound NRAS binds RAF. In the absence of an upstream stimulus, RAF kinases adopt a closed conformation, in which the N terminus inhibits the catalytic C terminus. When RAS binds RAF, it shifts to an open conformation through the disruption of the auto-inhibitory interaction between its N and C termini. Upon phosphorylation by RAS, RAF forms homo- (e.g. BRAF/BRAF) or hetero- (BRAF/CRAF) dimeric molecules. Active RAF kinases phosphorylate and activate MEK1 and MEK2, which in turn phosphorylate ERK. Active ERK phosphorylates serine or threonine residues within the Ser/Thr-Pro motifs in many cytoplasmic and nuclear proteins. In this way, ERK regulates cell survival, proliferation, adhesion, migration, and differentiation. More than 50 cytoplasmic substrates of ERK have been identified, including kinases (e.g. p90 ribosomal S6 kinase), apoptotic regulators (e.g. BIM), cytoskeletal proteins (e.g. paxillin) and others. In the nucleus, ERK regulates transcription factors, including members of the ternary complex factor and E-twenty-six (ETS) families. Ultimately, this results in the transcriptional activation of immediate/early and late response genes, including MYC, FOS and CCND1 that play key roles in cell cycle progression. A complex network of negative-feedback interactions limit activation of the ERK signaling. Negative-feedback regulation is mediated through direct phosphorylation of almost all components of the RTK-RAS MAPK cascade by ERK<sup>12,13</sup>.

The Cancer Genome Atlas (TCGA) program published in 2015 a systematic multi-platform characterization of 333 cutaneous melanomas at the DNA, RNA, and protein levels and established a genomic classification in four groups according to the most significantly mutated genes: BRAF, RAS (including N-, K- and H-RAS members), NF1 and triple negative

subtypes (Fig. 4). Such genomic classification provides signposts for the identification of actionable targets and predictive biomarkers, as well as potentially useful guidance for therapeutic decisions<sup>14</sup>. In 2017 Hayward N. *et al.* implemented the genomic classification of the TCGA in a study that included also acral and mucosal melanomas and drew the most updated genomic landscape of melanoma (Fig. 5)<sup>11</sup>.

The gene encoding the serine/threonine protein kinase BRAF maps to chromosome 7q34. Approximately 50% of melanomas harbor activating BRAF mutations, which are considered *driver* mutations<sup>13,15</sup>. Almost 90% of the BRAF mutations observed in melanoma are at codon 600 (V600mut), and among these, over 90% consist of a T>A nucleotide change at position 1799 of the coding DNA resulting in a valine to glutamic acid substitution (V600E). The second most common (5-6%) mutation is the valine to lysine substitution at the same codon (1798\_1799delGTinsAA, V600K), followed by a valine to arginine substitution (1798\_1799delGTinsAG, V600R), a two-nucleotide variation c.1799\_17800delTGinsAA (V600E-complex) or c.1799\_17800delTGinsAT (V600D) (COSMIC, <http://www.sanger.ac.uk/cosmic>)<sup>16,17</sup>. In contrast to the wild-type (wt) protein, BRAF V600mut can activate the downstream MEK protein in a monomeric form and independently from RAS activation. BRAF mutation is associated with young age at diagnosis, intermittently sun-exposed sites such as the trunk, superficial spreading subtype, absence of solar elastosis. Mutations in BRAF alone do not induce melanoma, but are initiation events for nevi formation. After acquiring an initiation mutation, a melanocyte undergoes limited proliferation before entering a senescent-like state, resulting in a cell-cycle arrest. Additional genetic events, such as acquisition of TERT promoter mutations or deletion of CDKN2A, are needed to elicit a fully cancerous phenotype<sup>18, 19</sup>.

The oncogene NRAS is altered in 15–20% of melanomas especially at codon Q61, and represents the second most common oncogenic *driver* mutation in this disease. These mutations prevent efficient GTP hydrolysis, thus maintaining Ras in an active, GTP-bound state. In this conformation, Ras binds and activates its effectors including Raf. Usually, NRAS mutations occur in all non-uvexposed sites of melanoma, including both sun exposed and non-sun exposed skin, mucosal, and acral sites. Unlike BRAF, NRAS mutations are rarely present in benign melanocytic nevi, with the exception of congenital nevi. NRAS mutations are associated with thicker primary tumors, high mitotic rate, and lower incidence of ulceration. Mutations in NRAS constitutively activate intracellular signaling through a variety of pathways, most notably the RAS-RAF-MAPK and PI3K-AKT pathways<sup>20</sup>. NRAS and BRAF mutations are usually mutually exclusive.

The Neurofibromatosis type 1 (NF1) tumor suppressor gene is frequently mutated in melanoma. NF1 negatively regulates RAS by enhancing its RAS GTPase activity, hence converting active RAS-GTP to inactive RAS-GDP. Inactivating NF1 mutations have been detected throughout the gene in 38-46% of melanomas expressing BRAFwt and RAS<sup>14, 21</sup>. Functional studies showed that NF1 suppression leads to increased RAS activation<sup>22</sup>.

Another key pathway in melanoma is the PI3K-AKT cascade. PI3K, which consists of a dimer of catalytic and regulatory subunits, can be activated by multiple signals, including receptor tyrosine kinases (RTKs), RAS proteins, and cell-cell contacts. Activated PI3K phosphorylates phosphatidyl-inositols in the plasma membrane at the 3'-OH group. These 3'-phospholipids attract proteins that contain a pleckstrin homology (PH) domain to the cell membrane, including AKT. AKT, which has 3 isoforms (AKT1/2/3), is phosphorylated at two critical and conserved residues, Thr308 (by PDK1) and Ser473 (by the mTORC2 complex), which fully activates its catalytic activity. Activated AKT then phosphorylates a number of effector proteins, thereby regulating multiple key cellular processes, including proliferation, survival, motility, metabolism, angiogenesis. PTEN regulates the activity of the pathway by dephosphorylating phosphatidyl-inositols at the 3'-position, thereby antagonizing the activity of PI3K. PTEN loss, most commonly via allelic loss and focal deletions, frequently occurs in melanomas with activating BRAF mutations. Point mutations in PIK3CA, which encodes the catalytic subunit of PI3K, and in AKT1/3, are detected in 2-6% and in 1-2% of melanomas, respectively<sup>23</sup>.

Activating mutations in KIT have been identified in melanomas of acral and mucosal types and in those arising in chronically sun-damaged skin. KIT (c-kit), a type III receptor tyrosine kinase, and its ligand, stem cell factor (SCF), also known as c-kit ligand, are essential for the development of melanocytes in vertebrates, regulating growth, migration, survival, and differentiation. Depending on the cellular context in which KIT is activated, downstream effectors include Src family kinases, the p85 subunit of PI3K, phospholipase C-gamma, and MAP kinases. KIT mutations or amplifications are observed in ~30% of mucosal, 20% of acral, and 20% of melanomas arising in chronically sun-damaged skin. KIT mutations show heterogeneous distribution through the gene, and they are most frequently detected in exon 11 (L576P) and 13 (K642E)<sup>24, 25</sup>.

Activating mutations in GNAQ and GNA11 are detected in uveal melanoma. The GNAQ and GNA11 genes encode members of the G-protein  $\alpha$  subunits involved in mediating signals between G-protein coupled receptors (GPCRs) and downstream effectors, such as

MEK, PI3-kinase/Akt, protein kinase C, and YAP. GNAQ and GNA11 mutations are found in 33% and in 39% of uveal melanomas, respectively, and about 90% occur at codon Q209<sup>26</sup>.

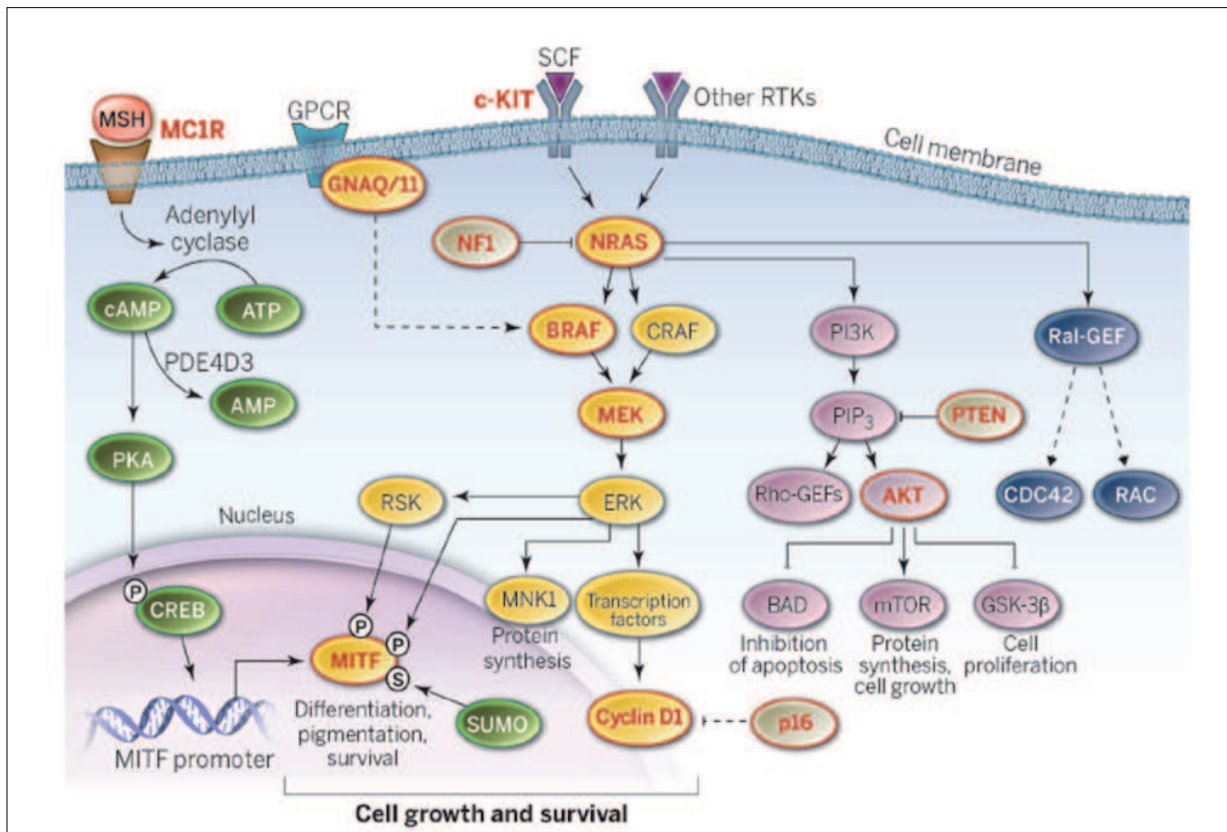


**Figure 3.** Key signaling pathways in melanoma. MAPK signaling promotes cell growth and survival and is constitutively active in most melanomas. Oncogenic BRAF and NRAS mutations are found in 40-60% and 10-30% of melanomas, respectively. c-KIT signaling is essential for melanocyte development and is associated with melanomas arising on acral, mucosal, and chronically sun-damaged skin. Mutations in GNAQ and GNA11 are the dominant lesions in uveal melanomas. Known melanoma oncogenes and tumor suppressors are labeled in red. Dotted lines represent omitted pathway components.

*From Lo JA et al. The melanoma revolution: from UV carcinogenesis to a new era in therapeutics  
Science 2014*

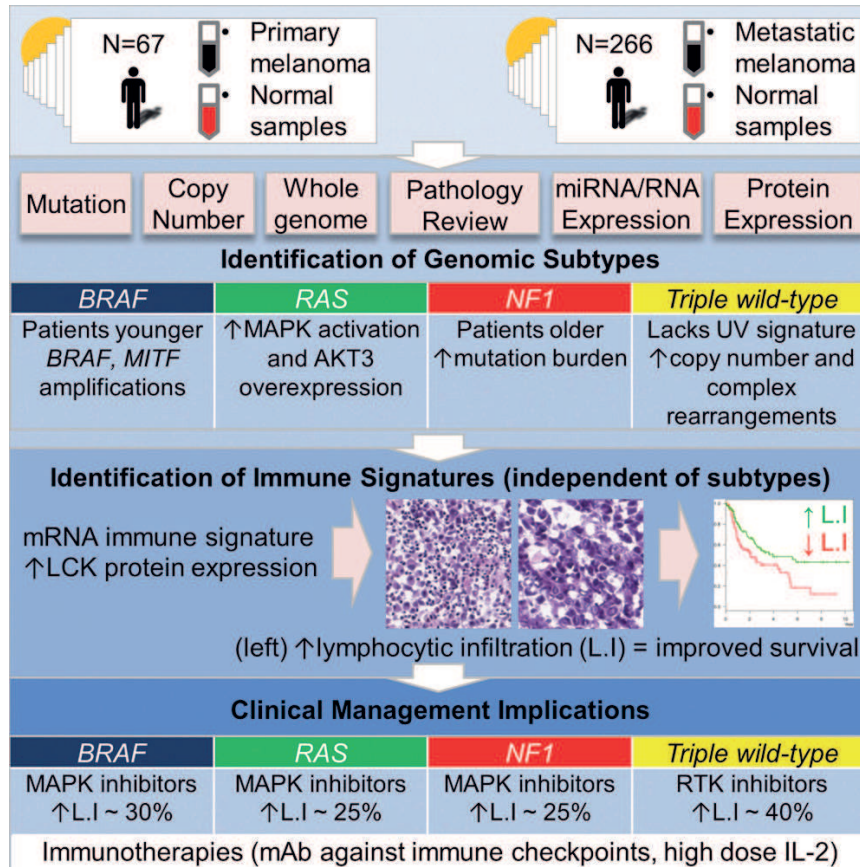


**Figure 4.** The genomic classification of cutaneous melanoma, as outlined by TCGA.

From Cancer Genome Atlas Network. Genomic Classification of Cutaneous Melanoma  
Cell 2015



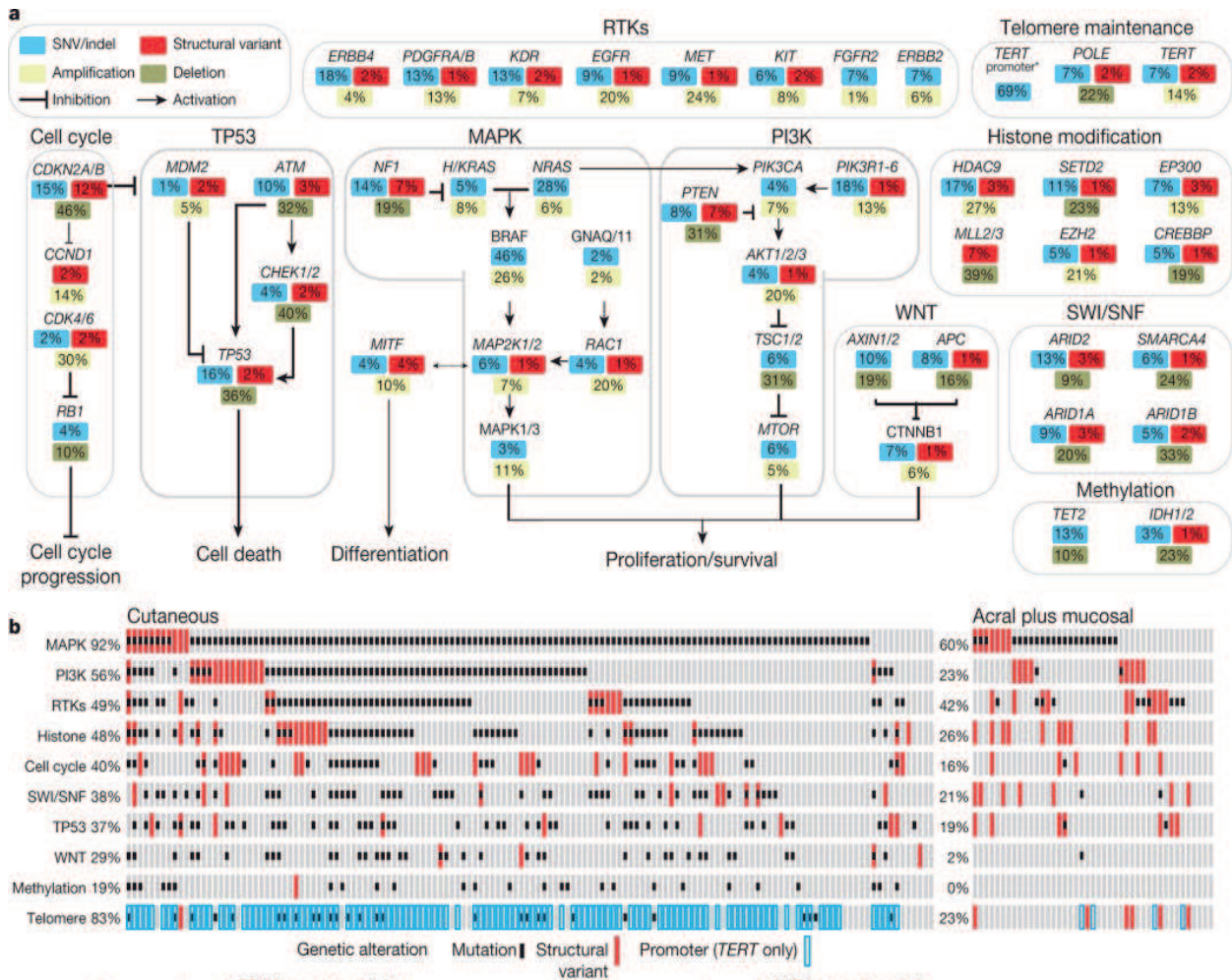


**Figure 5.** Genes and signaling pathways recurrently altered in melanoma. (a) Percentage of samples with aberrations in candidate driver genes, grouped by pathway. Substitution/indels (blue), structural variants (red), copy number amplification (yellow), homozygous deletion (green). (b) Frequency of aberrations in pathways as percentage of cutaneous or acral/mucosal melanomas.

From Hayward N. et al. Whole-genome landscapes of major melanoma subtypes  
*Nature* 2017

## 2.5 Progression from melanocyte to metastatic melanoma

Cutaneous melanoma can be categorized based upon its origin from non-chronically sun damaged (non-CSD) or chronically sun damaged (CSD) skin. In non-CSD melanoma, the progression cascade is initiated by BRAF V600E, the only pathogenic mutation that can be found in benign nevi. In the absence of other driver mutations, nevus melanocytes stop proliferating and enter senescence. Progression to melanoma requires the nevus to acquire additional mutations, such as TERT promoter mutations and CDKN2A hemizygous alterations. By contrast, CSD melanomas show a different set of driver mutations, i.e. NRAS, NF1 or BRAF non-V600E mutations. They do not originate from nevi, but from melanoma *in situ* or intermediate lesions (Fig. 4).

Melanoma *in situ* tend to have a high mutation burden with a strong mutation signature associated to UV exposure, which is the predominant mutagen acting at this stage, together with other mutations that promote proliferation, such as mutations in PTEN and TP53. Melanoma becomes invasive once melanoma cells leave the epithelium of the epidermis and invade the subjacent mesenchymal tissue. Invasive melanoma also inherits the driver mutations activating the MAPK pathway, as well as TERT mutations that accumulated during earlier stages of progression. However, invasive melanomas display higher frequencies of bi-allelic inactivation of CDKN2A, which is not seen in precursor lesions. In addition, mutations affecting members of the SWI/SNF chromatin-remodeling complex, particularly ARID1A and ARID2, which maintain chromatin remodeling, emerge at the transition to invasive melanoma and correlate with the appearance of widespread chromosomal aberrations. There seems to be no further substantial increase in the burden of point mutations between the early stage and advanced melanoma. In contrast, copy number alterations increase throughout the evolution of melanoma and are considered the principal mutagen at late stages of melanoma progression. Although there might be instances in which pathogenic mutations promote metastatic dissemination, the pattern of recurrent alterations associated with metastatic progression is still poorly defined<sup>19,27</sup>.

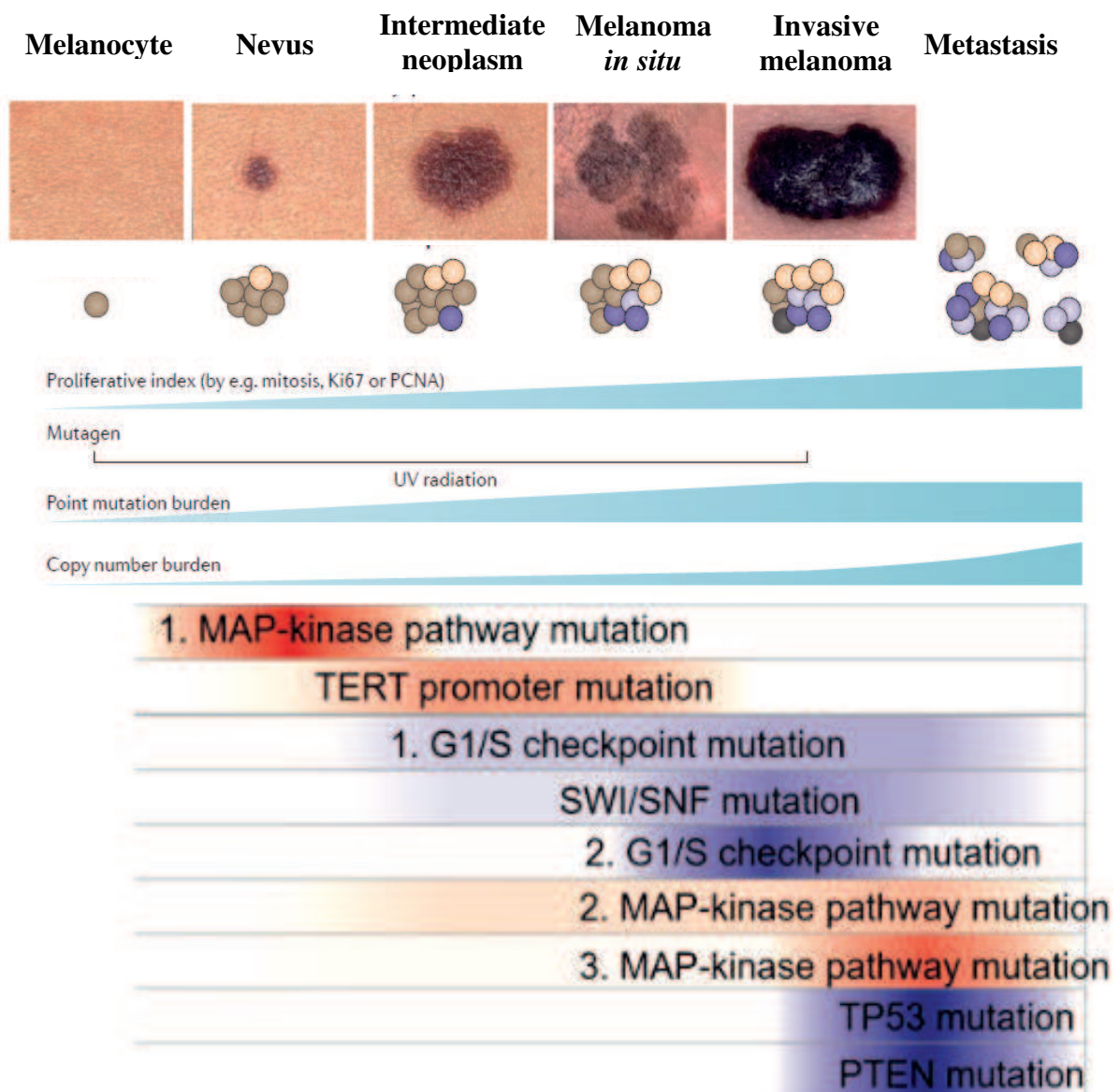


**Figure 6.** Genetic evolution of cutaneous melanoma.

Adapted from:

Cancer Genome Atlas Network. Genomic Classification of Cutaneous Melanoma  
Cell 2015

SMR06-4 presentation, World Melanoma Congress 2017

## 2.6 Treatment options for melanoma

While wide local surgical excision has a high potential to cure pts with early-stage melanoma, until recently, there has been a dearth of effective treatments for surgically unresectable or metastatic melanoma and prognosis of stage IV melanoma pts was poor, with a median survival ranging from 8 to 18 months. Standard-of-care treatments during this time included dacarbazine-based chemotherapy and cytokine IL-2<sup>28,29</sup>. Therapy of advanced stage melanoma has improved dramatically with the development of BRAF and MEK inhibitors and of cytotoxic T-lymphocyte-associated antigen 4 (CTLA-4) and programmed cell-death protein 1 (PD-1) blocking antibodies, which have been shown to improve the overall survival of pts<sup>30</sup>.

Vemurafenib and Dabrafenib are potent inhibitors of V600-mutated BRAF. Marked antitumor effects were shown against melanoma cell lines carrying the BRAF V600E mutation but not against cells with BRAFwt cells, in which, instead, Vemurafenib and Dabrafenib triggered a paradoxical effect of MAPK pathway activation<sup>31</sup>. In phase III trials, both Vemurafenib and Dabrafenib produced improved rates of OS and PFS compared to Dacarbazine (Vemurafenib: median PFS 5.3 vs. 1.6 months; Dabrafenib: median PFS 5.1 vs. 2.7 months). Common side effects are cutaneous squamous-cell carcinoma and keratoacanthoma, due to the paradoxical activation of the MAPK pathway in BRAFwt cells<sup>24,32,33</sup>.

Unfortunately, though initial responses to these agents are impressive, resistance develops in approximately 6–7 months. Since most reported resistance mechanisms reactivate the MAPK pathway, the MEK-inhibitor Trametinib was combined to BRAF inhibitor Dabrafenib to strengthen the MAPK pathway inhibition. The combination, compared to BRAF inhibition alone, delayed the emergence of resistance thus prolonging PFS and reduced toxicity<sup>34</sup>. Several such combinations of BRAF and MEK inhibitors (BRAFi/MEKi) are currently available. Due to the superior effects of the combinations vs. BRAFi alone, they have become the standard targeted therapy for BRAF V600 mutation positive melanoma. Nevertheless, resistance remains a significant problem.

Another systemic treatment focuses on the activation of the immune system by blocking inhibitory checkpoints. Ipilimumab, a monoclonal antibody against CTLA-4 and more recently, Nivolumab and Pembrolizumab, both anti-PD-1 monoclonal antibodies, have considerably improved the survival of metastatic pts and can be considered as first-line treatments even in the presence of a BRAF mutation. Combinations of anti-CTLA4 and anti-PD1 are currently being tested in clinical trials and seem to confer improved effects compared

to monotherapies, despite an increased toxicity. Targeted and immunotherapy combinations are currently under investigation, supported by the positive effect of MAPK inhibition on the immune recognition<sup>35</sup>. Ongoing studies are also exploring the use of combination targeted therapy and immunotherapy in the adjuvant setting for resected stage III melanoma pts<sup>36, 37</sup>.

## 2.7 Resistance to MAPK inhibitors

Resistance may arise under the selective pressure of therapy from pre-existing resistant tumor subclones (primary/intrinsic resistance), as a result of an evolutionary process that takes place during treatment (secondary/acquired resistance), or as a combination of both. While in the first case complete lack of response is observed, in the second one the progression follows an initial clinical benefit.

A major effect of resistance to BRAFi therapy occurs via the reactivation of the MAPK pathway, which leads to uncontrolled cellular proliferation (Fig. 7). Different aberrations have been found to contribute to MAPK re-activation, such as:

- upregulation and activation of receptor tyrosine kinases: increased levels of IGF-IR were found in progressing tumors or in cell lines resistant to BRAFi<sup>38-40</sup>;
- expression of BRAF splice variants lacking the RAS-binding domain<sup>38, 41</sup>;
- BRAF V600 amplification<sup>42, 43</sup>;
- activating mutations of NRAS, which bypass BRAF inhibition by activating CRAF;
- loss of expression of the NRAS negative regulator NF1<sup>42, 44, 45</sup>;
- activating MEK mutations<sup>38, 42, 46-49</sup>;
- COT kinase (MAP3K8) upregulation, which activates ERK through MEK, bypassing RAF<sup>50</sup>;
- Overexpression of the RAC1<sup>P29S</sup> mutant protein, a RAS-related GTPase that regulates cell proliferation and migration<sup>47, 51</sup>;
- CDKN2A loss, as a MAPK-reactivating mechanism, given that one of its gene products, p16/INK4A, negatively regulates the MAPK pathway effector complex cyclinD/cdk4<sup>42</sup>;
- CDK4 and cyclin D1 amplification<sup>52</sup>.

Similar resistance mechanisms have been described with combined BRAF/MEK inhibition; these include MEK1/2 mutations, BRAF amplifications, NRAS mutations, and loss of NF1<sup>53</sup>.

Among the mentioned alterations, BRAF amplification is described as one of the main mechanisms of acquired resistance. A higher number of BRAF gene copies has been detected in specimens from pts at disease progression compared to baseline biopsies<sup>43, 53-55</sup>. An

increased BRAF gene copy number has been also reported both in pre-treatment specimens from metastatic melanoma pts who did not respond to therapy and in MAPKi resistant cell lines<sup>56,57</sup>. Thus, it is still debated if BRAF amplification is an acquired mechanism of resistance, which develops *de novo* in the tumor cells to overcome BRAF inhibition, or if it can also play a role as an intrinsic mechanism when detected in the tumor prior to MAPKi exposure.

Of note, the BRAF gene maps to chromosome 7, which is frequently gained, as a whole or in part, especially in BRAFmut melanoma, contributing to variation of the amount of the mutant allele. Indeed, the percentage of the BRAFmut allele, although expected to be 50% as mutations in oncogenes are usually heterozygous, reportedly spans across a wide range of values in melanoma samples<sup>58-61</sup>. Because the BRAF V600 mutation is the target of BRAFi, the percentage of the BRAFmut allele was suggested to influence the clinical efficacy of the treatment but its association with pts' response is still controversial<sup>58, 62-64</sup>.

Resistance can be also induced by the activation of parallel signaling pathways, such as the PI3K-AKT pathway<sup>38, 42, 65</sup>. Mutations in additional PI3K-AKT positive-regulatory genes (e.g. PIK3CA and PIK3CG) and in negative-regulatory genes (e.g. PIK3R2, PTEN, and PHLPP1) are found throughout melanoma progression. The tumor suppressor PTEN, which inhibits PI3K signaling, is frequently lost in melanoma. PTEN loss was described as a mechanism underlying intrinsic resistance via increased PI3K/AKT signaling because melanoma cell lines with functional inactivation of PTEN seemed to be less sensitive than wt ones to MAPKi. However, in the clinical setting, even tumors with complete loss of PTEN responded to MAPKi<sup>47, 48, 56, 66, 67</sup>. Beside PTEN loss, also gain-of-function AKT1/3 mutations have been shown to be involved in resistance<sup>42, 65</sup>.

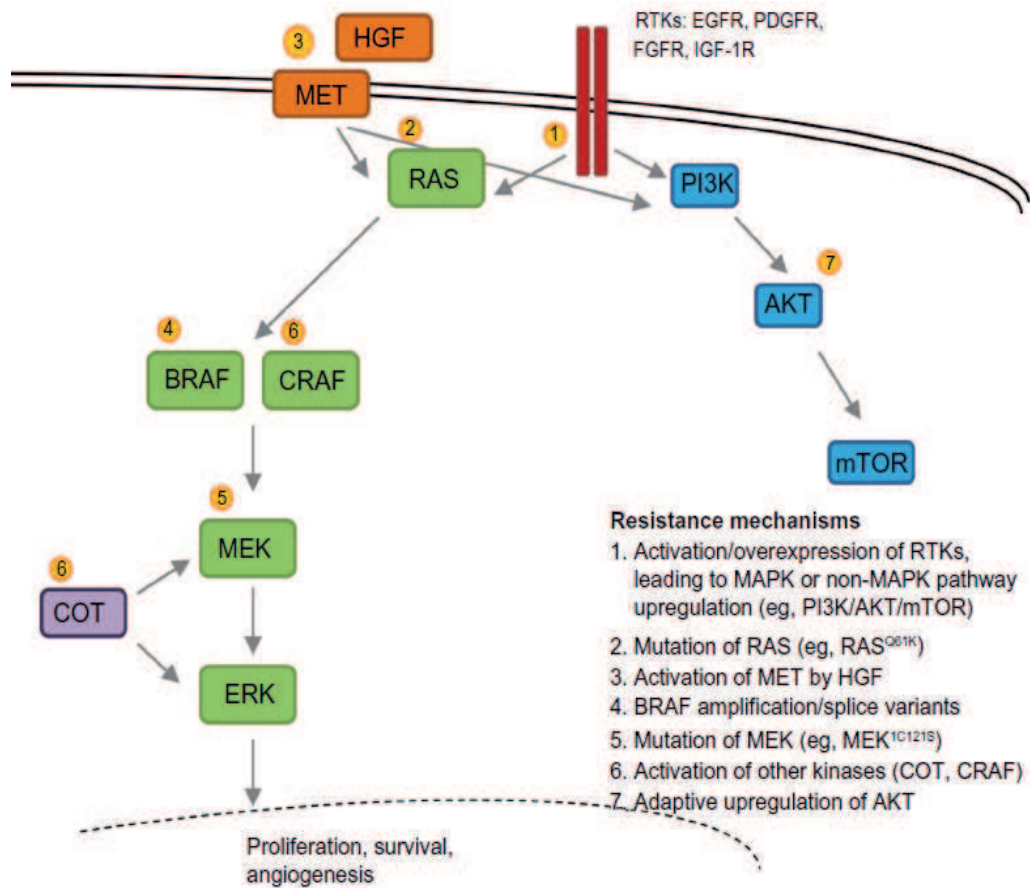


**Figure 7.** Main mechanisms of resistance to MAPK inhibitors.

*From Luke JJ et al. Targeted agents and immunotherapies: optimizing outcomes in melanoma. Nat Rev Clin Oncol 2017.*

## 2.8 TERT promoter gene mutations in melanoma

Telomerase reactivation is reportedly an early event in melanoma progression. Telomerase is the enzyme responsible for the maintenance of telomeres—nucleoprotein structures that protect the ends of eukaryotic chromosomes from being recognized as broken ends with consequent activation of the repair machinery. Telomeres shorten at each replicative cycle and, when they reach a critical length, cells are triggered to enter a permanent growth arrest stage called senescence, conferring to the cell a limited life-span<sup>68,69</sup>. Overcoming the senescence barrier by telomere stabilization is prerequisite to the acquisition of uncontrolled cell proliferation potential. In most cases, this is achieved by transcriptional induction of TERT expression accompanied by telomerase activation.

Telomerase comprises a catalytic subunit, encoded by the telomerase reverse transcriptase (TERT) gene, and an RNA component transcribed from the Telomerase RNA component (TERC). Telomerase is active in germ cells and proliferative cells of self-renewing tissues and is mostly silenced in differentiated cells, leading to gradual telomere attrition. Non-coding mutations within the core promoter of TERT (i.e. -124C>T alias C228T and -146C>T alias C250T) create *de novo* binding sites for E twenty-six/ternary complex (ETS/TCF) transcription factors, thus leading to increased TERT transcription and activation. Other non-frequent nucleotide changes that occur as somatic mutations include the -124/-125CC>TT and the -138/-139CC>TT (Fig. 8). A mutation at -57 was also found in a case of familial melanoma<sup>70-72</sup>.

In cutaneous melanoma, TERT promoter mutations associate with BRAF mutations, features of aggressiveness, such as increased tumor thickness and mitotic rate, advanced stage, presence of ulceration and absence of regression<sup>73</sup>. In addition, poor prognosis was described for pts with TERT promoter mutations<sup>74</sup>. Some studies reported a modification of the effect of the TERT promoter mutations on survival by the rs2853669 polymorphism at -245 bp within the TERT promoter, which disrupts a preexisting non-canonical ETS2 site<sup>75</sup>. The effect of the TERT promoter mutations on survival and disease recurrence is reportedly present or even enhanced in pts that did not carry the variant allele of the polymorphism. Analysis of melanoma-specific survival showed that the number of deaths among pts that carried the variant allele was significantly lower than in those who did not<sup>76</sup>.



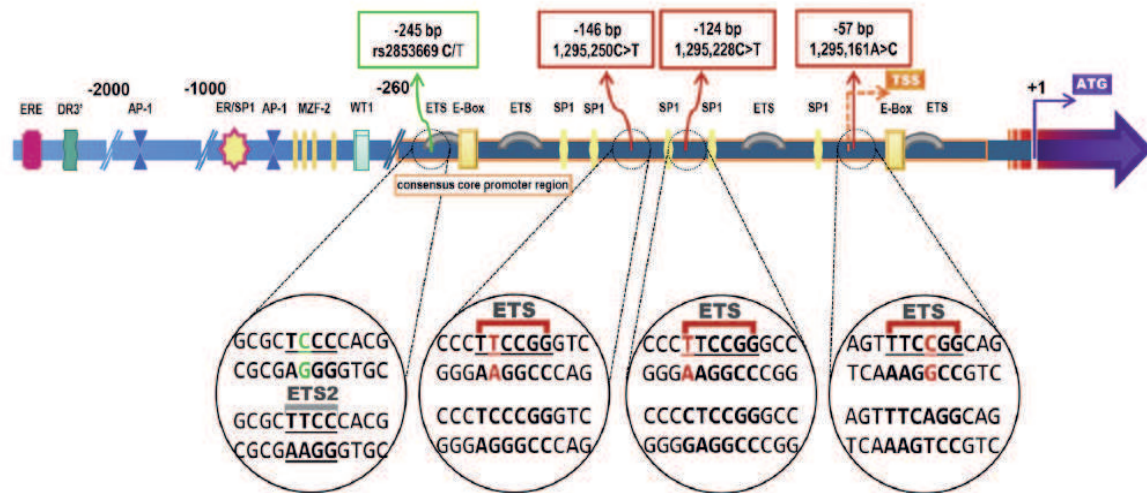


**Fig. 8.** Structure of the *TERT* promoter. Different regulatory elements and location of mutations at -57, -124 and -146 bp and the rs2853669 at -245 bp from the ATG start site are indicated.

*From Heidenreich B, Kumar R. TERT promoter mutations in telomere biology  
Mutat Res 2017*

## **AIMS OF THE STUDY**

### **AIM 1: Identification of molecular signatures associated with response to MAPK inhibitors.**

Melanoma patients' response to MAPKi is heterogeneous and still unpredictable. In our study, we sought to identify any correlation(s) between molecular alterations in pre-treatment specimens and different types of response that could guide patient stratification for appropriate treatment selection. Specifically, we investigated:

- A. BRAF gene copy number and mutant allele frequency
- B. PTEN loss
- C. TERT promoter mutations

and correlated them with PFS.

We also applied a comprehensive and unbiased approach using genome-wide CNV analysis to identify additional genomic aberrations, which could be associated with response.

### **AIM 2: Research of molecular biomarkers to classify acral melanoma**

Acral lentiginous melanoma (ALM) is a rare subtype of cutaneous melanoma with peculiar morphological, epidemiological, and genetic features. Since ALM develops on sun-protected sites as palms, soles, or beneath the nail plate, it shows genetic alterations unrelated to sun exposure and, hence, differs from the most common cutaneous non-acral melanoma (NAM), which, instead, is associated with a typical UV-signature. Because the genomic landscape of ALM is still incompletely described, we used whole genome CNV analysis to characterize ALM and detail the genomic signatures that differentiate ALM from NAM.

## **MATERIALS AND METHODS**

### **4.1 Patient cohort**

Eighty-one pre-treatment specimens (21 from primary tumors and 60 from metastases) were collected from 72 pts diagnosed with BRAFmut unresectable stage III or stage IV cutaneous melanoma, who were treated at the Veneto Institute of Oncology IOV – IRCCS in Padua. Multiple biopsies were available for 7 pts. Forty-six pts (64%) received monotherapy [(Vemurafenib (33) or Dabrafenib (13)] and 26 (36%) a combination (Combo) of BRAF and MEK inhibitors (Dabrafenib and Trametinib, respectively). Demographic and clinical characteristics were documented and included age, gender, stage, histopathological features, therapy, and ECOG performance status at baseline. PFS, assessed by imaging or clinical evaluation, was the clinical outcome measure we evaluated in this study, considered as a continuous variable or as a categorized variable. In the latter case, taking into account the reported improved response to combination therapy vs. monotherapy, pts were divided into 3 groups: no-response (PFS<3 mo.), short-response (PFS 3-12 mo., in BRAFi-treated, and 3-18 mo., in Combo-treated pts) and long-response (PFS>12 mo. and >18 mo., in BRAFi- and Combo-treated pts, respectively). Clinical-pathological features of the cohort are summarized in Table 1. Written informed consent was obtained from all pts upon enrollment in the study, as approved by the local institutional ethics committee.

**Table 1. Summary of clinical, tissue and molecular characteristics of the patient cohort at baseline.**

		<b>Overall</b>	<b>BRAF analysis</b>	<b>PTEN analysis</b>	<b>TERT analysis</b>	<b>CNV analysis</b>
		<i>N</i> (%)	<i>N</i> (%)	<i>N</i> (%)	<i>N</i> (%)	<i>N</i> (%)
<b>Patients</b>		72 (100%)	46 (100%)	26 (100%)	55 (100%)	44 (100%)
<b>Gender</b>	Male	39 (54%)	24 (52%)	11 (42%)	26 (47%)	23 (52%)
	Female	33 (46%)	22 (48%)	15 (58%)	29 (53%)	21 (48%)
<b>Age (years)</b>	Median (range)	59 (28 - 81)	55 (28 - 80)	57 (32 - 80)	59 (28-81)	56 (28 - 80)
<b>Therapy</b>	Vemurafenib	33 (46%)	22 (48%)	11 (42%)	25 (45%)	21 (48%)
	Dabrafenib	13 (18%)	12 (26%)	8 (31%)	7 (13%)	10 (23%)
	Combo	26 (36%)	12 (26%)	7 (27%)	23 (42%)	13 (29%)
<b>Stage</b>	III	15 (21%)	10 (22%)	3 (12%)	9 (16%)	7 (16%)
	IV	57 (79%)	36 (78%)	23 (88%)	46 (84%)	37 (84%)
<b>ECOG PF</b>	0	54 (75%)	34 (74%)	18 (69%)	40 (73%)	32 (73%)
	1	11 (15%)	10 (22%)	7 (27%)	9 (16%)	9 (20%)
	>1	7 (10%)	2 (4%)	1 (4%)	6 (11%)	3 (7%)
<b>Median PFS (months)</b>	Overall (95% CI)	7.36 (5.59-9.15)	7.5 (5.5-12.8)	7 (3.63-10.37)	7.37 (4.14-10.6)	5.57 (3.87-7.26)
<b>Response groups</b>	No-response	14 (19%)	7 (15%)	5 (19%)	12 (22%)	10 (23%)
	Short-response	33 (46%)	24 (52%)	14 (54%)	23 (43%)	22 (50%)
	Long-response	18 (25%)	14 (30%)	7 (27%)	14 (25%)	12 (27%)
	Censored	7 (10%)	1(3%)	0	6 (10%)	0
<b>Tumor specimens</b>		81 (100%)	51 (100%)	29 (100%)	61 (100%)	51 (100%)
<b>Tissue</b>	Primary	21 (26%)	9 (18%)	4 (14%)	15 (25%)	7 (14%)
	Metastasis	60 (74%)	42 (82%)	25 (86%)	46 (75%)	44 (86%)
<b>BRAF mutation</b>	V600E	71 (88%)	42 (82%)	23 (80%)	57 (93%)	43 (84%)
	V600K	8 (10%)	7 (14%)	4 (14%)	3 (5%)	6 (12%)
	V600R	1 (1%)	1 (2%)	1 (3%)	1 (2%)	1 (2%)
	V600_K601E	1 (1%)	1 (2%)	1 (3%)	0	1 (2%)

## 4.2 Tumor samples and DNA extraction and quantification

All samples were formalin-fixed paraffin-embedded (FFPE). A pathologist contoured and estimated the tumor area on hematoxylin and eosin-stained (H&E) slides. For 5 samples, tumor cell percentage was also evaluated by the Aperio ScanScope CS system and ImageScope software (Leica Biosystems, Milton Keynes, UK) on digital images of H&E slides; the results confirmed the accuracy of the pathology evaluation.

Samples with tumor content  $\geq 70\%$  were hand-macrodissected to enrich the tumor cell population and incubated overnight at  $56^{\circ}\text{C}$  with  $20\mu\text{l}$  of proteinase K and  $180\mu\text{l}$  of ATL buffer (Qiagen, Hilden, Germany) to obtain cell lysate. DNA was purified using spin-columns from the QIAmp DNA micro/mini kit (Qiagen, Hilden, Germany) or by magnetic bead technology with the MagNA Pure Compact Instrument (Roche Diagnostics, Mannheim, Germany), according to the manufacturer's instructions. Total DNA was quantified using a spectrophotometer (NanoDrop). Double-stranded DNA was measured using the Quant-iT PicoGreen dsDNA Assay Kit (ThermoFisher Scientific, Waltham, MA, USA) and the Victor X4 fluorometer (Perkin Elmer, Waltham, MA, USA).

## 4.3 Real-time PCR

BRAF gene copy number was assessed by real-time quantitative PCR (qPCR) using the TaqMan technology on a Light-Cycler 480 instrument (Roche Diagnostics, Mannheim, Germany). A 149 bp region was amplified with primers encompassing the 600 codon in a multiplex reaction that also included primers for the albumin (ALB) gene as a reference gene. We used the relative quantification measured using the  $2^{-\Delta\Delta\text{Ct}}$  method with a BRAF reference standard (Horizon Diagnostics, Cambridge, UK) in each experiment and adjusted it according to the estimated tumor cell percentage. To validate our approach, we analyzed control DNA from FFPE normal skin samples that showed a BRAF/ALB ratio ranging from 0.93 to 1.1 and denoting an equal copy number of the BRAF and ALB genes (1.9-2.2 copies). The adenocarcinoma cell line HT-29, for which chromosome 7 trisomy has been reported<sup>77</sup>, was used as an additional control and showed a BRAF/ALB ratio of 1.5, as expected. We set a copy number of 2.3 as a cut-off to discriminate between a diploid BRAF status and BRAF gain.

The quantification of the BRAF mutant allele in each sample was obtained by *ad hoc* real-time PCR reactions set up to amplify the V600E/K mutant and wt alleles. The forward primer was mutation-specific, with a 3' terminus matching the V600E, V600K or the wt

codon, while the reverse primer and the probe were identical in each reaction. To increase allele specificity, an additional nucleotide mismatch was incorporated 2 nucleotides upstream the 3' end of each forward primer. Both mutant- and wt- specific PCRs were performed using the ALB gene as a control to normalize for DNA content. Standard curves with serial dilutions of the commercially available BRAF V600E or V600K 50% allele standards (Horizon Diagnostics, Cambridge, UK) in BRAFwt sample were used to evaluate the reaction efficiency and to calculate the fraction of BRAF V600 mutant allele as in Kristensen *et al.*<sup>78</sup> The BRAF mutant allele % was calculated as a ratio of BRAF mutant/BRAF mutant + BRAFwt adjusted by tumor cell percentage. To validate the method, we compared the BRAF mutant allele % as measured by allele-specific real-time qPCR to that evaluated by pyrosequencing for 5 representative samples and for the BRAF V600E HT-29 cell line. The two methods yielded comparable results with an average difference of 10.7% (data not shown).

Sequences of primers and probes are provided in Table 2. All PCR reactions were carried out in duplicate in a final volume of 20 $\mu$ l containing 10 $\mu$ l of LightCycler 480 Probes Master 10X (Roche Diagnostics, Mannheim, Germany), 0.5 $\mu$ M of each primer, 0.3 $\mu$ M of BRAF hydrolysis probe, 0.1 $\mu$ M of albumin hydrolysis probe and 5 $\mu$ l of DNA. Thermal-cycler conditions were as follows: initial denaturation step of 10 min at 95°C, followed by 40 amplification cycles at 95°C for 10 sec, 60°C for 60 sec and 72°C for 1 sec, with a final extension step of 30 sec at 72°C.

Table 2. Primers and probes used in real-time qPCR.

Target	Forward primer	Reverse primer	Probe
Albumin	5'- GCTGTCATCTCTTTGTGGGCT-3'	5'-GGGAGCTGCTGGTTCTCTTT-3'	5'-VIC-CAAAACCTGTCATGCCCCACA-MGB-3'
<b>BRAF V600E</b>	5'-TAGGTGATTTTGGTCTAGCTACcGA-3'	5'-GTAACTCAGCAGCATCTCAGGG-3'	5'-FAM-GGAGTGGGTCCCATCAGTTT-MGB-3'
<b>BRAF wt</b>	5'-TAGGTGATTTTGGTCTAGCTACcGT-3'	5'-GTAACTCAGCAGCATCTCAGGG-3'	5'-FAM-GGAGTGGGTCCCATCAGTTT-MGB-3'
<b>BRAF V600K</b>	5'-AGGTGATTTTGGTCTAGCTAaAA-3'	5'-GTAACTCAGCAGCATCTCAGGG-3'	5'-FAM-GGAGTGGGTCCCATCAGTTT-MGB-3'
<b>BRAF total</b>	5'-ATAGGTGATTTTGGTCTAGCTACA-3'	5'-GTAACTCAGCAGCATCTCAGGG-3'	5'-FAM-GGAGTGGGTCCCATCAGTTT-MGB-3'

#### 4.4 End-point PCR and Sanger sequencing

Mutational status of the PTEN gene and TERT promoter were assessed by Sanger sequencing. For PTEN, PCR was performed for exons 5, 6, 7 and 8, because they are the most frequently mutated ones in melanoma<sup>79</sup>. To amplify genomic regions sized no more than 300 bp, exon 5 was amplified in 2 reactions and exon 8 in 3. We used 1X buffer, 0.2mM dNTPs, 1.5mM MgCl<sub>2</sub>, 5% DMSO, T4, 0.5μM of each M13-tailed primer, 5 U/μl of AmpliTaq Gold polymerase in a 30μl total volume. Cycling conditions were: 8 min at 95°C, 30 cycles of 95°C for 1 min, 55°C for 1 min, 72°C for 1 min, followed by 7 min at 72°C.

Mutational status of the TERT core promoter region from position -27 to -286 upstream of the ATG start site, including the rs2853669 polymorphic site, was amplified in a 50μl volume containing 100ng DNA, 5μl AmpliTaq Gold 360 10X Buffer, 1mM MgCl<sub>2</sub>, 10μl of GC Enhancer for each sample to amplify, 0.2mM dNTPs, 0.5μM of each M13-tailed primer, 5 U/μl of AmpliTaq Gold 360 Polimerase. AmpliTaq Gold 360 reagents were purchased from Applied Biosystems (Austin, TX, USA). Thermal Cycler conditions were as follows: 10 min at 95°C, 35 cycles at 95°C for 30 sec, 64°C for 40 sec, 72°C for 75 sec, followed by 7 min at 72°C.

All PCR reactions were carried out using the K562 cell line DNA as positive control and water as negative control. The amplified products were purified with Illustra GFX 96 PCR Purification Kit (GE Healthcare, Buckinghamshire, UK) to remove the excess of primers and unused nucleotides. The purified product (1μl) was subjected to 25 cycles of sequencing reaction with BigDye terminator v1.1 Cycle Sequencing Kit (Applied Biosystems, Austin, TX, USA), 0.16μM M13 universal primer (M13\_Fw: 5'TGTAAAACGACGGCCAGT3'; M13\_Rv: 5'CAGGAAACAGCTATG ACC3'), forward and reverse primers in separate reactions. The products were purified with BigDye XTerminator Purification Kit (ThermoFisher Scientific, Waltham, MA, USA), and analyzed on a 96-capillary sequencer (AB3730xl Genetic Analyzer). Primers sequences are provided in Table 3.



#### 4.5 Copy Number Variation (CNV) analysis

For CNV assessment, we used the OncoScan CNV Assay (Affymetrix, Santa Clara, CA, USA) on an Affymetrix SNP-array platform according to the manufacturer's protocol. This assay is based on a molecular inversion probe technology (MIP), specifically designed to handle limited amounts of highly degraded FFPE-extracted DNA and enabling the analysis of over 220,000 SNPs distributed across the genome. The MIP method is summarized in Fig. 9.

In OncoScan assay, 80ng of double-stranded DNA were hybridized overnight with the MIP probes—single stranded DNA probes with complementary regions to the 5' and 3' of the genomic target. After hybridization between the complementary regions to the target, the single nucleotide gap (typically a SNP) left between the ends was subsequently filled in, resulting in a circularized probe. Genomic DNA is a limiting factor in the reaction so that the number of circularized probes is proportional to the absolute amount of template DNA. Non-reactive probes and genomic DNA were removed by exonuclease treatment. The circularized MIP probes were linearized with a cleavage enzyme and a first PCR amplification was performed followed by a second amplification. The amplified products were digested with HaeIII enzyme and hybridized overnight on the OncoScan Array. The arrays were washed and stained in GeneChip Fluidics Station and scanned in GeneChip Scanner 7G. The raw probe signal intensities (CEL files) obtained were processed using the OncoScan Console software (Affymetrix, Santa Clara, CA, USA), which converts the probe intensities into  $\log_2$ ratio and B-allele frequencies, resulting in OSCHP files. To establish the expected normal copy number state for a given locus, a universal reference dataset was used, composed of about 400 normal FFPE samples from a wide range of tissues. The last step for the data analysis workflow is the copy number segmentation, which results in the copy number calls. For this, we used OncoScan Nexus Express software (Biodiscovery, El Segundo, CA, USA) and the TuScan segmentation algorithm.

As quality control parameters, we used *median absolute pairwise difference* (MAPD)  $\leq 0.3$ , *ndSNPQC*  $\geq 26$  and *ndWaviness SD*  $\leq 0.12$ . Copy number variants (CNVs) detected in each sample were compared to the Database of Genomic Variants (DGV) to exclude potential polymorphic CNVs (<http://dgv.tcag.ca/>).

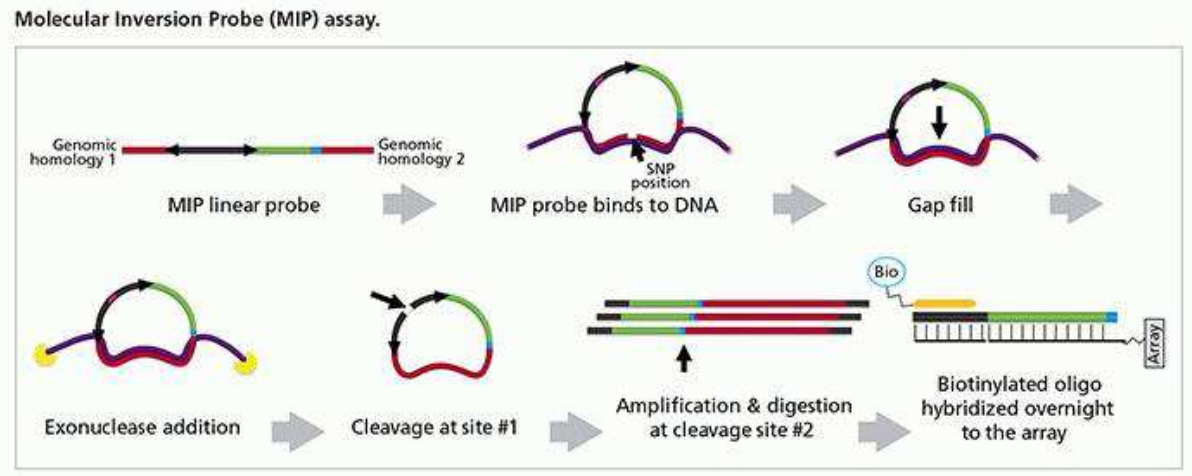


**Figure 9. Molecular Inversion Probe (MIP) assay.**

*From Thermofisher.com*

#### 4.6 Fluorescence *in situ* hybridization (FISH) analysis

A total of 18 FFPE samples (2 primary melanomas and 16 metastases) from 15 pts were analyzed by FISH using the Vysis BRAF SpectrumGold FISH probe kit, which covers a region encompassing the entire BRAF gene, and the Vysis CEP7 SpectrumGreen probe, which hybridizes to the alpha satellite DNA at the chromosome 7 centromere. To determine PTEN gene copy number, the Vysis PTEN/CEP 10 FISH probe kit was used, which contains a mixture of probes hybridizing to the 10q23 region of chromosome 10 and to the alpha satellite DNA at the chromosome 10 centromere (Abbott Molecular, Des Plaines, IL, USA).

Four  $\mu\text{m}$ -sections were pretreated with the Paraffin Pretreatment Kit I (Abbott Molecular, Des Plaines, IL, USA), denatured, and hybridized with 10 $\mu\text{l}$  of probe mixture. After washing, the slides were counterstained with 10 $\mu\text{l}$  of DAPI I (Abbott Molecular, Des Plaines, IL, USA) and analyzed at high-power (X100) magnification using a LEICA DM4000 B LED epifluorescence microscope (Leica Biosystems, Milton Keynes, UK). The Leica Application Suite software was used for image acquisition. For each sample, the number of copies of the gene and of the chromosome were estimated by calculating the mean number of signals for each probe in 100 nuclei.

FISH analysis was performed in collaboration with the Dr Cristina Montesco's group (Anatomy and Histology Unit, IOV - IRCCS, Padua).

#### **4.7 Statistical analysis**

Statistical analysis was performed in collaboration with Dr Paola Del Bianco (Clinical Trials and Biostatistics Unit, IOV – IRCCS Padua). Quantitative variables were summarized as median and range; categorical variables were reported as counts and percentages. PFS was calculated from the date of treatment initiation to progression. Patients who did not develop an event during the study period were censored at the date of last observation. PFS probability, computed using the Kaplan-Meier method, was compared among strata with the log-rank test. The median PFS time and 95% confidence interval (CI) were reported. Hazard ratios (HR) and 95% CI for each group were estimated using univariate Cox proportional hazards models with low risk as the reference class. The independent role of each covariate in predicting the PFS was verified in a multivariate model considering all characteristics significantly associated to the outcome in the univariate analysis. All tests were two-sided and a  $p$  value  $<0.05$  was considered statistically significant. Statistical analyses were performed using the SAS version 9.4 (SAS Institute, Cary, NC, USA).

## RESULTS - PROJECT 1

### 5.1 Summary of the work reported in the submitted manuscript *BRAF gene copy number and mutant allele frequency correlate with melanoma patients' response to MAPK inhibitors* by Stagni C. et al.

During the first part of the Ph.D. project, we characterized BRAF copy number and BRAFmut allele percentage at baseline in a cohort of 46 MAPKi-treated pts and we examined the correlation with PFS. The manuscript, which is currently under revision, is enclosed as Appendix 1.

We determined BRAF copy number by a multimodal approach, including qPCR, OncoScan assay and FISH, in 51 pre-treatment samples from 46 pts with BRAFmut metastatic melanoma who were treated with MAPKi. Overall, BRAF copy number gains were detected in 30 pts (65%), while 14 pts (30%) displayed a diploid BRAF status. Notably, the increased amount of BRAF gene copies was frequently supported by whole or partial chromosome 7 polysomy. BRAF gene amplification (i.e. >6 gene copies) was never detected in our cohort. Two samples were excluded from further analyses due to discordant results among the techniques.

We quantified the percentage of BRAFmut allele by allele-specific qPCR in 48 available samples from 44 pts. We observed a wide spectrum of BRAFmut allele % values (20-98%, median 54%) and set a range of 35-65% to define the balanced heterozygous BRAF status and distinguish it from cases with a low (<35%) or high (>65%) BRAFmut allele %. As a result, 64.5% of the analyzed samples (63.6% of pts) were classified as heterozygous, while 12.5% and 23% of them (13.6% and 22.7% of pts) showed a low (average 24.3%) and high (average 88.6%) BRAFmut allele %, respectively. Upon integration of BRAFmut allele frequency and BRAF gene copy number data, balanced heterozygosity remained the most represented category, both in BRAF diploid samples (79%) and in those with gains (60%).

We then investigated the relationship between BRAF copy number and BRAFmut allele % at baseline and patient response to MAPKi. Pts with BRAF gains showed a trend toward longer PFS (median 12.1 mo.; 95% CI 5.6–18.5) compared to those with diploid BRAF status (median 4.7 mo.; 95% CI 2.5–8.2) in univariate analysis ( $p$ -log rank = 0.056). A significantly longer PFS was also observed in pts with balanced heterozygous mutation status (median 12.0 mo.; 95% CI 5.6–15.8) and high BRAFmut allele % (median 7.5 mo.; 95% CI 2.1–21.7) compared to those with low BRAFmut allele % (median 3.0 mo.; 95% CI 1.4–5.5) ( $p$ -log rank <0.001). Consistently, pts with low BRAFmut allele % presented a seven- and

five-fold increased hazard ratio for disease progression when compared to the heterozygous and high BRAFmut allele % groups, respectively. In the multivariate model, adjusted for clinical characteristics, both BRAF copy number and BRAFmut allele frequency appeared to be independent predictors of disease progression. Patients with tumor characterized by diploid BRAF status had a significantly higher risk of progression than those with BRAF gains (HR=2.86; 95% CI 1.29–6.35;  $p = 0.01$ ). Patients with low BRAFmut allele % still showed a significantly higher risk of progression compared to those with balanced heterozygous BRAF status (HR=4.54, 95% CI 1.33–15.53;  $p = 0.016$ ).

Our data suggest that pts whose tumors display BRAF gains or balanced heterozygous BRAFmut allele frequency have an improved response, which is independent of type of therapy and tumor stage.

## 5.2 Analysis of the PTEN gene

The PI3K/Akt pathway is often activated to overcome the block caused by MAPKi. One of the major mechanisms of activation of the PI3K/Akt pathway is loss of the PTEN gene. To investigate the contribution of this mechanism to MAPKi resistance in our cohort, we assessed the PTEN gene mutational status and copy number on 29 samples, 4 primary tumors and 25 metastases, from 26 pts, who received monotherapy with Vemurafenib or Dabrafenib (19 pts, 73%) or combo therapy (7 pts, 27%).

Complete PTEN gene loss was detected in 42% pts (Fig. 10a) and was supported either by focal homozygous deletion of the PTEN locus (in 6 pts/8 samples) or by deletion of one allele, due to whole or partial chromosomal loss, and mutation of the other one (in 5 pts/6 samples). Partial loss of PTEN, due to chromosomal loss (in 7 pts) or loss-of-heterozygosity (LOH) and mutations (in 2 pts), was detected in 35% pts. Overall, we identified PTEN mutations that affected the catalytic and the C2 domains of the protein in 27% pts. The mutations were: F104\* (c.311\_325del), D252V (c.755A>T), K267fs\*9 (c.800delA), W274\* (c.822 G>A), R335\* (c.1003 C>T), K197Rfs\*2 (c.590delA) and I300fs\*7 (c.900delC) (Fig. 10b). We found no copy loss in 23% pts (6 pts/6 samples) who showed, instead, a copy number of 2 or 3. No significant differences were detected between primary tumors and metastases.

We then investigated the relationship between PTEN status at baseline and response to treatment evaluating the frequency of PTEN loss in pts grouped as no-, short- and long-response. We observed that complete loss of PTEN was present in 20% (n=1) of no-response pts, 50% (n=7) of short-response pts and 43% (n=3) of long-response pts (Fig. 10c). Partial

loss was found in 40% (n=2) of no-response, 36% (n=5) of short-response and 28.5% (n=2) of long-response pts, respectively. Forty % (n=2) of no-response pts, 14% (n=2) of short-response pts and 28.5% (n=2) of long-response pts did not present any PTEN gene copy loss. Our data do not show any relevant differences in PTEN copy number status between pts who responded differently or did not at all to MAPKi therapy. Because PTEN loss was present also in long-response pts, our findings suggest that PTEN loss does not correlate with resistance to MAPKi.

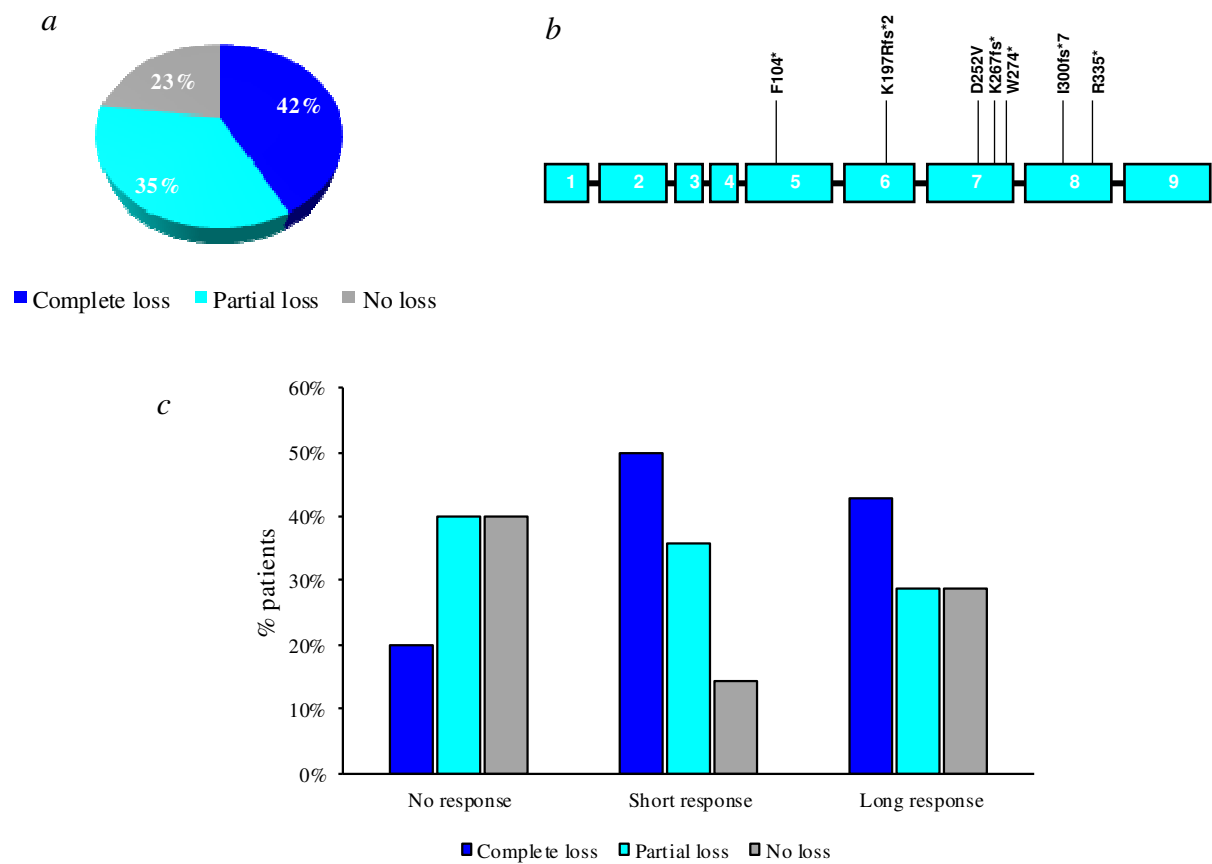


**Figure 10.** *PTEN* gene analysis. (a) Frequency of complete loss, partial loss and no loss of the *PTEN* gene in our cohort. (b) *PTEN* gene mutations identified in our cohort. (c) Histogram representation of *PTEN* status according to PFS groups.

### 5.3 Analysis of TERT promoter status

To investigate if there is an association between presence of TERT promoter mutations and treatment response, we sequenced a 260 bp-region of the TERT promoter in 61 samples (15 primary and 46 metastases) from 55 pts and correlated the results with PFS. Patients were treated with BRAFi monotherapy (32 pts, 58%) or with combo therapy (23 pts, 42%). Other clinical and molecular characteristics of the cohort are summarized in Table 1. For 4 pts, more than one lesion was analyzed and, in all cases, the mutation status matched between the paired samples. Overall, 43 pts (78%) had tumors with mutations in the TERT promoter (TERTmut). The two hot-spot mutations, -124C>T and -146C>T, were equally frequent (each present in 20 pts out of 55, 36%) while the -138-139CC>TT was present only in 3 pts (5%). The 3 mutations were mutually exclusive. In 3 cases, we found other co-occurrent mutations, such as -101C>T or -126C>T with -124C>T and -149C>T with -146C>T. Mutation frequency was not significantly different between primary (n=12, 19%) and metastatic (n=34, 55%) tumor samples. We also analyzed the SNP rs2853669 (at -245 bp in the TERT promoter), which reportedly counteracts the activating effect of the mutations, we analyzed this SNP in our cohort<sup>75</sup>. A total of 28 pts (51%) carried the polymorphism (SNPcarriers), 53% of TERTmut and 42% of TERTwt pts.

We then investigated by non-parametric Kaplan-Meier analysis, the relationship between TERT promoter gene status and patient response to MAPKi. Overall, data analysis showed that TERTmut and TERTwt pts had similar PFS, as did carriers and non-carriers of the SNP rs2853669. Upon stratification of the TERTmut cohort based on presence/absence of the polymorphism, we observed a trend toward better PFS for TERTmut/SNPcarrier pts (median PFS 11.5 mo., 95% CI 3.12–19.88) compared to TERTmut/SNPnon-carrier pts (median 7 mo., 95% CI 4.27–9.72,  $p=0.17$ ; Fig. 11a). Upon stratification based on mutation type, the presence of -146C>T mutation correlated with worse PFS (median PFS 5.45 mo., 95% CI 2.80–9.20) compared to the -124C>T (median PFS 15.2 mo., 95% CI 5.57–) and was associated with a three-fold increased risk of progression ( $p=0.003$ , Table 4). In the multivariate model, adjusted for clinical characteristics, pts with -146C>T mutation still showed a shorter PFS than those with the -124C>T mutation, but the difference was not statistically significant (HR=1.94, 95% CI 0.78–4.81,  $p=0.153$ ). When the SNP status was taken into account, the difference in HR between -124 C>T and -146 C>T mutations remained significant only in individuals who were non-carriers of the rs2853669 polymorphism ( $p=0.046$ , Table 5).

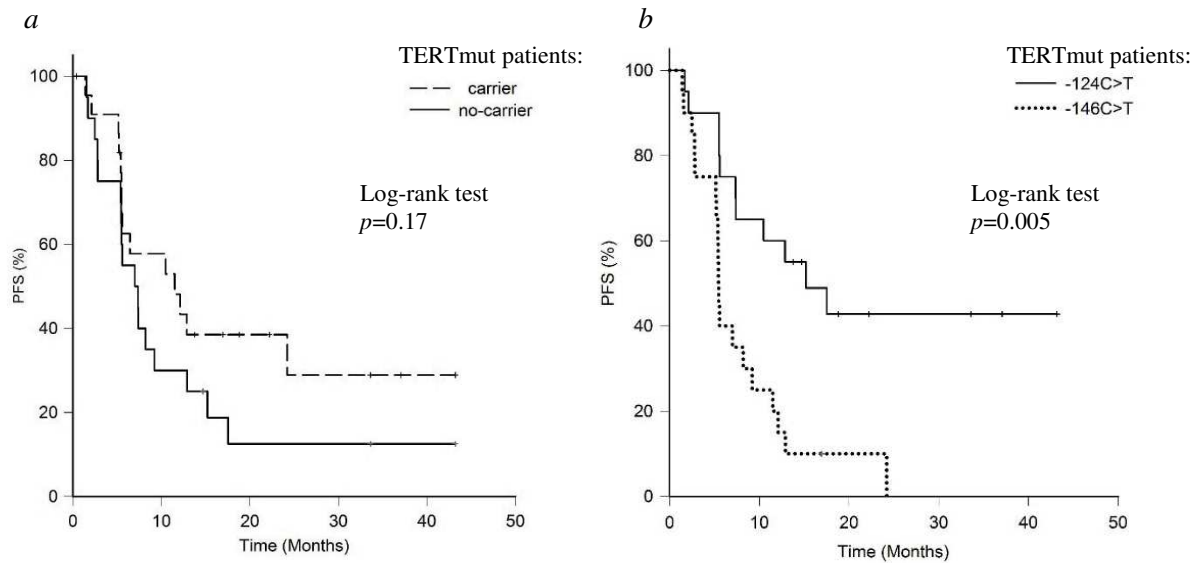


**Table 4. Univariate and multiple survival analysis.**

	Median PFS months (95% CI)	<i>p</i> - <i>logrank</i>	Univariate analysis			Multiple analysis 1		
			HR	95% CI	<i>P</i> - <i>value</i>	HR	95% CI	<i>p</i> - <i>value</i>
<b>Gender</b>								
M	5.40 (3.57–7.00)	0.0003	3.07	1.62–5.82	0.0006	2.10	0.94–4.66	0.0693
F	12.87 (7.37–)		1			1		
<b>Age (years)</b>			1.01	0.99–1.04	0.2283			
<b>ECOG PS</b>								
0	11.50 (6.43–15.67)	0.0269	1			1		
1-3	5.50 (2.77–6.50)		2.17	1.08–4.34	0.0292	2.03	0.91–4.51	0.0827
<b>Stage</b>								
III	–	0.0272	1			1		
IV	6.43 (5.43–8.20)		3.04	1.08–8.58	0.0358	3.24	1.10–9.57	0.0333
<b>Therapy</b>								
Combo	12.10 (7.33–)	0.0103	1			1		
Mono	5.57 (5.20–7.37)		2.33	1.20–4.55	0.0127	2.52	1.17–5.42	0.0184
<b>SNP</b>								
C/C	5.50 (2.10–)	0.9108	1					
C/T	6.50 (5.40–24.20)		0.78	0.26–2.37	0.6663			
T/T	7.67 (5.43–15.67)		0.81	0.28–2.38	0.7058			
<b>Mutation</b>								
-124C>T	15.20 (5.57–)	0.0221	1			1		
-138-139C>T	6.43 (–)		2.30	0.29–18.39	0.4325	1.64	0.19–14.12	0.6503
-146C>T	5.45 (2.80–9.20)		3.12	1.46–6.66	0.0033	1.94	0.78–4.81	0.1536
WT	7.08 (3.13–15.80)		1.71	0.70–4.14	0.2357	1.81	0.72–4.53	0.2044



**Table 5. Multiple survival analysis.**

		<b>Multiple analysis 2</b>		
		<b>HR</b>	<b>95% CI</b>	<b><i>p-value</i></b>
<b>Gender</b>	M	2.67	1.21;5.91	<i>0.0154</i>
	F	1		
<b>Stage</b>	III	1		
	IV	4.72	1.53;14.57	<i>0.0069</i>
<b>Therapy</b>	Combo	1		
	Mono	2.65	1.19;5.89	<i>0.0170</i>
<b>Mutation</b>	-124/SNP carrier	1	0.25;2.70	<i>0.7341</i>
	-146/SNP carrier	0.81		
	-124/SNP no-carrier	1	1.02;12.5	<i>0.0462</i>
	-146/SNP no-carrier	3.45		

## 5.4 Genome-wide CNV analysis

To identify new molecular features potentially correlated with response to therapy, we performed a genome-wide analysis to define the CNV profile of 51 pre-treatment samples from 44 pts (31 treated with BRAFi monotherapy and 13 with combo therapy). Five pts were still on therapy at the time of the study, one ceased the treatment due to other comorbidities.

First, we examined the overall copy number profile of the cohort. Consistent with the known high degree of genomic aberration in melanoma<sup>80, 81</sup>, we found that 15 samples had a diploid genome (26%), while 36 (71%) were aneuploid: specifically, 2 were triploid, 8 tetraploid while the overall ploidy could not be defined for the remaining 26, owing to the high frequency of aberrations. As shown in Fig. 12, the overall CNV profile of our samples comprised frequent (i.e. identified in >50% samples) copy gains, involving chromosomes 1q, 6p, 7, 8q, 12p, 20, Xp, and losses in chromosomes 9p and 10. Isochromosomes were also present and involved chromosomes 1, 6, 7, 8, 10, X.

For each specimen, we annotated the number and length of copy number aberrations, including gains (=3 copies), high copy gains ( $\geq 4$  copies), losses and homozygous copy losses, in order to evaluate the extent of genome instability (Table 6). We observed a significant heterogeneity in the amount of CNV within our cohort as some lesions displayed few alterations while others were characterized by a high degree of genomic damage (range 7-92.8% of genome affected by CNV). Gains were more frequently detected than losses, involving an average 21% vs. 12% of the genome, respectively. Alterations affected mainly the whole chromosome or one arm, while focal events (i.e. with a length <1Mb) were rare. Although the available number of primary tumors was limited, when we compared CNV profiles between primary and metastases, we did not find any significant difference.

To verify whether the amount of CNV correlates with response to therapy, we compared the CNV profiles of samples from the no-response (n=10), short-response (n=28) and long-response (n=13) groups of pts. The no-response group showed the highest amount of genome affected by CNV (median 51.8% vs. 37.45% in the short-response vs. 36.1 in the long-response group, Fig. 13a). The long-response group was characterized by more frequent high copy gains compared to the no-response one, which, instead, had more homozygous copy losses.

To identify new genes possibly involved in the response to MAPKi, we compared the CNV profiles of the two extreme groups of pts, i.e. no-response and long-response. The most striking differences were detected in chromosomes 1, 3, 11, 17, and 21. Specifically, losses of

chr1p31.1, chr3p24.1-p24.2, chr17p13.1 and LOH of chr3p14, chr3p21 and chr3p22, characterized the no-response group, while gains in chr11q21.1-q21.3, chr11q22.2 and in chr21q11.2 characterized the long-response group (Fig. 13b). Gene enrichment analysis identified numerous genes mapping in these regions, including some genes that were reported to be involved in cancer. For instance, chr3p24 was described as a cancer susceptibility locus in breast cancer, lung cancer and Hodgkin lymphoma, and the low expression and aberrant methylation of the RARB gene, which maps to this region, was reported in melanoma<sup>82-84</sup>. Furthermore, chr3p21.2 harbors multiple genes that exhibit various degrees of tumor suppression activity, including RASSF1, which is frequently hypermethylated in cancer and covers a central position in a tumor suppressor cluster regulating key biological processes, such as proliferation, cell cycle, signal transduction and apoptosis<sup>85</sup>. Moreover, TP53, a known tumor suppressor frequently aberrant at late stages of melanoma, maps to chr17p13.1.

In addition to the above-described analyses, the copy number of 51 preselected genes that play a role in melanomagenesis was evaluated for a potential association with response to treatment in our cohort (Fig. 14). Notably, the no-response group showed a higher number of deletions in these genes, while the long-response group had more gains. BRAF, MET and TRRAP were the genes with higher frequency of gains in both groups, while CDKN2A and PTEN were those most frequently lost. This analysis also confirmed the difference in TP53 copy number: 50% of no-response pts and none of the long-response pts had a loss.

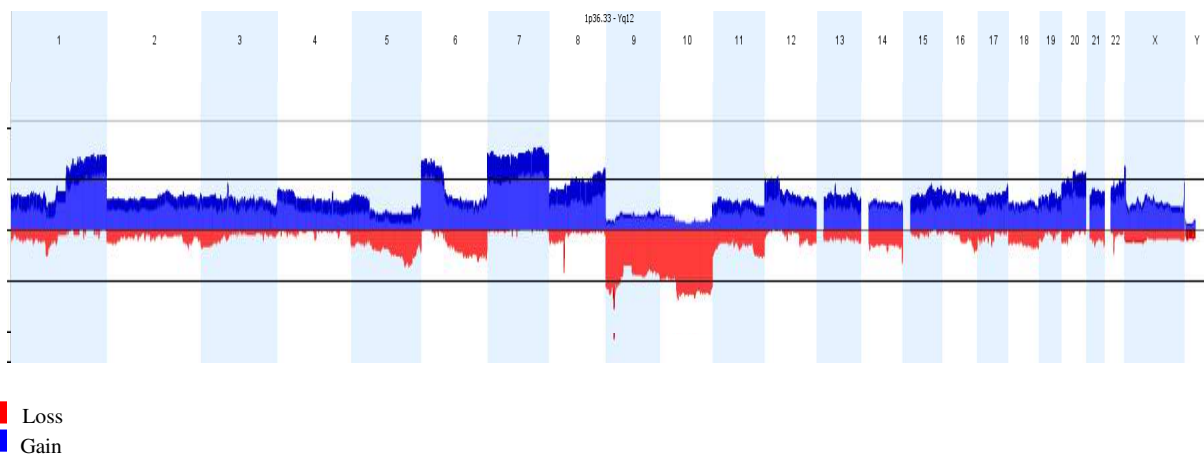


**Figure 12.** Overall CNV profile of our pre-treatment cohort. The y-axis indicates the percentage of the population in the selected samples having an aberration at a specific point along the genome. Amplifications are plotted in blue above the 0% baseline. Deletions are plotted in red below the 0% baseline. Dark blue and dark red in the plot indicate two or more copy gain and homozygous loss, respectively.

**Table 6. Copy number alterations detected in 51 cutaneous melanomas by OncoScan assay.**

<b>Number of events</b>			
	<b>Mean ± SD</b>	<b>Median</b>	<b>Range</b>
Total copy number events	124.16±74.14	115	20-304
Gains	63.82±49.21	49	5-225
High copy gains	29.25±49.8	3	0-180
Losses	29.45±21.78	26	0-86
Homozygous copy losses	1.63±1.66	1	0-8
<b>Relative length (as percentage of genome altered)</b>			
% genome changed	45.66±26.42	37.7	7-92.8
% gain	21.16±18.11	13.8	1.87-75.9
% high copy gain	11.91± 22.47	0.34	0-73.6
% loss	12.45 ±11.81	10.10	0-45.9
% homozygous copy loss	0.15±0.35	0.01	0-1.8
<b>Relative frequencies of copy number aberration type (%)</b>			
Gains	51 ±21	46	16-93
High copy gains	16±23	5	0-76
Losses	32±22	33	0-78
Homozygous copy losses	2±2	1	0-7

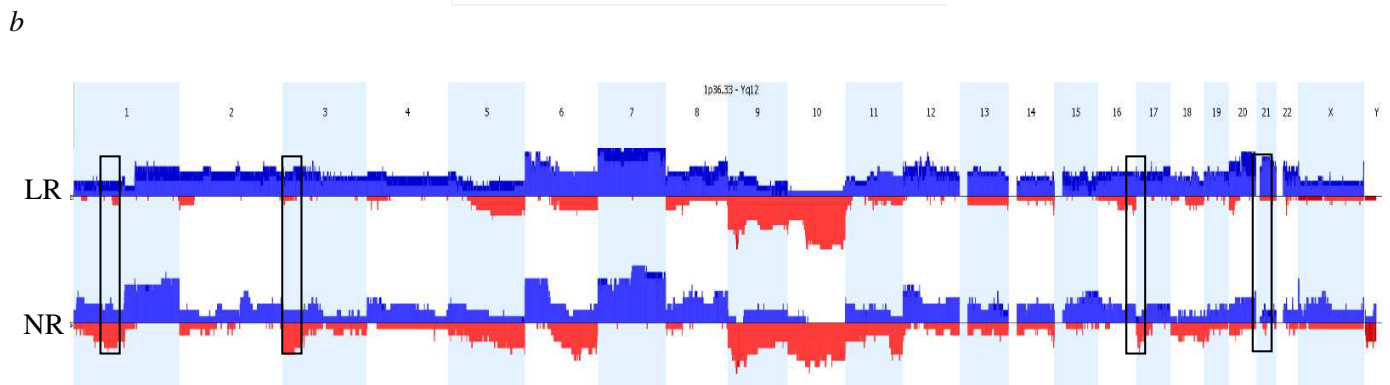
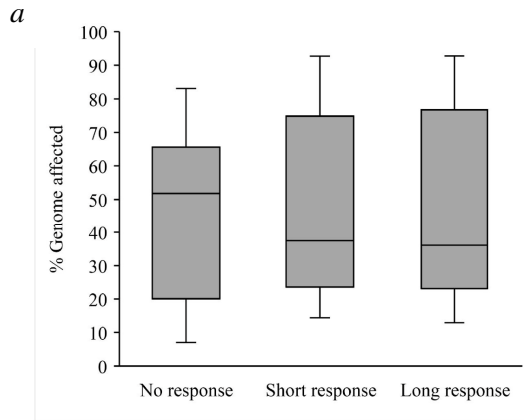


**Figure 13.** CNV profiles according to PFS. (a) Box-plot showing the % genome affected by copy number aberrations according to PFS. (b) CNV profiles of no-response (NR) and long-response (LR) groups. Regions with a significant difference are boxed.

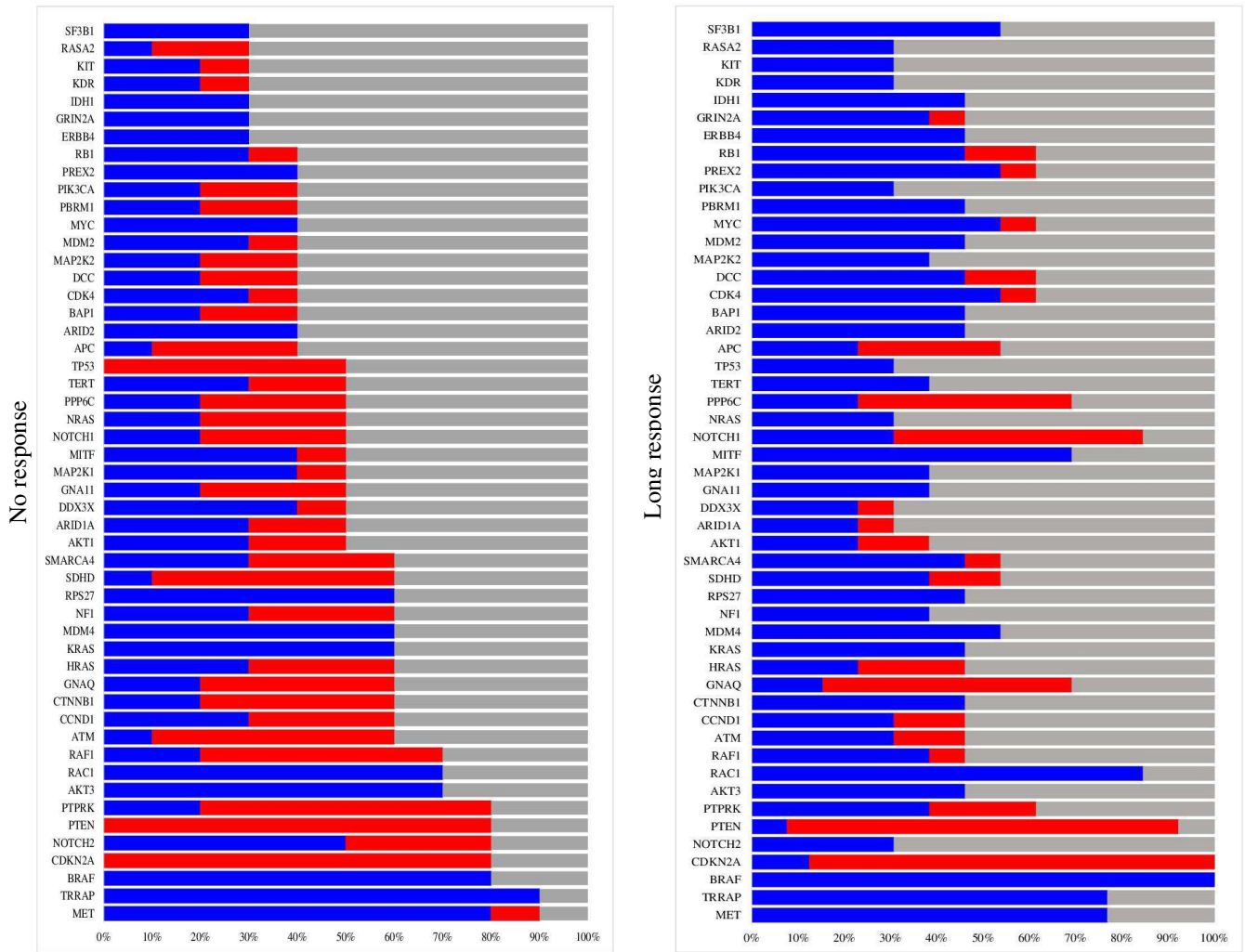


**Figure 14.** Bar charts showing the frequency of copy number aberrations in 51 genes involved in melanoma progression. (Left) no-response patients, (right) long-response patients.

## RESULTS - PROJECT 2

### 6.1 Genome-wide CNV analysis of acral lentiginous melanoma

To investigate the molecular mechanisms underlying ALM and differentiating it from NAM, we performed OncoScan analysis and made a preliminary comparison of the CNV profile of 17 ALM (13 primary and 4 metastases) with that of 20 NAM (5 primary and 15 metastases). The characteristics of the ALM cases analyzed are summarized in Table 7.

Among the 17 ALM, 10 samples presented a high level of genomic CNV, which did not allow definition of the ploidy, while one sample resulted tetraploid, another one triploid and 5 samples had overall diploidy. Among 20 NAM, for 7 cases the ploidy was non-assessable, 4 were tetraploid, one was triploid and 8 were diploid. The amount of genome affected by CNV was similar in the two groups (mean 44.2% in ALM, 44.52% in NAM). However, NAM were more frequently characterized by high copy gains, while ALM were more frequently characterized by losses and homozygous copy losses (Tables 8 and 9). When considering the number of events, ALM showed a mean of 136.47 total events, of which 66% were gains (65.3 + 24.9) and 34% were losses (43.9 + 2.3). NAM, instead, had a mean of 123.75 events, of which 83% were gains (65.4 + 37.4) and 17% were losses (19.6 + 1.5). Thus, in our cohort, therefore, we did not find a difference in the total percentage of genome altered or in the total number of copy number aberrations between ALM and NAM, but ALM CNV profiles resulted characterized by a higher degree of deletions, while NAM of copy gains.

Overall, in ALM the regions mostly affected (frequency >50%) by copy number gains were in chromosomes 1q, 5p, 6, 7p, 8q, 13q, 22q and Xp, while losses were frequent in chromosomes 9, 10p and 16q. In NAM, copy number gains were mainly present in chromosomes 1, 3p, 4, 6p, 7, 8, 12, 13q, 15q, 17q, 19q, 20, 21, 22q and X, while losses were frequent in 9p and 10q. Altogether, common altered regions in the two melanoma groups were gains in chromosomes 1q, 6p, 8q, 13q, 22q, Xp and losses in chromosomes 9p and 10q.

The major differences between ALM and NAM ( $p < 0.05$ ) involved chromosome 7q21.2-7q33 where NAM exhibited a higher frequency of gains (75-87% of samples affected) than ALM (23.5-29.4%), and chromosome 16q24.2-16q24.3 where copy number losses were present in 64.7% of ALM samples vs. only 10% of NAM samples (Fig. 15).

We observed also differences in the type of aberrations. Indeed, in ALM, clusters of breakpoints (i. e. consecutive genomic fragments of different copy number, Fig. 16.) were

frequent and mainly involved chromosome 5, 11 and 22. In addition, we observed that isochromosomes characterized the genome of ALM and affected especially chromosome 6.

Finally, since ALM are known to have high frequency of gene amplifications throughout the genome, even detectable at earliest stages of the disease, we investigated the presence of focal amplification (i.e.  $\geq 4$  copies, sized  $< 1\text{Mb}$ ) in genes known to be recurrently affected in cutaneous melanoma. We identified focal amplification of TERT in 3 cases (17%), of CCND1 in 2 cases (12%), of MDM2 and MITF in 1 case each (6%). In NAM, instead, we found only two focal amplifications, involving BRAF and MITF (1 case each, 0.5%). Focal homozygous copy losses of CDKN2A and PTEN genes were found in both ALM and NAM, but were more frequent in NAM (8 and 4 cases, 40% and 20%, respectively) than ALM (2 and 1 cases, 12% and 6%, respectively).

**Table 7. Patient and specimen characteristics from the ALM cohort**

			ALM
			<i>N</i> (%)
<b>Patients</b>			17(100)
<b>Gender</b>	Male		7 (41)
	Female		10 (59)
<b>Age (years)</b>	Median (range)		66.77 (37 – 88)
	Mean (SD)		65.24 (16.59)
<b>Specimens</b>			
			<i>N</i> (%)
<b>Tissue</b>	Primary		13 (76)
	Metastasis		4 (24)
<b>Breslow thickness (cm)</b>	Median (range)		3.52 (2.04 – 13.5)
	Mean (SD)		4.75 (3.09)
<b>Clark level</b>	3		1 (6)
	4		10 (59)
	5		5 (29)
	NA		1 (6)
<b>Ulceration</b>	YES		8 (47)
	NO		9 (53)
<b>Regression</b>	YES		1 (6)
	NO		16 (94)
<b>Vascular invasion</b>	YES		4 (24)
	NO		13 (76)

NA: not available



**Table 8. Copy number alterations detected in ALM by OncoScan assay**

<b>Number of events</b>			
	Mean ± SD	Median	Range
Total copy number events	136.5±75.3	120	28-304
Gains	65.3±42.5	56	19-170
High copy gains	24.9±37.2	11	0-140
Losses	43.9±25.1	48	4-86
Homozygous copy losses	2.3±2.3	2	0-9
<b>Relative length (as percentage of genome altered)</b>			
% genome changed	44.2±24	36.7	8.06-87
% gain	19.5±15.7	11.9	3.87-56.7
% high copy gain	6.4±14.4	0.7	0-56.7
% loss	18.1±13.2	12.5	0.1-41.1
% homozygous copy loss	0.2±0.3	0	0-1.07

**Table 9. Copy number alterations detected in NAM by OncoScan assay**

<b>Number of events</b>			
	Mean ± SD	Median	Range
Total copy number events	123.8±84.2	96	23-287
Gains	65.4±48.9	47.5	5-160
High copy gains	37.4±58.5	8	0-180
Losses	19.6±17.8	17	0-71
Homozygous copy losses	1.5±1.1	2	0-3
<b>Relative length (as percentage of genome altered)</b>			
% genome changed	44.5±30.2	29	7.02-92.8
% gain	21.5±20	14.5	2-73.3
% high copy gain	15.7±26.3	1.2	0-73.6
% loss	7.3±6	6.8	0-19.5
% homozygous copy loss	0.1±0.2	0	0-0.83

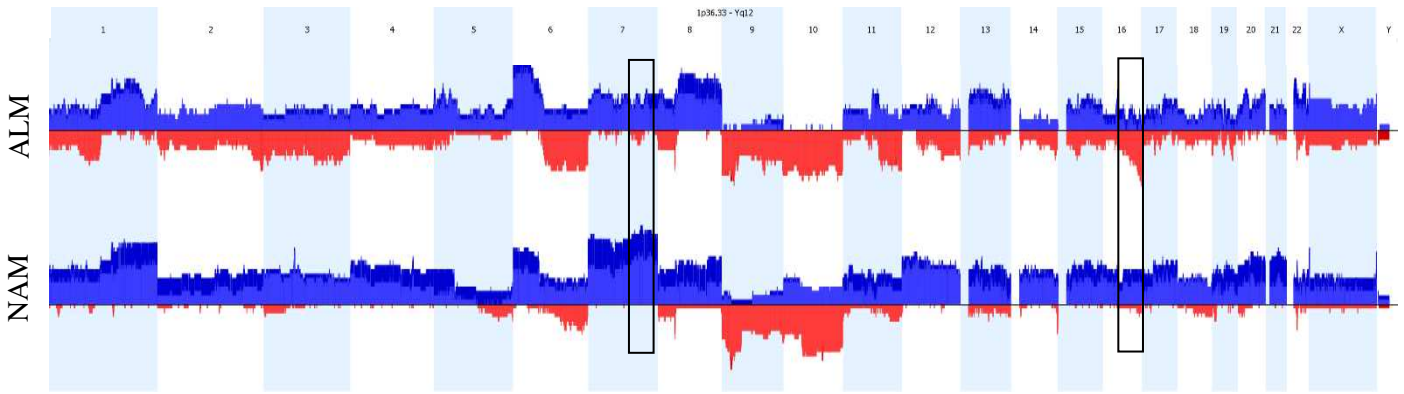


**Figure 15.** Comparison of CNV profiles between ALM and NAM.

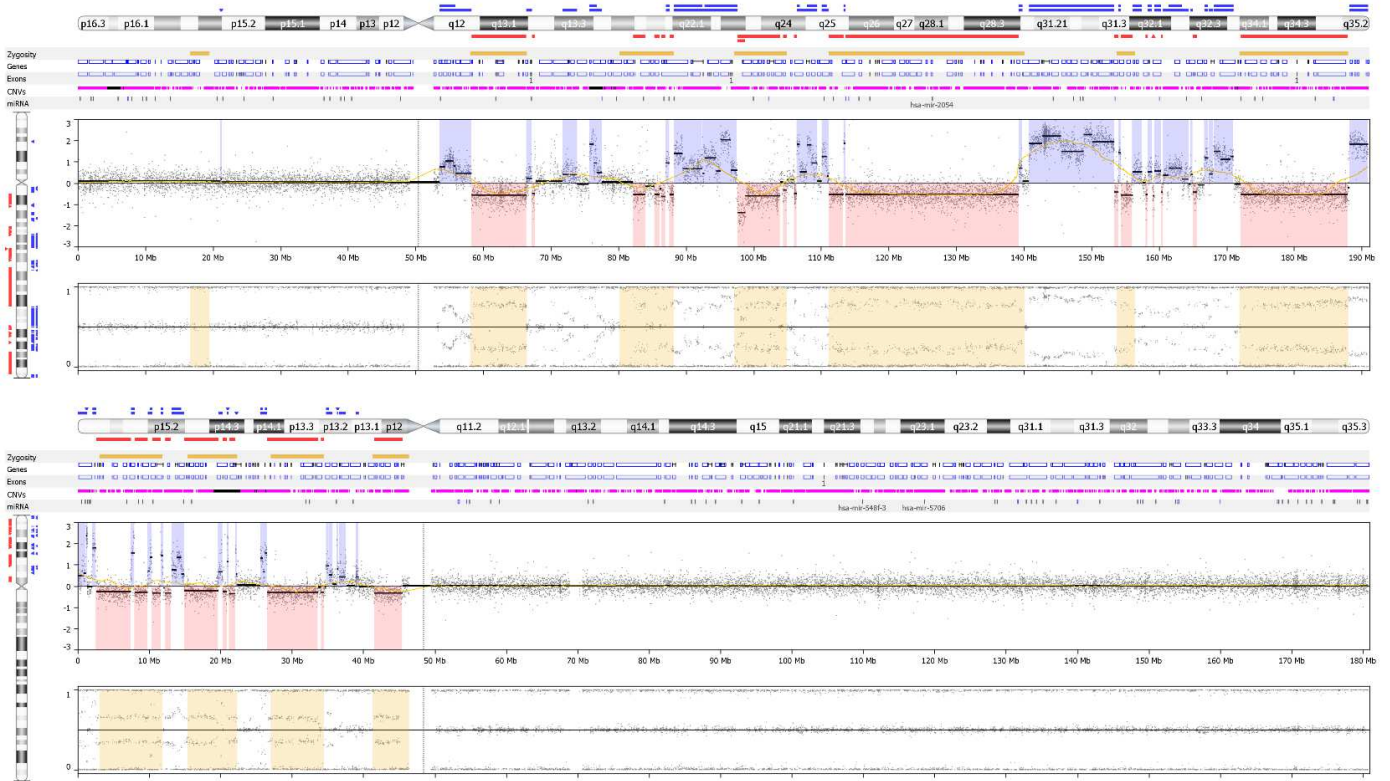


**Figure 16.** Examples of clusters of breakpoints in chromosome 4 (upper panel) and in chromosome 5 (lower panel).

## DISCUSSION

The onset of resistance represents a major hindrance to long-term effectiveness of MAPKi in metastatic melanoma pts and predictive biomarkers are urgently needed. For this purpose, we have quantitatively studied the BRAF gene - the direct target of the MAPKi-based therapy - and investigated the correlation between gene copy number or mutant allele frequency at baseline and PFS. Our findings show that pts with melanoma displaying gains of the BRAF gene or with BRAFmut allele percentage similar to or higher than that of the wt allele seem to benefit the most from MAPKi therapy. In this light, assessment of BRAF copy number and/or mutant allele load could be considered prior to treatment choice as a useful tool for patient selection to targeted therapy.

We also explored the still controversial relationship between aberrations of the PTEN tumor suppressor gene and patient response to MAPKi. Indeed, although *in vitro* studies reported decreased effectiveness of MAPKi in cells with PTEN loss<sup>66, 67</sup>, complete responses to MAPKi have been observed even in pts with deleted/mutated PTEN<sup>48,56</sup>. Our data confirm that PTEN loss is a frequent event in BRAFmut metastatic melanoma, but it does not correlate with resistance to MAPKi. Conceivably, even though PTEN loss concurs to create an adverse context to MAPKi, other clinical factors and/or resistance mechanisms are prevalent in influencing the response. For these reasons, PTEN loss cannot be used as a biomarker to predict patient responsiveness to therapy.

TERT promoter mutations are frequent somatic alterations in melanoma, which can be found at early stages of melanoma progression and often co-occur with BRAF mutations<sup>11,19,71</sup>. Consistently, in our BRAFmut cohort we found 73% TERT mutant pts. TERT promoter mutations were outlined as markers of aggressiveness and poor prognosis<sup>73,74</sup>. Herein, we describe their correlation with response to targeted therapies. Specifically, we identified a still unreported association between the -146C>T mutation and shorter PFS compared to the -124C>T. Although both the -124C>T and the -146C>T have been shown to increase transcription of the TERT gene (and hence telomerase activity) by creating new binding sites for ETS transcription factors, a stronger effect on TERT activation was reported for the -124C>T<sup>86</sup>. In addition, a peculiar pathway of activation by non-canonical NF-kB signaling was described for the -146C>T mutation<sup>87</sup>. Thus, it is possible that functional differences between -124C>T and -146C>T affect the response to MAPKi treatment. We also explored the polymorphism rs2853669 located at -245 bp within the TERT promoter, which was reported to disrupt an ETS transcription factor binding site<sup>75</sup>,

counteracting the effect of the mutations on TERT expression. The presence of the C variant allele of rs2853669 was shown to be protective because among TERT mutant pts, those who did not carry the SNP showed worse survival compared to SNP carriers. In agreement with these data and with our previous results, we observed that TERTmut/SNPnon-carriers exhibited shorter PFS than TERTmut/SNPcarriers, and this effect was especially pronounced in pts with the -146C>T mutation without SNP.

In this study, we used a high-density probe SNP array to analyze whole-genome alteration profiles in melanoma samples and to explore their correlation with clinical response. The CNV analysis might allow one to uncover new oncogenes and tumor suppressors. Overall, the copy number profiles of our cases concurred with those previously published for BRAF mutant cutaneous melanoma, with frequent copy number gains in chromosomes 1q, 6p, 7, 8q, 12p, 20, Xp, and frequent losses in chromosomes 9p and 10<sup>81</sup>. Although a high incidence of genomic damage was associated with melanoma aggressiveness and worse clinical outcome<sup>88,89</sup>, we found no correlation between the overall amount of CNV and PFS. To determine if specific copy number aberrations are associated with therapeutic response, we compared the genomic profile of the no-response and long-response groups of pts. We identified different patterns of aberrations in chromosomes 1, 3, 11, 17 and 21. Specifically, no-response pts were characterized by loss of known regions associated with cancer susceptibility or harboring tumor suppressors (chr3p21, chr3p24, chr17p13)<sup>83</sup>. Thus, loss of specific regions, rather than the overall CNV, seem to correlate with poor response to MAPKi.

The second part of the study focused on the molecular characterization of acral lentiginous melanoma, a subtype of cutaneous melanoma with epidemiological and morphological features that set it aside from other subtypes. The genetic landscape of acral melanoma is still poorly characterized, as opposed to that of cutaneous non-acral melanoma. With the intent to shed light on it, we performed CNV analysis of a cohort of acral melanomas and compared their profile with that of cutaneous non-acral melanomas. Although further validation is needed, our preliminary data showed no difference in the total amount of CNV between ALM and NAM. Instead, the genomic profile of ALM was specifically characterized by a high frequency of deletions throughout the whole genome and that of NAM by numerous high copy gains. The major differences involved chromosome 7, where NAM presented more gains, and chromosome 16, where ALM had more losses. Moreover, ALM showed several amplifications in small genomic regions, which were rare in NAM.

Among the amplified genes, TERT and CCND1 were the most frequently affected, supporting a likely pivotal role in ALM oncogenesis.

In conclusion, we provided a characterization of different molecular aspects related to patient response to MAPKi. Our data on BRAF copy number and mutant allele frequency are intriguing and promote further analyses in larger cohorts. We highlighted a key role of TERT in the response to MAPKi and a possible functional difference between the two most frequent mutations in the promoter region, -124C>T and -146C>T. Future investigations on each single mutation will clarify the link between MAPK pathway and TERT activation. CNV analysis provided a genome-wide characterization of cutaneous melanoma and allowed us to pinpoint regions with potential involvement in response to therapy. Integration of additional layers of information will help us to confirm these results. Finally, we have outlined some genomic features of acral melanoma, which could ease comprehension of its oncogenesis and guide the design of therapeutic strategies. We plan to expand the cohort and perform a detailed comparison, not only by CNV profiling but also by whole-genome mutational analysis, of acral vs. non-acral melanomas to highlight the main features of each melanoma subtype.

*I hope that my work has contributed and will contribute  
to further our knowledge of melanoma.*

## REFERENCES

1. Ali Z, Yousaf N, Larkin J. Melanoma epidemiology, biology and prognosis. *EJC Suppl* 2013;**11**:81-91.
2. Kibbi N, Kluger H, Choi JN. Melanoma: Clinical Presentations. *Cancer Treat Res* 2016;**167**:107-29.
3. Greenwald HS, Friedman EB, Osman I. Superficial spreading and nodular melanoma are distinct biological entities: a challenge to the linear progression model. *Melanoma Res* 2012;**22**:1-8.
4. Durbec F, Martin L, Derancourt C, Grange F. Melanoma of the hand and foot: epidemiological, prognostic and genetic features. A systematic review. *Br J Dermatol* 2012;**166**:727-39.
5. Goydos JS, Shoen SL. Acral Lentiginous Melanoma. *Cancer Treat Res* 2016;**167**:321-9.
6. Gershenwald JE, Scolyer RA, Hess KR, Sondak VK, Long GV, Ross MI, Lazar AJ, Faries MB, Kirkwood JM, McArthur GA, Haydu LE, Eggermont AMM, *et al.* Melanoma staging: Evidence-based changes in the American Joint Committee on Cancer eighth edition cancer staging manual. *CA Cancer J Clin* 2017;.
7. MacKie RM, Hauschild A, Eggermont AM. Epidemiology of invasive cutaneous melanoma. *Ann Oncol* 2009;**20 Suppl 6**:vi1-7.
8. Rastrelli M, Tropea S, Rossi CR, Alaibac M. Melanoma: epidemiology, risk factors, pathogenesis, diagnosis and classification. *In Vivo* 2014;**28**:1005-11.
9. Berwick M, Buller DB, Cust A, Gallagher R, Lee TK, Meyskens F, Pandey S, Thomas NE, Veierod MB, Ward S. Melanoma Epidemiology and Prevention. *Cancer Treat Res* 2016;**167**:17-49.
10. Vogelstein B, Papadopoulos N, Velculescu VE, Zhou S, Diaz LA, Jr, Kinzler KW. Cancer genome landscapes. *Science* 2013;**339**:1546-58.
11. Hayward NK, Wilmott JS, Waddell N, Johansson PA, Field MA, Nones K, Patch AM, Kakavand H, Alexandrov LB, Burke H, Jakrot V, Kazakoff S, *et al.* Whole-genome landscapes of major melanoma subtypes. *Nature* 2017;**545**:175-80.
12. Lito P, Rosen N, Solit DB. Tumor adaptation and resistance to RAF inhibitors. *Nat Med* 2013;**19**:1401-9.
13. Fecher LA, Amaravadi RK, Flaherty KT. The MAPK pathway in melanoma. *Curr Opin Oncol* 2008;**20**:183-9.
14. Cancer Genome Atlas Network. Genomic Classification of Cutaneous Melanoma. *Cell* 2015;**161**:1681-96.

15. Davies H, Bignell GR, Cox C, Stephens P, Edkins S, Clegg S, Teague J, Woffendin H, Garnett MJ, Bottomley W, Davis N, Dicks E, *et al.* Mutations of the BRAF gene in human cancer. *Nature* 2002;**417**:949-54.
16. Heinzerling L, Kuhnappel S, Meckbach D, Baiter M, Kaempgen E, Keikavoussi P, Schuler G, Agaimy A, Bauer J, Hartmann A, Kiesewetter F, Schneider-Stock R. Rare BRAF mutations in melanoma patients: implications for molecular testing in clinical practice. *Br J Cancer* 2013;**108**:2164-71.
17. Lovly CM, Dahlman KB, Fohn LE, Su Z, Dias-Santagata D, Hicks DJ, Hucks D, Berry E, Terry C, Duke M, Su Y, Sobolik-Delmaire T, *et al.* Routine multiplex mutational profiling of melanomas enables enrollment in genotype-driven therapeutic trials. *PLoS One* 2012;**7**:e35309.
18. Ascierto PA, Kirkwood JM, Grob JJ, Simeone E, Grimaldi AM, Maio M, Palmieri G, Testori A, Marincola FM, Mozzillo N. The role of BRAF V600 mutation in melanoma. *J Transl Med* 2012;**10**:85,5876-10-85.
19. Shain AH, Yeh I, Kovalyshyn I, Sriharan A, Talevich E, Gagnon A, Dummer R, North J, Pincus L, Ruben B, Rickaby W, D'Arrigo C, *et al.* The Genetic Evolution of Melanoma from Precursor Lesions. *N Engl J Med* 2015;**373**:1926-36.
20. Johnson DB, Puzanov I. Treatment of NRAS-mutant melanoma. *Curr Treat Options Oncol* 2015;**16**:15,015-0330-z.
21. Krauthammer M, Kong Y, Bacchiocchi A, Evans P, Pornputtpong N, Wu C, McCusker JP, Ma S, Cheng E, Straub R, Serin M, Bosenberg M, *et al.* Exome sequencing identifies recurrent mutations in NF1 and RASopathy genes in sun-exposed melanomas. *Nat Genet* 2015;**47**:996-1002.
22. Nissan MH, Pratilas CA, Jones AM, Ramirez R, Won H, Liu C, Tiwari S, Kong L, Hanrahan AJ, Yao Z, Merghoub T, Ribas A, *et al.* Loss of NF1 in cutaneous melanoma is associated with RAS activation and MEK dependence. *Cancer Res* 2014;**74**:2340-50.
23. Kwong LN, Davies MA. Navigating the therapeutic complexity of PI3K pathway inhibition in melanoma. *Clin Cancer Res* 2013;**19**:5310-9.
24. Beadling C, Jacobson-Dunlop E, Hodi FS, Le C, Warrick A, Patterson J, Town A, Harlow A, Cruz F, 3rd, Azar S, Rubin BP, Muller S, *et al.* KIT gene mutations and copy number in melanoma subtypes. *Clin Cancer Res* 2008;**14**:6821-8.
25. Curtin JA, Busam K, Pinkel D, Bastian BC. Somatic activation of KIT in distinct subtypes of melanoma. *J Clin Oncol* 2006;**24**:4340-6.
26. Shoushtari AN, Carvajal RD. GNAQ and GNA11 mutations in uveal melanoma. *Melanoma Res* 2014;**24**:525-34.
27. Shain AH, Bastian BC. From melanocytes to melanomas. *Nat Rev Cancer* 2016;**16**:345-58.

28. Chapman PB, Einhorn LH, Meyers ML, Saxman S, Destro AN, Panageas KS, Begg CB, Agarwala SS, Schuchter LM, Ernstoff MS, Houghton AN, Kirkwood JM. Phase III multicenter randomized trial of the Dartmouth regimen versus dacarbazine in patients with metastatic melanoma. *J Clin Oncol* 1999;**17**:2745-51.
29. Middleton MR, Grob JJ, Aaronson N, Fierlbeck G, Tilgen W, Seiter S, Gore M, Aamdal S, Cebon J, Coates A, Dreno B, Henz M, *et al.* Randomized phase III study of temozolomide versus dacarbazine in the treatment of patients with advanced metastatic malignant melanoma. *J Clin Oncol* 2000;**18**:158-66.
30. Luke JJ, Flaherty KT, Ribas A, Long GV. Targeted agents and immunotherapies: optimizing outcomes in melanoma. *Nat Rev Clin Oncol* 2017;**14**:463-82.
31. Joseph EW, Pratilas CA, Poulikakos PI, Tadi M, Wang W, Taylor BS, Halilovic E, Persaud Y, Xing F, Viale A, Tsai J, Chapman PB, *et al.* The RAF inhibitor PLX4032 inhibits ERK signaling and tumor cell proliferation in a V600E BRAF-selective manner. *Proc Natl Acad Sci U S A* 2010;**107**:14903-8.
32. McArthur GA, Chapman PB, Robert C, Larkin J, Haanen JB, Dummer R, Ribas A, Hogg D, Hamid O, Ascierto PA, Garbe C, Testori A, *et al.* Safety and efficacy of vemurafenib in BRAF(V600E) and BRAF(V600K) mutation-positive melanoma (BRIM-3): extended follow-up of a phase 3, randomised, open-label study. *Lancet Oncol* 2014;**15**:323-32.
33. Hauschild A, Grob JJ, Demidov LV, Jouary T, Gutzmer R, Millward M, Rutkowski P, Blank CU, Miller WH, Jr, Kaempgen E, Martin-Algarra S, Karaszewska B, *et al.* Dabrafenib in BRAF-mutated metastatic melanoma: a multicentre, open-label, phase 3 randomised controlled trial. *Lancet* 2012;**380**:358-65.
34. Long GV, Stroyakovskiy D, Gogas H, Levchenko E, de Braud F, Larkin J, Garbe C, Jouary T, Hauschild A, Grob JJ, Chiarion-Sileni V, Lebbe C, *et al.* Dabrafenib and trametinib versus dabrafenib and placebo for Val600 BRAF-mutant melanoma: a multicentre, double-blind, phase 3 randomised controlled trial. *Lancet* 2015;**386**:444-51.
35. Luke JJ, Flaherty KT, Ribas A, Long GV. Targeted agents and immunotherapies: optimizing outcomes in melanoma. *Nat Rev Clin Oncol* 2017;**14**:463-82.
36. Weber J, Mandala M, Del Vecchio M, Gogas HJ, Arance AM, Cowey CL, Dalle S, Schenker M, Chiarion-Sileni V, Marquez-Rodas I, Grob JJ, Butler MO, *et al.* Adjuvant Nivolumab versus Ipilimumab in Resected Stage III or IV Melanoma. *N Engl J Med* 2017;.
37. Long GV, Hauschild A, Santinami M, Atkinson V, Mandala M, Chiarion-Sileni V, Larkin J, Nyakas M, Dutriaux C, Haydon A, Robert C, Mortier L, *et al.* Adjuvant Dabrafenib plus Trametinib in Stage III BRAF-Mutated Melanoma. *N Engl J Med* 2017;.
38. Rizos H, Menzies AM, Pupo GM, Carlino MS, Fung C, Hyman J, Haydu LE, Mijatov B, Becker TM, Boyd SC, Howle J, Saw R, *et al.* BRAF inhibitor resistance mechanisms in metastatic melanoma: spectrum and clinical impact. *Clin Cancer Res* 2014;**20**:1965-77.



39. Girotti MR, Pedersen M, Sanchez-Laorden B, Viros A, Turajlic S, Niculescu-Duvaz D, Zambon A, Sinclair J, Hayes A, Gore M, Lorigan P, Springer C, *et al.* Inhibiting EGF receptor or SRC family kinase signaling overcomes BRAF inhibitor resistance in melanoma. *Cancer Discov* 2013;**3**:158-67.
40. Abel EV, Basile KJ, Kugel CH, 3rd, Witkiewicz AK, Le K, Amaravadi RK, Karakousis GC, Xu X, Xu W, Schuchter LM, Lee JB, Ertel A, *et al.* Melanoma adapts to RAF/MEK inhibitors through FOXD3-mediated upregulation of ERBB3. *J Clin Invest* 2013;**123**:2155-68.
41. Poulikakos PI, Persaud Y, Janakiraman M, Kong X, Ng C, Moriceau G, Shi H, Atefi M, Titz B, Gabay MT, Salton M, Dahlman KB, *et al.* RAF inhibitor resistance is mediated by dimerization of aberrantly spliced BRAF(V600E). *Nature* 2011;**480**:387-90.
42. Shi H, Hugo W, Kong X, Hong A, Koya RC, Moriceau G, Chodon T, Guo R, Johnson DB, Dahlman KB, Kelley MC, Kefford RF, *et al.* Acquired resistance and clonal evolution in melanoma during BRAF inhibitor therapy. *Cancer Discov* 2014;**4**:80-93.
43. Shi H, Moriceau G, Kong X, Lee MK, Lee H, Koya RC, Ng C, Chodon T, Scolyer RA, Dahlman KB, Sosman JA, Kefford RF, *et al.* Melanoma whole-exome sequencing identifies (V600E)B-RAF amplification-mediated acquired B-RAF inhibitor resistance. *Nat Commun* 2012;**3**:724.
44. Nazarian R, Shi H, Wang Q, Kong X, Koya RC, Lee H, Chen Z, Lee MK, Attar N, Sazegar H, Chodon T, Nelson SF, *et al.* Melanomas acquire resistance to B-RAF(V600E) inhibition by RTK or N-RAS upregulation. *Nature* 2010;**468**:973-7.
45. Whittaker SR, Theurillat JP, Van Allen E, Wagle N, Hsiao J, Cowley GS, Schadendorf D, Root DE, Garraway LA. A genome-scale RNA interference screen implicates NF1 loss in resistance to RAF inhibition. *Cancer Discov* 2013;**3**:350-62.
46. Wagle N, Van Allen EM, Treacy DJ, Frederick DT, Cooper ZA, Taylor-Weiner A, Rosenberg M, Goetz EM, Sullivan RJ, Farlow DN, Friedrich DC, Anderka K, *et al.* MAP kinase pathway alterations in BRAF-mutant melanoma patients with acquired resistance to combined RAF/MEK inhibition. *Cancer Discov* 2014;**4**:61-8.
47. Van Allen EM, Wagle N, Sucker A, Treacy DJ, Johannessen CM, Goetz EM, Place CS, Taylor-Weiner A, Whittaker S, Kryukov GV, Hodis E, Rosenberg M, *et al.* The genetic landscape of clinical resistance to RAF inhibition in metastatic melanoma. *Cancer Discov* 2014;**4**:94-109.
48. Trunzer K, Pavlick AC, Schuchter L, Gonzalez R, McArthur GA, Hutson TE, Moschos SJ, Flaherty KT, Kim KB, Weber JS, Hersey P, Long GV, *et al.* Pharmacodynamic effects and mechanisms of resistance to vemurafenib in patients with metastatic melanoma. *J Clin Oncol* 2013;**31**:1767-74.
49. Emery CM, Vijayendran KG, Zipser MC, Sawyer AM, Niu L, Kim JJ, Hatton C, Chopra R, Oberholzer PA, Karpova MB, MacConaill LE, Zhang J, *et al.* MEK1 mutations confer resistance to MEK and B-RAF inhibition. *Proc Natl Acad Sci U S A* 2009;**106**:20411-6.

50. Johannessen CM, Boehm JS, Kim SY, Thomas SR, Wardwell L, Johnson LA, Emery CM, Stransky N, Cogdill AP, Barretina J, Caponigro G, Hieronymus H, *et al.* COT drives resistance to RAF inhibition through MAP kinase pathway reactivation. *Nature* 2010;**468**:968-72.
51. Watson IR, Li L, Cabeceiras PK, Mahdavi M, Gutschner T, Genovese G, Wang G, Fang Z, Tepper JM, Stenke-Hale K, Tsai KY, Davies MA, *et al.* The RAC1 P29S hotspot mutation in melanoma confers resistance to pharmacological inhibition of RAF. *Cancer Res* 2014;**74**:4845-52.
52. Smalley KS, Lioni M, Dalla Palma M, Xiao M, Desai B, Egyhazi S, Hansson J, Wu H, King AJ, Van Belle P, Elder DE, Flaherty KT, *et al.* Increased cyclin D1 expression can mediate BRAF inhibitor resistance in BRAF V600E-mutated melanomas. *Mol Cancer Ther* 2008;**7**:2876-83.
53. Moriceau G, Hugo W, Hong A, Shi H, Kong X, Yu CC, Koya RC, Samatar AA, Khanlou N, Braun J, Ruchalski K, Seifert H, *et al.* Tunable-combinatorial mechanisms of acquired resistance limit the efficacy of BRAF/MEK cotargeting but result in melanoma drug addiction. *Cancer Cell* 2015;**27**:240-56.
54. Johnson DB, Menzies AM, Zimmer L, Eroglu Z, Ye F, Zhao S, Rizos H, Sucker A, Scolyer RA, Gutzmer R, Gogas H, Kefford RF, *et al.* Acquired BRAF inhibitor resistance: A multicenter meta-analysis of the spectrum and frequencies, clinical behaviour, and phenotypic associations of resistance mechanisms. *Eur J Cancer* 2015;**51**:2792-9.
55. Shi H, Moriceau G, Kong X, Lee MK, Lee H, Koya RC, Ng C, Chodon T, Scolyer RA, Dahlman KB, Sosman JA, Kefford RF, *et al.* Melanoma whole-exome sequencing identifies (V600E)B-RAF amplification-mediated acquired B-RAF inhibitor resistance. *Nat Commun* 2012;**3**:724.
56. Nathanson KL, Martin AM, Wubbenhorst B, Greshock J, Letrero R, D'Andrea K, O'Day S, Infante JR, Falchook GS, Arkenau HT, Millward M, Brown MP, *et al.* Tumor genetic analyses of patients with metastatic melanoma treated with the BRAF inhibitor dabrafenib (GSK2118436). *Clin Cancer Res* 2013;**19**:4868-78.
57. Villanueva J, Infante JR, Krepler C, Reyes-Uribe P, Samanta M, Chen HY, Li B, Swoboda RK, Wilson M, Vultur A, Fukunaba-Kalabis M, Wubbenhorst B, *et al.* Concurrent MEK2 mutation and BRAF amplification confer resistance to BRAF and MEK inhibitors in melanoma. *Cell Rep* 2013;**4**:1090-9.
58. Mesbah Ardakani N, Leslie C, Grieu-Iacopetta F, Lam WS, Budgeon C, Millward M, Amanuel B. Clinical and therapeutic implications of BRAF mutation heterogeneity in metastatic melanoma. *Pigment Cell Melanoma Res* 2017;**30**:233-42.
59. Yu CC, Qiu W, Juang CS, Mansukhani MM, Halmos B, Su GH. Mutant allele specific imbalance in oncogenes with copy number alterations: Occurrence, mechanisms, and potential clinical implications. *Cancer Lett* 2017;**384**:86-93.

60. Soh J, Okumura N, Lockwood WW, Yamamoto H, Shigematsu H, Zhang W, Chari R, Shames DS, Tang X, MacAulay C, Varella-Garcia M, Voorder T, *et al.* Oncogene mutations, copy number gains and mutant allele specific imbalance (MASI) frequently occur together in tumor cells. *PLoS One* 2009;**4**:e7464.
61. Helias-Rodzewicz Z, Funck-Brentano E, Baudoux L, Jung CK, Zimmermann U, Marin C, Clerici T, Le Gall C, Peschaud F, Taly V, Saiag P, Emile JF. Variations of BRAF mutant allele percentage in melanomas. *BMC Cancer* 2015;**15**:497,015-1515-3.
62. Lebbe C, How-Kit A, Battistella M, Sadoux A, Podgorniak MP, Sidina I, Pages C, Roux J, Porcher R, Tost J, Mourah S. BRAF(V600) mutation levels predict response to vemurafenib in metastatic melanoma. *Melanoma Res* 2014;**24**:415-8.
63. Satzger I, Marks L, Kerick M, Klages S, Berking C, Herbst R, Volker B, Schacht V, Timmermann B, Gutzmer R. Allele frequencies of BRAFV600 mutations in primary melanomas and matched metastases and their relevance for BRAF inhibitor therapy in metastatic melanoma. *Oncotarget* 2015;**6**:37895-905.
64. Boespflug A, Funck-Brentano E, Helias-Rodzewicz Z, Maucort-Boulch D, Beauchet A, Bringuier PP, Dumontet C, Emile JF, Saiag P, Dalle S. Reply to "Clinical and therapeutic implications of BRAF mutation heterogeneity in metastatic melanoma" by Mesbah Ardakani *et al.* *Pigment Cell Melanoma Res* 2017;**30**:498-500.
65. Shi H, Hong A, Kong X, Koya RC, Song C, Moriceau G, Hugo W, Yu CC, Ng C, Chodon T, Scolyer RA, Kefford RF, *et al.* A novel AKT1 mutant amplifies an adaptive melanoma response to BRAF inhibition. *Cancer Discov* 2014;**4**:69-79.
66. Paraiso KH, Xiang Y, Rebecca VW, Abel EV, Chen YA, Munko AC, Wood E, Fedorenko IV, Sondak VK, Anderson AR, Ribas A, Palma MD, *et al.* PTEN loss confers BRAF inhibitor resistance to melanoma cells through the suppression of BIM expression. *Cancer Res* 2011;**71**:2750-60.
67. Xing F, Persaud Y, Pratilas CA, Taylor BS, Janakiraman M, She QB, Gallardo H, Liu C, Merghoub T, Hefter B, Dolgalev I, Viale A, *et al.* Concurrent loss of the PTEN and RB1 tumor suppressors attenuates RAF dependence in melanomas harboring (V600E)BRAF. *Oncogene* 2012;**31**:446-57.
68. Blackburn EH, Epel ES, Lin J. Human telomere biology: A contributory and interactive factor in aging, disease risks, and protection. *Science* 2015;**350**:1193-8.
69. de Lange T. How telomeres solve the end-protection problem. *Science* 2009;**326**:948-52.
70. Xu L, Li S, Stohr BA. The role of telomere biology in cancer. *Annu Rev Pathol* 2013;**8**:49-78.
71. Heidenreich B, Nagore E, Rachakonda PS, Garcia-Casado Z, Requena C, Traves V, Becker J, Soufir N, Hemminki K, Kumar R. Telomerase reverse transcriptase promoter mutations in primary cutaneous melanoma. *Nat Commun* 2014;**5**:3401.

72. Horn S, Figl A, Rachakonda PS, Fischer C, Sucker A, Gast A, Kadel S, Moll I, Nagore E, Hemminki K, Schadendorf D, Kumar R. TERT promoter mutations in familial and sporadic melanoma. *Science* 2013;**339**:959-61.
73. Macerola E, Loggini B, Giannini R, Garavello G, Giordano M, Proietti A, Niccoli C, Basolo F, Fontanini G. Coexistence of TERT promoter and BRAF mutations in cutaneous melanoma is associated with more clinicopathological features of aggressiveness. *Virchows Arch* 2015;**467**:177-84.
74. Griewank KG, Murali R, Puig-Butille JA, Schilling B, Livingstone E, Potrony M, Carrera C, Schimming T, Moller I, Schwamborn M, Sucker A, Hillen U, *et al.* TERT promoter mutation status as an independent prognostic factor in cutaneous melanoma. *J Natl Cancer Inst* 2014;**106**:10.1093/jnci/dju246. Print 2014 Sep.
75. Rachakonda PS, Hosen I, de Verdier PJ, Fallah M, Heidenreich B, Ryk C, Wiklund NP, Steineck G, Schadendorf D, Hemminki K, Kumar R. TERT promoter mutations in bladder cancer affect patient survival and disease recurrence through modification by a common polymorphism. *Proc Natl Acad Sci U S A* 2013;**110**:17426-31.
76. Nagore E, Heidenreich B, Rachakonda S, Garcia-Casado Z, Requena C, Soriano V, Frank C, Traves V, Quecedo E, Sanjuan-Gimenez J, Hemminki K, Landi MT, *et al.* TERT promoter mutations in melanoma survival. *Int J Cancer* 2016;**139**:75-84.
77. Kawai K, Viars C, Arden K, Tarin D, Urquidi V, Goodison S. Comprehensive karyotyping of the HT-29 colon adenocarcinoma cell line. *Genes Chromosomes Cancer* 2002;**34**:1-8.
78. Kristensen T, Clemmensen O, Hoejberg L. Low incidence of minor BRAF V600 mutation-positive subclones in primary and metastatic melanoma determined by sensitive and quantitative real-time PCR. *J Mol Diagn* 2013;**15**:355-61.
79. Aguiassa-Toure AH, Li G. Genetic alterations of PTEN in human melanoma. *Cell Mol Life Sci* 2012;**69**:1475-91.
80. Bastian BC, LeBoit PE, Hamm H, Brocker EB, Pinkel D. Chromosomal gains and losses in primary cutaneous melanomas detected by comparative genomic hybridization. *Cancer Res* 1998;**58**:2170-5.
81. Greshock J, Nathanson K, Medina A, Ward MR, Herlyn M, Weber BL, Zaks TZ. Distinct patterns of DNA copy number alterations associate with BRAF mutations in melanomas and melanoma-derived cell lines. *Genes Chromosomes Cancer* 2009;**48**:419-28.
82. Furuta J, Umebayashi Y, Miyamoto K, Kikuchi K, Otsuka F, Sugimura T, Ushijima T. Promoter methylation profiling of 30 genes in human malignant melanoma. *Cancer Sci* 2004;**95**:962-8.
83. Frampton M, da Silva Filho MI, Broderick P, Thomsen H, Forsti A, Vijayakrishnan J, Cooke R, Enciso-Mora V, Hoffmann P, Nothen MM, Lloyd A, Holroyd A, *et al.* Variation at 3p24.1 and 6q23.3 influences the risk of Hodgkin's lymphoma. *Nat Commun* 2013;**4**:2549.

84. Sarkar D, Leung EY, Baguley BC, Finlay GJ, Askarian-Amiri ME. Epigenetic regulation in human melanoma: past and future. *Epigenetics* 2015;**10**:103-21.
85. da Costa Prando E, Cavalli LR, Rainho CA. Evidence of epigenetic regulation of the tumor suppressor gene cluster flanking RASSF1 in breast cancer cell lines. *Epigenetics* 2011;**6**:1413-24.
86. Heidenreich B, Kumar R. TERT promoter mutations in telomere biology. *Mutat Res* 2017;**771**:15-31.
87. Li Y, Zhou QL, Sun W, Chandrasekharan P, Cheng HS, Ying Z, Lakshmanan M, Raju A, Tenen DG, Cheng SY, Chuang KH, Li J, *et al.* Non-canonical NF-kappaB signalling and ETS1/2 cooperatively drive C250T mutant TERT promoter activation. *Nat Cell Biol* 2015;**17**:1327-38.
88. Hirsch D, Kemmerling R, Davis S, Camps J, Meltzer PS, Ried T, Gaiser T. Chromothripsis and focal copy number alterations determine poor outcome in malignant melanoma. *Cancer Res* 2013;**73**:1454-60.
89. Gandolfi G, Longo C, Moscarella E, Zalaudek I, Sancisi V, Raucci M, Manzotti G, Gugnoni M, Piana S, Argenziano G, Ciarrocchi A. The extent of whole-genome copy number alterations predicts aggressive features in primary melanomas. *Pigment Cell Melanoma Res* 2016;**29**:163-75.

## APPENDIX 1

### **BRAF gene copy number and mutant allele frequency correlate with time to progression in metastatic melanoma patients treated with MAPK inhibitors.**

Camilla Stagni<sup>1</sup>, Carolina Zamuner<sup>2</sup>, Lisa Elefanti<sup>3</sup>, Tiziana Zanin<sup>2</sup>, Paola Del Bianco<sup>4</sup>, Antonio Sommariva<sup>5</sup>, Alessio Fabozzi<sup>6</sup>, Jacopo Pigozzo<sup>6</sup>, Simone Mocellin<sup>5</sup>, Maria Cristina Montesco<sup>2</sup>, Vanna Chiarion-Sileni<sup>6</sup>, Arcangela De Nicolò<sup>7,8</sup>, Chiara Menin<sup>3,8</sup>.

*<sup>1</sup>Oncology and Immunology Section, Department of Surgery, Oncology and Gastroenterology, University of Padua; <sup>2</sup>Anatomy and Histology Unit, <sup>3</sup>Diagnostic Immunology and Molecular Oncology Unit, <sup>4</sup>Clinical Trials and Biostatistics Unit, <sup>5</sup>Surgical Oncology Unit, <sup>6</sup>Melanoma and Esophagus Oncology Unit, <sup>7</sup>Cancer Genomics Program, Veneto Institute of Oncology IOV - IRCCS, Padua, Italy; <sup>8</sup>Shared senior authorship.*

**Keywords:** melanoma, BRAF, MAPK inhibitors, copy number, mutant allele frequency

**Running Title:** BRAF CNV and mutant allele frequency in metastatic melanoma

**Correspondence to:** Chiara Menin, Immunology and Molecular Oncology Unit, Veneto Institute of Oncology IOV - IRCCS, Via Gattamelata 64, 35128 Padova, Italy, Tel: +39 0498215882, Fax: +39 0498072854, Email: [chiara.menin@iov.veneto.it](mailto:chiara.menin@iov.veneto.it)

**Abbreviations:** MAPKi, MAPK inhibitors; CNV, copy number variation; PFS, progression free survival; mut, V600-mutated; pts, patients; FFPE, formalin-fixed paraffin-embedded; H&E, hematoxylin and eosin-stained; qPCR, real-time quantitative PCR; wt, wild-type; FISH, fluorescence in situ hybridization; CI, confidence interval; HR, hazard ratios.

**Article category:** Tumor Markers and Signatures

**Novelty and Impact:** BRAF-mutated melanoma benefits from MAPKi-based therapy. Yet, the onset of resistance impacts long-term efficacy and can even be immediate. By analyzing 46 MAPKi-treated melanoma patients at baseline, the authors showed an association between

diploid BRAF status and low BRAF mutant allele percentage with increased risk of disease progression. These preliminary results point at the determination of BRAF copy number and/or mutant allele load as a potentially useful tool for a more accurate patient selection.

## **Abstract**

Metastatic melanoma is characterized by complex genomic alterations including a high rate of mutations in driver genes and widespread deletions and amplifications encompassing various chromosome regions. Among them, chromosome 7 is frequently gained in BRAF mutant melanoma, inducing a mutant allele-specific imbalance. Although BRAF amplification is a known mechanism of acquired resistance to therapy with MAPK inhibitors (MAPKi), it is still unclear if BRAF copy number variation (CNV) and BRAF mutant allele imbalance at baseline can be associated with response to treatment.

In this study, we used a multimodal approach to assess BRAF CNV and mutant allele frequency in pre-treatment melanoma samples from 46 patients who received MAPKi-based therapy and we analyzed the association with progression free survival (PFS).

We found that 65% patients displayed BRAF gains, often supported by chromosome 7 polysomy. In addition, we observed that 64% patients had a balanced BRAF mutant/wild-type allele ratio, while 14% and 23% patients had low and high BRAF mutant allele frequency, respectively. Notably, a significantly higher risk of progression was observed in patients with a diploid BRAF status vs. those with BRAF gains (HR = 2.86; 95% CI 1.29-6.35;  $p = 0.01$ ) and in patients with low percentage vs. those with a balanced BRAF mutant allele percentage (HR = 4.54, 95% CI 1.33-15.53;  $p = 0.016$ ).

Our data suggest that quantitative analysis of the BRAF gene could be useful to select the melanoma patients who are most likely to benefit from MAPKi therapy.

## Introduction

Approximately 50% of cutaneous melanomas carry a *BRAF* mutation that leads to constitutive activation of the mitogen-activated protein kinase (MAPK) pathway.<sup>1, 2</sup> In more than 80% of cases, the mutation causes a valine to glutamic acid, less frequently, a valine to lysine, substitution at codon 600 (p.V600E and p.V600K, respectively). Rarer mutations, including *BRAF* p.V600D, p.V600R, p.V600\_K6001E have also been reported (COSMIC, <http://www.sanger.ac.uk/cosmic>).<sup>3, 4</sup> In recent years, the advent of selective inhibitors of the MAPK pathway (i.e. *BRAF* and *MEK* inhibitors) has improved both the overall and the progression-free survival (PFS) of *BRAF* V600-mutated (mut) metastatic melanoma patients (pts). After initial response, however, the majority of pts invariably experience the onset of resistance, which limits long-term treatment effectiveness.<sup>5-9</sup> In some cases, disease progression is immediate, occurring within three months.<sup>10</sup> Therefore, the identification of biomarkers that predict response to therapy is a pre-requisite for patient stratification and treatment selection.

*BRAF* gene amplification is described as one of the main mechanisms of acquired resistance on *BRAF* inhibitor-based therapy (with or without *MEK* inhibitors) supporting reactivation of the MAPK pathway (hence tumor cell proliferation) that leads to relapse. A higher number of *BRAF* gene copies has been detected in specimens from pts at disease progression compared to baseline biopsies.<sup>11-14</sup> An increased *BRAF* gene copy number has been also reported both in pre-treatment specimens from metastatic melanoma pts who did not respond to therapy and in MAPK inhibitors (MAPKi) resistant cell lines.<sup>15, 16</sup> Thus, it is still debated if *BRAF* amplification is an acquired mechanism of resistance, which develops *de novo* in the tumor cells to overcome *BRAF* inhibition, or if it can also play a role as an intrinsic mechanism when detected in the tumor prior to MAPKi exposure.

A high rate of chromosome instability is a hallmark of melanoma. It is also known that copy number variation (CNV) becomes more pronounced with the progression from *in situ* to metastatic melanoma. Cutaneous melanoma is characterized by a pattern of copy number alterations that typically include chromosome 1, 6, and 7 gains and chromosome 9 and 10 losses.<sup>17, 18</sup> The *BRAF* gene maps to chromosome 7, which is frequently gained, as a whole or in part, especially in *BRAF*mut melanoma, contributing to variation of the amount of the mutant allele. Indeed, the percentage of the *BRAF*mut allele, although expected to be 50% as mutations in oncogenes are usually heterozygous, reportedly spans across a wide range of values in melanoma samples.<sup>19-22</sup> Because the *BRAF* V600 mutation is the target of *BRAF*



inhibitors, the percentage of the BRAFmut allele was suggested to influence the clinical efficacy of the treatment but its association with patients' response is still controversial.<sup>19, 23-25</sup> The aim of our study was to assess BRAF copy number and mutant allele frequency in pre-therapy specimens from metastatic melanoma pts who received MAPKi and to investigate the correlation with patients' response to treatment. The identification of predictive biomarkers would allow the selection of pts who are most likely to benefit from MAPK-targeted therapy, thus improving clinical management.

## **Material and Methods**

### **Patient cohort**

Fifty-one specimens (9 from primary tumors and 42 from metastases) were collected, prior to MAPK-targeted therapy initiation, from 46 pts diagnosed with BRAFmut unresectable stage III or stage IV cutaneous melanoma, who were treated at the Veneto Institute of Oncology IOV – IRCCS in Padua. Multiple biopsies were available for 5 pts.

All pts received MAPK-targeted therapy: 34 (74%) were treated with monotherapy [(Vemurafenib (22) or Dabrafenib (12))] and 12 (26%) with a combination of BRAF and MEK inhibitors (Combo: Dabrafenib and Trametinib, respectively). Age, gender and clinical history including stage, histopathological features, therapy, and ECOG performance status at baseline were collected. Progression-free survival, assessed by total body imaging or physical examination, was the used clinical outcome measure. Written informed consent was obtained from all pts before the enrollment into the study, which was approved by the local institutional ethics committee.

### **Tumor samples and DNA extraction**

All samples were formalin-fixed paraffin-embedded (FFPE). A pathologist contoured and estimated the tumor area on hematoxylin and eosin-stained (H&E) slides. For five samples, tumor cell percentage was also evaluated by the Aperio ScanScope CS system and ImageScope software (Leica Biosystems, Milton Keynes, UK) on digital images of H&E slides; the results confirmed the accuracy of the pathology evaluation. Samples with tumor content  $\geq 70\%$  were macrodissected to enrich the tumor cell population. DNA was extracted using the QIAmp DNA micro/mini kit (Qiagen, Hilden, Germany) or the MagNA Pure

Compact Instrument (Roche Diagnostics, Mannheim, Germany) according to the manufacturer's instructions.

### **Real-time PCR reactions**

BRAF gene copy number was assessed by real-time quantitative PCR (qPCR) using the TaqMan technology on a Light-Cycler 480 instrument (Roche Diagnostics, Mannheim, Germany). A 149 bp region was amplified with primers encompassing the 600 codon in a multiplex reaction that also included primers for albumin (ALB) as a reference gene. We used the relative quantification measured using the delta-Ct method with a BRAF reference standard (Horizon Diagnostics, Cambridge, UK) in each experiment and adjusted it according to the estimated tumor cell percentage. To validate our approach, we analyzed control DNA from FFPE normal skin samples that showed a BRAF/ALB ratio ranging from 0.93 to 1.1 and denoting an equal copy number of the BRAF and ALB genes (range 1.9-2.2 copies). The adenocarcinoma cell line HT-29, for which chromosome 7 trisomy has been reported,<sup>26</sup> was used as an additional control and showed a BRAF/ALB ratio of 1.5, as expected. We therefore set a copy number of 2.3 as a cut-off to discriminate between a diploid BRAF status and BRAF gain.

The quantification of the BRAF mut allele in each sample was obtained by *ad hoc* real-time PCR reactions set up to amplify the V600E/K mut and wild-type (wt) alleles. The forward primer was mutation-specific, with a 3' terminus matching the V600E, V600K or the wt codon, while the reverse primer and the probe were identical in each reaction. To increase allele specificity, an additional nucleotide mismatch was incorporated 2 nucleotides upstream the 3' end of each forward primer. Both mut- and wt-specific PCRs were performed using the ALB gene as a control to normalize for DNA content. Standard curves with serial dilutions of the commercially available BRAF V600E or V600K 50% allele standards (Horizon Diagnostics, Cambridge, UK) in BRAF wt sample were used to evaluate the reaction efficiency and to calculate the fraction of BRAF V600mut allele as in Kristensen *et al.*<sup>27</sup> The BRAFmut allele % was calculated as a ratio of BRAFmut/BRAFmut+BRAFwt adjusted by tumor cell percentage. To validate the method, we compared the BRAFmut allele % as measured by allele-specific real-time qPCR to that evaluated by pyrosequencing for five representative samples and for the BRAF V600E HT-29 cell line.<sup>22, 23, 27</sup> The two methods yielded comparable results with an average difference of 10.7% (data not shown).

Sequences of primers and probes are provided in the Supplementary Table S1. All PCR reactions were carried out in duplicate (cycle conditions are available upon request).

### **Copy number variation analysis**

For the CNV assessment, 80 nanograms of dsDNA were analyzed using the OncoScan CNV Assay (Affymetrix, Santa Clara, CA, USA) on an Affymetrix SNP-array platform according to the manufacturer's protocol. This assay is based on a molecular inversion probe technology specifically designed to handle limited amounts of highly degraded, FFPE-extracted DNA. The raw probe signal intensities (CEL files) obtained were processed using the OncoScan Console software (Affymetrix, Santa Clara, CA, USA). Normal controls from the OncoScan assay kit were used to calculate log<sub>2</sub>ratio and B-allele frequencies. Copy number aberrations were identified by OncoScan Nexus Express (Biodiscovery, El Segundo, CA, USA) using the TuScan segmentation algorithm.

### **Fluorescence *in situ* hybridization (FISH) analysis**

A total of 18 FFPE samples (2 primary melanomas and 16 metastases) from 15 pts were analyzed by FISH using the Vysis BRAF SpectrumGold FISH Probe Kit, which covers a region encompassing the entire BRAF gene, and the Vysis CEP7 SpectrumGreen Probe, which hybridizes to the alpha satellite DNA at the chromosome 7 centromere (Abbott Molecular, Des Plaines, IL, USA). Four micrometer-sections were pretreated with the Paraffin Pretreatment Kit I (Abbott Molecular, Des Plaines, IL, USA), denatured, and hybridized with 10 microliters of probe mixture. After washing, the slides were counterstained with 10 microliters of DAPI I (Abbott Molecular, Des Plaines, IL, USA) and analyzed at high-power magnification (X100) using a LEICA DM4000 B LED epifluorescence microscope (Leica Biosystems, Milton Keynes, UK). The Leica Application Suite software was used for image acquisition. For each sample, the number of copies of the BRAF gene and of the chromosome 7 were estimated by calculating the mean number of signals for each probe in 100 nuclei.

### **Statistical analysis**

Quantitative variables were summarized as median and range; categorical variables were reported as counts and percentages. PFS was calculated from the date of treatment initiation to progression. Patients who did not develop an event during the study period were censored at the date of last observation. The PFS rates were estimated by the Kaplan-Meier method and compared with the log-rank test. Hazard ratios (HR) and 95% Confidence Interval (CI) for each group of interest were estimated using the Cox proportional hazards model with low risk

group being used as the reference. The independent role of each covariate in predicting the PFS was verified in a multivariate model considering all characteristics significantly associated to the outcome in the univariate analysis. No deviation from the proportional hazards assumption were found by the numerical methods of Lin *et al.*<sup>28</sup> All tests were two-sided and a *p* value <0.05 was considered statistically significant. Statistical analyses were performed using the SAS version 9.4 (SAS Institute, Cary, NC).

## Results

We retrospectively studied 51 samples from 46 pts treated for BRAFmut metastatic melanoma at the Veneto Institute of Oncology IOV – IRCCS in Padua. Routine diagnostic mutation analysis detected the BRAF V600E (c.1799T>A) mutation in 42 samples (82%), the V600K (c.1798\_1799delGTinsAA) in 7 (14%), the V600R (c.1798\_1799delGTinsAG) and V600\_K601E (c.1799\_1801delTGA) each in one sample (2%). Patients demographics and clinical/pathological characteristics are summarized in Table 1 and detailed in Table 2.

Patients received either BRAFi monotherapy (Vemurafenib or Dabrafenib) or a combination of BRAF and MEK inhibitors. Six pts were still on therapy at the time of the analysis; one (O-199) suspended the treatment due to toxicity. The median time to progression was 5.6 months (95% CI 4.5-7.5) for pts treated with monotherapy, 15.7 months (95% CI 8.2 - ) for those treated with Combo therapy, and 7.5 months (95% CI 5.5-12.8) overall.

### Assessment of BRAF gene copy number

BRAF gene copy number was first assessed by qPCR. After setting a cut-off of 2.3 copies to discriminate between diploid BRAF status and BRAF gain, we identified gains (median of 3 copies, range 2.4-4) in 26 samples from 23 pts (50%) and a diploid status (median of 2.2 copies, range 1.9-2.3) in the remainder (Fig. 1a and Supporting Information Table 2). Different specimens from the same patient showed concordant copy number results in all cases but one, O-0557 (Supporting Information Table 2).

To confirm the results obtained by qPCR and investigate the possible mechanisms underlying the detected BRAF gains, we derived data relating to the 39 pts (43 specimens) in this study from a genome-wide CNV analysis, which we carried out for other purposes (unpublished data). Consistent with previous reports, most pts (72%) displayed widespread genome aneuploidy, while only 28% showed a diploid genome (Supporting Information Table 2).

BRAF-focused CNV analysis identified more than two BRAF copies (median of 3 copies, range 2.4-7) in 29 samples from 25 pts (64%). As exemplified in Fig. 1b, these detected BRAF gains were often coupled with polysomy of chromosome 7 (i.e. more than 2.3 copies of the 7p11-q21 region encompassing the centromere), thus assigning 18 pts (72%) to the ‘gain/polysomy’ category. Also 2 samples (O-4519 and O-4769) with 7 BRAF gene copies, which could be considered as gene amplification, were included in this group owing to the associated whole chromosome 7 polysomy. The 7 pts who showed 2.7 to 6 BRAF copies and chromosome 7 disomy, were assigned to the category ‘gain/disomy’. In the remaining 14 pts (36%), BRAF CNV analysis showed diploid BRAF gene (median of 2 copies, range 2-2.3) and chromosome 7 disomy and they were assigned to the category ‘diploid/disomy’ (Supporting Information Table 2).

Comparing the results obtained by qPCR with those obtained by CNV analysis, we observed that all gains identified with the former approach were confirmed by the latter one. Instead, 8 out of the 22 qPCR-assessed pts with diploid BRAF status displayed, in fact, BRAF gains by CNV analysis (Italicized in Supporting Information Table 2). For 4 of them (O-0477, O-0550, O-2386, O-3854), CNV analysis uncovered polysomy of chromosome 4, where the ALB gene maps. Thus, the BRAF status for these cases was reclassified as ‘BRAF gain’. To resolve the discrepancy related to the other 4 pts (O-0482, O-0557, O-0559, O-1977), we carried out FISH analysis, which we extended to a total number of 18 samples from 17 pts. FISH confirmed all BRAF gains detected by CNV analysis. The above-mentioned 4 cases were, therefore, re-classified as gains. Notably, FISH analysis disclosed a previously undetected chromosome 7 polysomy in one case (O-0482) (Supporting Information Table 2) showing intra-tumor heterogeneity with few cells that harbored more than two BRAF copies. Both CNV and FISH analysis displayed the same BRAF copy number when multiple biopsies from one patient were evaluated.

Our results indicate that while the qPCR-assessed BRAF gains are a robust result, the qPCR-assessed diploid BRAF status needs validation by another approach. Because samples O-0592 and O-1681 were analyzed only by qPCR, we could not define their BRAF copy number (NA, not assigned; Table 2). Overall, based on these criteria, we found that BRAF gains were present in melanoma samples from 30 pts (65%), while 14 pts (30%) displayed a diploid BRAF status (Table 2). Notably, the increased amount of BRAF gene copies was frequently due to whole or partial chromosome 7 polysomy while BRAF gene amplification (namely >6 gene copies and chromosome disomy) was never detected in our pre-treatment cohort.

### **Assessment of BRAF mutant allele percentage**

To determine if BRAF CNV was associated with changes in the percentage of the BRAF V600E/V600K allele in the tumor, we evaluated the BRAFmut allele frequency and integrated the information with the copy number data.

Analyzing 48 samples from 44 pts (pts with V600R and V600\_K601E mutations were excluded), we observed a wide spectrum of BRAFmut allele % values, ranging from 20% to 98% (median 54%) (Supporting Information Table 2) and noticed that more than a half of them (56%) had a 40-60% BRAFmut allele frequency (Fig. 2a). Taking into account that, upon validation of this analysis, we observed a 10% mean difference when comparing the results by allele-specific qPCR with those by pyrosequencing, we set a range of 35-65% to distinguish the balanced heterozygous BRAF status and the cases with a low (<35%) or high (>65%) BRAFmut allele % (Fig. 2b). As a result, 64.6% of the analyzed samples (63.6% of pts) were classified as heterozygous, while 12.5% and 23% of them (13.6% and 22.7% of pts) showed a low (average 24.3%) and high (average 88.6%) BRAFmut allele %, respectively (Supporting Information Table 2).

Upon integration of BRAFmut allele frequency and BRAF gene copy number data (Fig. 2c), balanced heterozygosity remained the most represented category, both in BRAF diploid samples (79%) and in those with gains (60%). Notably, however, 34% of samples with BRAF gains were supported by high BRAFmut allele %, which was never detected in diploid BRAF samples. The latter ones showed instead a low BRAFmut allele % in almost one fifth of the cases (21.4%).

### **Association of baseline BRAF copy number and mutant allele frequency with PFS**

We then investigated, by nonparametric Kaplan-Meier analysis, the relationship between BRAF copy number and BRAFmut allele % at baseline and patient's response to MAPKi treatment. In univariate analysis (Table 3), patients with BRAF gain showed a trend toward longer PFS (median 12.1 months; 95% CI 5.6-15.8) compared to pts with diploid BRAF status (median 4.7 months; 95% CI 2.5-8.2) ( $p$ -log rank = 0.056; Fig. 3a). A significantly longer PFS was also observed in pts with balanced heterozygous BRAFmut status (median 12.0 months; 95% CI 5.6-15.8) and high BRAFmut allele % (median 7.5 months; 95% CI 2.1-21.7) compared to those with low BRAFmut allele % (median 3.0 months; 95% CI 1.4-5.5) ( $p$ -log rank <0.001; Fig. 3b). Notably, pts with low BRAFmut allele % presented a more than seven- and five-fold increased HR for disease progression when compared to the heterozygous and high BRAFmut allele % groups, respectively. As expected, in univariate

analysis also age, ECOG performance status, disease stage, and type of therapy were correlated to the PFS (Table 3).

In the multivariate model, adjusted for patients' clinical characteristics, both BRAF copy number and mutation allele frequency appeared to be independent predictors of disease progression (Table 3). Patients with tumor characterized by diploid BRAF status had a significantly higher risk of progression than those with BRAF gains (HR = 2.86; 95% CI 1.29-6.35;  $p = 0.01$ ). Patients with low BRAFmut allele % still showed a significantly higher risk of progression compared to those with balanced heterozygous BRAF status (HR = 4.54, 95% CI 1.33-15.53;  $p = 0.016$ ).

Our data suggest that pts whose tumors display BRAF gains or heterozygous BRAFmut allele % have a longer response, independently of type of therapy and tumor stage.

## Discussion

The onset of resistance represents a major hindrance to the long-term effectiveness of MAPKi therapy in metastatic melanoma pts. Predictive biomarkers of resistance are urgently needed. For this purpose, we have quantitatively studied the BRAF gene - the direct target of the MAPKi-based therapy - and investigated the correlation between PFS and gene copy number or mutant allele frequency at baseline. Our findings show that pts with melanoma displaying gains of the BRAF gene or BRAF mutant allele percentage similar to or higher than that of the wt allele seem to benefit the most from MAPKi therapy.

Given the complexity of the molecular alterations that characterize metastatic melanoma,<sup>29, 30</sup> we integrated data from three independent methods to achieve a confident assessment of BRAF copy number: qPCR, which is commonly used for gene quantification; CNV analysis, which provides a comprehensive picture of whole genome alterations; FISH, which has the potential to uncover tumor heterogeneity by analyzing single nuclei. Using the three techniques, we found BRAF gains in 65% of our patient cohort. Notably, our results failed to show the presence of BRAF amplification and indicate that, instead, BRAF gains are a common event that is often supported by total or partial chromosome 7 polysomy. Our data are consistent with previous findings showing that gains of chromosome 7 are frequently associated with the presence of BRAF mutations in metastatic melanoma.<sup>18, 31</sup>

Upon investigation of the impact of the BRAF copy number variation on allele frequency, even though most cases (64.5%) displayed a balanced BRAF mut/wt allele ratio, low and high

frequency of BRAFmut allele were detected in 12.5% and 23% of samples, respectively. The unbalanced ratio favoring the mutated allele of an oncogene is a frequent event during tumorigenesis. Moreover, mutant allele specific imbalance (MASI) is often coupled with copy number gains.<sup>20-22</sup> Indeed, we found that all samples with a high percentage of BRAFmut allele were also characterized by BRAF gains. On the other hand, we found that 21% of the samples with a diploid BRAF status showed an unbalanced allelic ratio favoring the wt allele (i.e. low BRAFmut allele %). We excluded the possibility of a contamination by normal cells (e.g. stromal and inflammatory cells) because our results took into account (and were adjusted based on) tumor cell percentage. Conceivably, intra-tumor heterogeneity contributes to the spectrum of BRAFmut allele %, whereby heterozygous, homozygous mutant or wt BRAF melanoma cells could coexist in one tumor lesion.<sup>19</sup> Indeed, this is a frequent scenario in primary melanoma as well as at the metastatic stage, even though the number of mutated cells tends to increase during tumor progression owing to the proliferative advantage conferred by the BRAF mutant allele.<sup>32, 33</sup> Thus, an unbalanced BRAF allelic ratio is always integral to the complexity of the metastatic melanoma genome.

Previous studies carried out in a very limited number of pretreatment specimens from pts treated with BRAF ± MEK inhibitors, had suggested that an increased BRAF copy number could be associated with disease progression.<sup>15, 16</sup> Instead, in our larger cohort of MAPKi-treated pts, we observed that BRAF gains at baseline were associated with a better clinical outcome, both by univariate and by multivariate analysis. Our results suggest a possible different effect of BRAF gains on the clinical response compared to the proved role of the BRAF gene amplification as an acquired mechanism of resistance to MAPKi.<sup>12, 34</sup> A similar effect on PFS was described for pts who received the multikinase inhibitor Sorafenib and whose melanoma harbored gains in one of the targeted genes, RAF1.<sup>35</sup> In addition, we observed a seven- or five-fold decrease of HR for disease progression in pts with melanoma harboring a balanced BRAF heterozygous mutation or a high BRAFmut allele %, respectively, compared to pts whose melanoma had a low BRAFmut allele %. Notably, we found that the significant correlation between BRAFmut allele frequency and response to MAPKi was independent of the other clinical characteristics, including therapy and stage. It can be speculated that a low mutational load would translate into reduced amount of accessible target to the inhibitor and hence less efficacy. Alternatively, targeting of the MAPK pathway in tumor cells with a higher amount of BRAFwt allele could trigger a paradoxical cell proliferation leading to tumor resistance.<sup>36</sup>



Previously, Lebbé et al. analyzed the correlation of BRAF mutant allele levels with best response rate to Vemurafenib, showing that complete responses were more frequent in pts with high BRAFmut allele, whose PFS advantage however decreased within 10 months.<sup>23</sup> Conversely, other two studies<sup>19, 24</sup> reported that pts with high or low mut allele % benefited equally from BRAF inhibitors. Recently, Boespflug A. et al. analyzing a large cohort, observed a trend in favor of a better PFS for pts with high mut allele %.<sup>25</sup> One of the major differences between these studies was the cut-off used to discriminate between high and low BRAFmut allele %. In none of the previous studies<sup>19, 23-25</sup> the heterozygous cases were considered as an independent group. Instead, we believed it was important to discriminate between pts with balanced heterozygosity and those with allelic imbalance. By doing so, we found that pts in the former group had the longest PFS. We acknowledge that, because many variables are considered, our results should be replicated in a larger cohort. Nevertheless, our study is monocentric and, hence, ensures homogeneity of clinical data.

In conclusion, we provide a characterization of the BRAF copy number and BRAFmut allele % profile in metastatic melanoma prior to MAPKi therapy. At this stage, we cannot exclude that these molecular traits have a prognostic rather than a predictive role. Future prospective clinical studies should clarify this aspect. Our results uncover the frequent occurrence of BRAF gene gains, which appear to be mostly responsible for the mutant allele imbalance, and show that BRAF copy number and BRAFmut allele % are associated with the response of metastatic melanoma pts to MAPKi, as do the stage and type of therapy. Patients with a melanoma characterized by a diploid BRAF status or low BRAFmut allele % have a remarkably increased risk of progression. In this light, assessment of BRAF copy number and/or mutant allele load could be considered prior to treatment choice as a useful tool for accurate patient selection to targeted therapy.

## References

1. Fecher LA, Amaravadi RK, Flaherty KT. The MAPK pathway in melanoma. *Curr Opin Oncol* 2008;20:183-9.
2. Davies H, Bignell GR, Cox C, Stephens P, Edkins S, Clegg S, Teague J, Woffendin H, Garnett MJ, Bottomley W, Davis N, Dicks E, Ewing R, Floyd Y, Gray K, Hall S, Hawes R, Hughes J, Kosmidou V, Menzies A, Mould C, Parker A, Stevens C, Watt S, Hooper S, Wilson R, Jayatilake H, Gusterson BA, Cooper C, Shipley J, Hargrave D, Pritchard-Jones K, Maitland N, Chenevix-Trench G, Riggins GJ, Bigner DD, Palmieri G, Cossu A, Flanagan A, Nicholson A, Ho JW, Leung SY, Yuen ST, Weber BL, Seigler HF, Darrow TL, Paterson H, Marais R, Marshall CJ, Wooster R, Stratton MR, Futreal PA. Mutations of the BRAF gene in human cancer. *Nature* 2002;417:949-54.
3. Heinzerling L, Kuhnappel S, Meckbach D, Baiter M, Kaempgen E, Keikavoussi P, Schuler G, Agaimy A, Bauer J, Hartmann A, Kiesewetter F, Schneider-Stock R. Rare BRAF mutations in melanoma patients: implications for molecular testing in clinical practice. *Br J Cancer* 2013;108:2164-71.
4. Lovly CM, Dahlman KB, Fohn LE, Su Z, Dias-Santagata D, Hicks DJ, Hucks D, Berry E, Terry C, Duke M, Su Y, Sobolik-Delmaire T, Richmond A, Kelley MC, Vnencak-Jones CL, Iafrate AJ, Sosman J, Pao W. Routine multiplex mutational profiling of melanomas enables enrollment in genotype-driven therapeutic trials. *PLoS One* 2012;7:e35309.
5. Schadendorf D, Long GV, Stroiakovski D, Karaszewska B, Hauschild A, Levchenko E, Chiarion-Sileni V, Schachter J, Garbe C, Dutriaux C, Gogas H, Mandala M, Haanen JBAG, Lebbe C, Mackiewicz A, Rutkowski P, Grob JJ, Nathan P, Ribas A, Davies MA, Zhang Y, Kaper M, Mookerjee B, Legos JJ, Flaherty KT, Robert C. Three-year pooled analysis of factors associated with clinical outcomes across dabrafenib and trametinib combination therapy phase 3 randomised trials. *Eur J Cancer* 2017;82:45-55.
6. Chapman PB, Hauschild A, Robert C, Haanen JB, Ascierto P, Larkin J, Dummer R, Garbe C, Testori A, Maio M, Hogg D, Lorigan P, Lebbe C, Jouary T, Schadendorf D, Ribas A, O'Day SJ, Sosman JA, Kirkwood JM, Eggermont AM, Dreno B, Nolop K, Li J, Nelson B, Hou J, Lee RJ, Flaherty KT, McArthur GA, BRIM-3 Study Group. Improved survival with vemurafenib in melanoma with BRAF V600E mutation. *N Engl J Med* 2011;364:2507-16.
7. Shi H, Hugo W, Kong X, Hong A, Koya RC, Moriceau G, Chodon T, Guo R, Johnson DB, Dahlman KB, Kelley MC, Kefford RF, Chmielowski B, Glaspy JA, Sosman JA, van

- Baren N, Long GV, Ribas A, Lo RS. Acquired resistance and clonal evolution in melanoma during BRAF inhibitor therapy. *Cancer Discov* 2014;4:80-93.
8. Van Allen EM, Wagle N, Sucker A, Treacy DJ, Johannessen CM, Goetz EM, Place CS, Taylor-Weiner A, Whittaker S, Kryukov GV, Hodis E, Rosenberg M, McKenna A, Cibulskis K, Farlow D, Zimmer L, Hillen U, Gutzmer R, Goldinger SM, Ugurel S, Gogas HJ, Egberts F, Berking C, Trefzer U, Loquai C, Weide B, Hassel JC, Gabriel SB, Carter SL, Getz G, Garraway LA, Schadendorf D, Dermatologic Cooperative Oncology Group of Germany (DeCOG). The genetic landscape of clinical resistance to RAF inhibition in metastatic melanoma. *Cancer Discov* 2014;4:94-109.
  9. Long GV, Weber JS, Infante JR, Kim KB, Daud A, Gonzalez R, Sosman JA, Hamid O, Schuchter L, Cebon J, Kefford RF, Lawrence D, Kudchadkar R, Burris HA, 3rd, Falchook GS, Algazi A, Lewis K, Puzanov I, Ibrahim N, Sun P, Cunningham E, Kline AS, Del Buono H, McDowell DO, Patel K, Flaherty KT. Overall Survival and Durable Responses in Patients With BRAF V600-Mutant Metastatic Melanoma Receiving Dabrafenib Combined With Trametinib. *J Clin Oncol* 2016;34:871-8.
  10. Flaherty KT, Puzanov I, Kim KB, Ribas A, McArthur GA, Sosman JA, O'Dwyer PJ, Lee RJ, Grippo JF, Nolop K, Chapman PB. Inhibition of mutated, activated BRAF in metastatic melanoma. *N Engl J Med* 2010;363:809-19.
  11. Johnson DB, Menzies AM, Zimmer L, Eroglu Z, Ye F, Zhao S, Rizos H, Sucker A, Scolyer RA, Gutzmer R, Gogas H, Kefford RF, Thompson JF, Becker JC, Berking C, Egberts F, Loquai C, Goldinger SM, Pupo GM, Hugo W, Kong X, Garraway LA, Sosman JA, Ribas A, Lo RS, Long GV, Schadendorf D. Acquired BRAF inhibitor resistance: A multicenter meta-analysis of the spectrum and frequencies, clinical behaviour, and phenotypic associations of resistance mechanisms. *Eur J Cancer* 2015;51:2792-9.
  12. Shi H, Moriceau G, Kong X, Lee MK, Lee H, Koya RC, Ng C, Chodon T, Scolyer RA, Dahlman KB, Sosman JA, Kefford RF, Long GV, Nelson SF, Ribas A, Lo RS. Melanoma whole-exome sequencing identifies (V600E)B-RAF amplification-mediated acquired B-RAF inhibitor resistance. *Nat Commun* 2012;3:724.
  13. Long GV, Fung C, Menzies AM, Pupo GM, Carlino MS, Hyman J, Shahheydari H, Tembe V, Thompson JF, Saw RP, Howle J, Hayward NK, Johansson P, Scolyer RA, Kefford RF, Rizos H. Increased MAPK reactivation in early resistance to dabrafenib/trametinib combination therapy of BRAF-mutant metastatic melanoma. *Nat Commun* 2014;5:5694.

14. Moriceau G, Hugo W, Hong A, Shi H, Kong X, Yu CC, Koya RC, Samatar AA, Khanlou N, Braun J, Ruchalski K, Seifert H, Larkin J, Dahlman KB, Johnson DB, Algazi A, Sosman JA, Ribas A, Lo RS. Tunable-combinatorial mechanisms of acquired resistance limit the efficacy of BRAF/MEK cotargeting but result in melanoma drug addiction. *Cancer Cell* 2015;27:240-56.
15. Nathanson KL, Martin AM, Wubbenhorst B, Greshock J, Letrero R, D'Andrea K, O'Day S, Infante JR, Falchook GS, Arkenau HT, Millward M, Brown MP, Pavlick A, Davies MA, Ma B, Gagnon R, Curtis M, Lebowitz PF, Kefford R, Long GV. Tumor genetic analyses of patients with metastatic melanoma treated with the BRAF inhibitor dabrafenib (GSK2118436). *Clin Cancer Res* 2013;19:4868-78.
16. Villanueva J, Infante JR, Krepler C, Reyes-Uribe P, Samanta M, Chen HY, Li B, Swoboda RK, Wilson M, Vultur A, Fukunaba-Kalabis M, Wubbenhorst B, Chen TY, Liu Q, Sproesser K, DeMarini DJ, Gilmer TM, Martin AM, Marmorstein R, Schultz DC, Speicher DW, Karakousis GC, Xu W, Amaravadi RK, Xu X, Schuchter LM, Herlyn M, Nathanson KL. Concurrent MEK2 mutation and BRAF amplification confer resistance to BRAF and MEK inhibitors in melanoma. *Cell Rep* 2013;4:1090-9.
17. Bastian BC, LeBoit PE, Hamm H, Brocker EB, Pinkel D. Chromosomal gains and losses in primary cutaneous melanomas detected by comparative genomic hybridization. *Cancer Res* 1998;58:2170-5.
18. Greshock J, Nathanson K, Medina A, Ward MR, Herlyn M, Weber BL, Zaks TZ. Distinct patterns of DNA copy number alterations associate with BRAF mutations in melanomas and melanoma-derived cell lines. *Genes Chromosomes Cancer* 2009;48:419-28.
19. Mesbah Ardakani N, Leslie C, Grieu-Iacopetta F, Lam WS, Budgeon C, Millward M, Amanuel B. Clinical and therapeutic implications of BRAF mutation heterogeneity in metastatic melanoma. *Pigment Cell Melanoma Res* 2017;30:233-42.
20. Yu CC, Qiu W, Juang CS, Mansukhani MM, Halmos B, Su GH. Mutant allele specific imbalance in oncogenes with copy number alterations: Occurrence, mechanisms, and potential clinical implications. *Cancer Lett* 2017;384:86-93.
21. Soh J, Okumura N, Lockwood WW, Yamamoto H, Shigematsu H, Zhang W, Chari R, Shames DS, Tang X, MacAulay C, Varella-Garcia M, Vooder T, Wistuba II, Lam S, Brekken R, Toyooka S, Minna JD, Lam WL, Gazdar AF. Oncogene mutations, copy number gains and mutant allele specific imbalance (MASI) frequently occur together in tumor cells. *PLoS One* 2009;4:e7464.

22. Helias-Rodzewicz Z, Funck-Brentano E, Baudoux L, Jung CK, Zimmermann U, Marin C, Clerici T, Le Gall C, Peschaud F, Taly V, Saiag P, Emile JF. Variations of BRAF mutant allele percentage in melanomas. *BMC Cancer* 2015;15:497,015-1515-3.
23. Lebbe C, How-Kit A, Battistella M, Sadoux A, Podgorniak MP, Sidina I, Pages C, Roux J, Porcher R, Tost J, Mourah S. BRAF(V600) mutation levels predict response to vemurafenib in metastatic melanoma. *Melanoma Res* 2014;24:415-8.
24. Satzger I, Marks L, Kerick M, Klages S, Berking C, Herbst R, Volker B, Schacht V, Timmermann B, Gutzmer R. Allele frequencies of BRAFV600 mutations in primary melanomas and matched metastases and their relevance for BRAF inhibitor therapy in metastatic melanoma. *Oncotarget* 2015;6:37895-905.
25. Boespflug A, Funck-Brentano E, Helias-Rodzewicz Z, Maucort-Boulch D, Beauchet A, Binguier PP, Dumontet C, Emile JF, Saiag P, Dalle S. Reply to "Clinical and therapeutic implications of BRAF mutation heterogeneity in metastatic melanoma" by Mesbah Ardakani et al. *Pigment Cell Melanoma Res* 2017;30:498–500.
26. Kawai K, Viars C, Arden K, Tarin D, Urquidi V, Goodison S. Comprehensive karyotyping of the HT-29 colon adenocarcinoma cell line. *Genes Chromosomes Cancer* 2002;34:1-8.
27. Kristensen T, Clemmensen O, Hoejberg L. Low incidence of minor BRAF V600 mutation-positive subclones in primary and metastatic melanoma determined by sensitive and quantitative real-time PCR. *J Mol Diagn* 2013;15:355-61.
28. Lin DY, Wei LJ, Ying Z. Checking the Cox model with cumulative sums of martingale-based residuals. *Biometrika* 1993;80:557-72.
29. Ding L, Kim M, Kanchi KL, Dees ND, Lu C, Griffith M, Fenstermacher D, Sung H, Miller CA, Goetz B, Wendl MC, Griffith O, Cornelius LA, Linette GP, McMichael JF, Sondak VK, Fields RC, Ley TJ, Mule JJ, Wilson RK, Weber JS. Clonal architectures and driver mutations in metastatic melanomas. *PLoS One* 2014;9:e111153.
30. Timar J, Vizkeleti L, Doma V, Barbai T, Raso E. Genetic progression of malignant melanoma. *Cancer Metastasis Rev* 2016;35:93-107.
31. Lazar V, Ecsedi S, Vizkeleti L, Rakosy Z, Boross G, Szappanos B, Begany A, Emri G, Adany R, Balazs M. Marked genetic differences between BRAF and NRAS mutated primary melanomas as revealed by array comparative genomic hybridization. *Melanoma Res* 2012;22:202-14.

32. Lin J, Goto Y, Murata H, Sakaizawa K, Uchiyama A, Saida T, Takata M. Polyclonality of BRAF mutations in primary melanoma and the selection of mutant alleles during progression. *Br J Cancer* 2011;104:464-8.
33. Yancovitz M, Litterman A, Yoon J, Ng E, Shapiro RL, Berman RS, Pavlick AC, Darvishian F, Christos P, Mazumdar M, Osman I, Polsky D. Intra- and inter-tumor heterogeneity of BRAF(V600E) mutations in primary and metastatic melanoma. *PLoS One* 2012;7:e29336.
34. Welsh SJ, Rizos H, Scolyer RA, Long GV. Resistance to combination BRAF and MEK inhibition in metastatic melanoma: Where to next? *Eur J Cancer* 2016;62:76-85.
35. Wilson MA, Zhao F, Khare S, Roszik J, Woodman SE, D'Andrea K, Wubbenhorst B, Rimm DL, Kirkwood JM, Kluger HM, Schuchter LM, Lee SJ, Flaherty KT, Nathanson KL. Copy Number Changes Are Associated with Response to Treatment with Carboplatin, Paclitaxel, and Sorafenib in Melanoma. *Clin Cancer Res* 2016;22:374-82.
36. Hatzivassiliou G, Song K, Yen I, Brandhuber BJ, Anderson DJ, Alvarado R, Ludlam MJ, Stokoe D, Gloor SL, Vigers G, Morales T, Aliagas I, Liu B, Sideris S, Hoeflich KP, Jaiswal BS, Seshagiri S, Koeppen H, Belvin M, Friedman LS, Malek S. RAF inhibitors prime wild-type RAF to activate the MAPK pathway and enhance growth. *Nature* 2010;464:431-5.

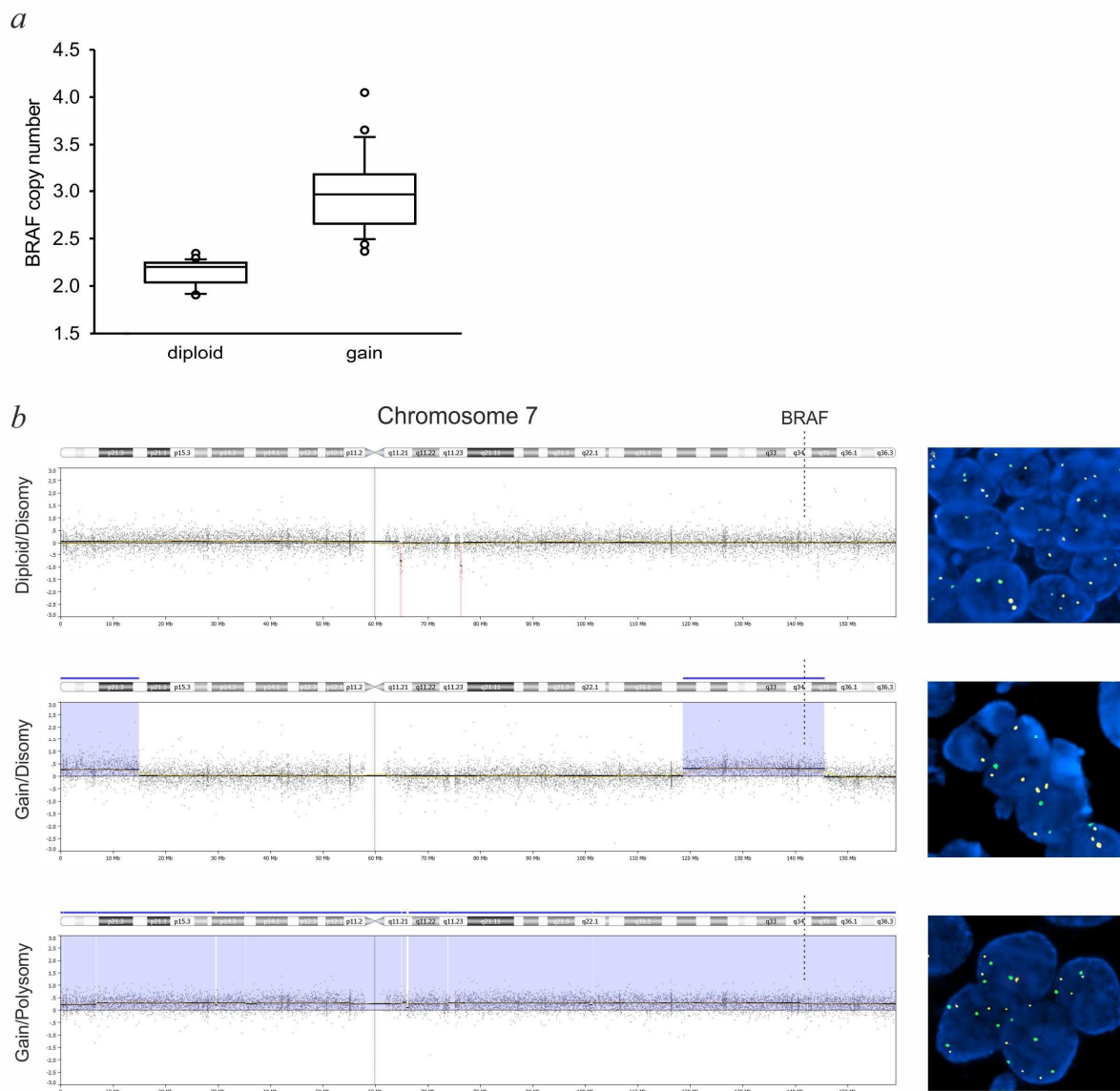


**Figure 1.** *Quantitative analysis of the BRAF gene.* (a) Boxplot of qPCR-derived BRAF copy number values. A cut-off of 2.3 copies was used to discriminate between diploid and gain status. (b) Representative cases of chromosome 7 and BRAF gene copy number aberrations as assessed by OncoScan assay (left panels) and FISH analysis (right panels).

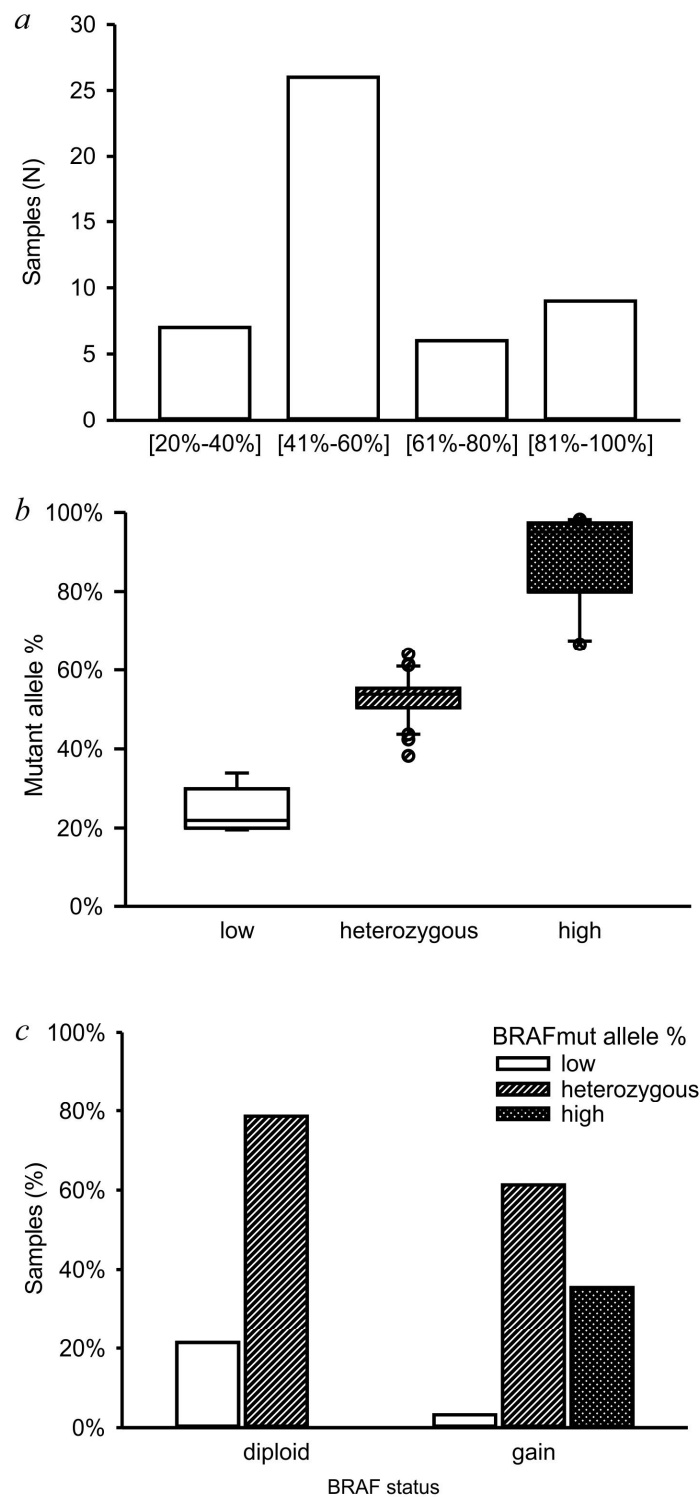


**Figure 2.** *Quantitative analysis of BRAF mutant allele frequency.* (a) Histogram representation of the % of mut allele in 48 melanoma samples obtained by allele-specific qPCR. (b) Boxplot of the % of mut allele in 48 samples divided into three categories: low (<35%), heterozygous (35%-65%), and high (>65%). (c) Histogram representation of the above-mentioned BRAFmut allele % categories according to diploid/gain status.



**Figure 3.**

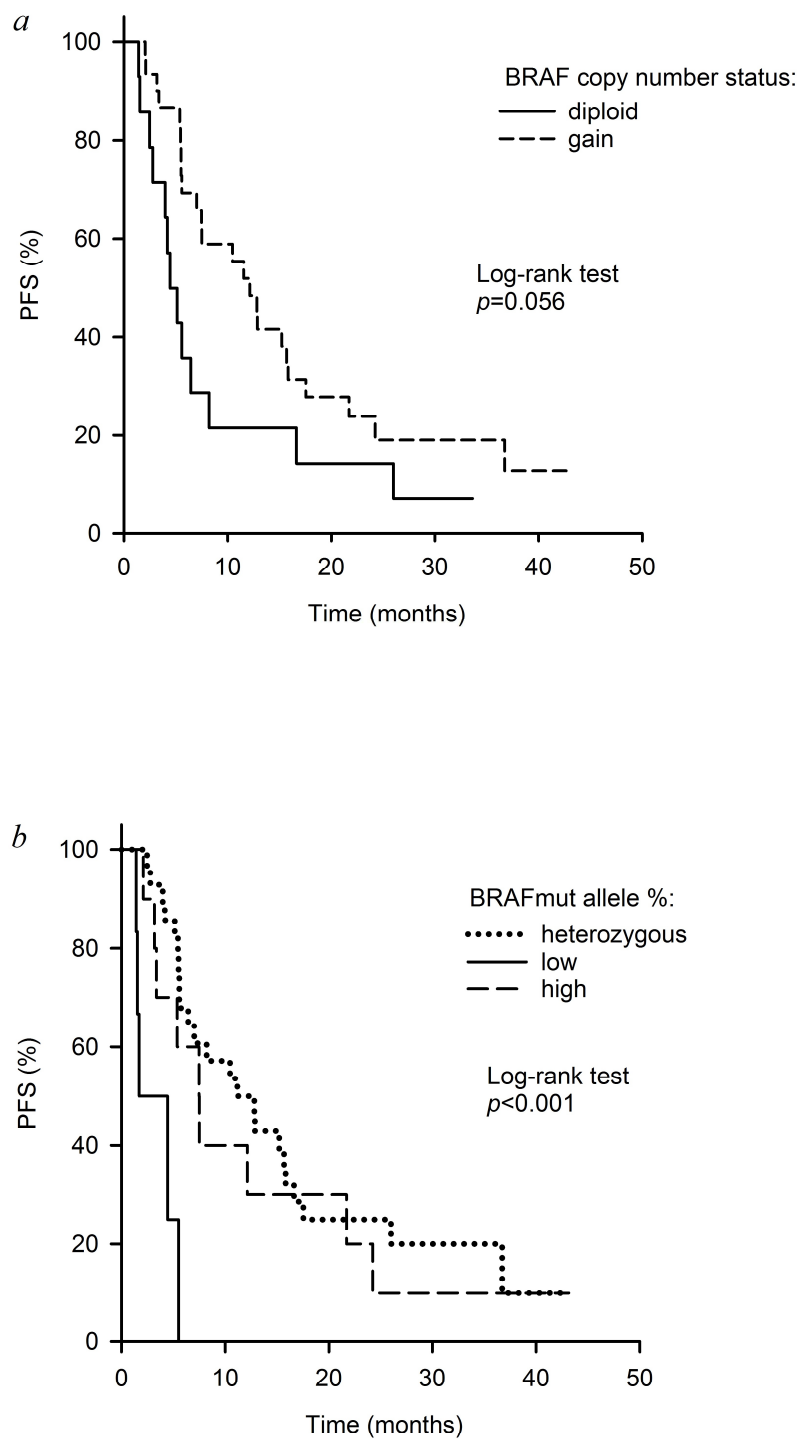


**Figure 3.** Progression-free survival according to BRAF quantitative analysis. (a) Kaplan-Meier plots of pts with diploid BRAF status (N=14) or BRAF gain (N=30). (b) Kaplan-Meier plots of pts with low (N=6), balanced heterozygous (N=28), and high (N=10) BRAFmut allele %.

**Table 1. Demographics and clinico-pathological characteristics of the melanoma patient cohort.**

	<i>N (%)</i>
<b>Patients</b>	46 (100%)
<b>Gender</b>	
Male	24 (52%)
Female	22 (48%)
<b>Median age years (range)</b>	55 (28-80)
<b>Therapy</b>	
Vemurafenib	22 (48%)
Dabrafenib	12 (26%)
Combo (Dabrafenib+Trametinib)	12 (26%)
<b>Stage</b>	
IIIB	4 (9%)
IIIC	6 (13%)
IV	36 (78%)
<b>ECOG PS</b>	
0	34 (74%)
1	10 (22%)
>1	2 (4%)
<b>Median PFS months (95% CI)</b>	7.5 (5.5-12.8)
<b>Tumor specimens</b>	
<b>Tissue</b>	51 (100%)
Primary	9 (18%)
Metastasis	42 (82%)
<b>BRAF mutation</b>	
V600E	42 (82%)
V600K	7 (14%)
V600R	1 (2%)
V600_K601E	1 (2%)

**Table 2. BRAF copy number status in melanoma samples according to tumor and patient characteristics.**

Patient	Tumor tissue analyzed	% Tumor cells	BRAF mutation	Therapy	PFS (months)	BRAF copy number status
O-0433	primary	90	V600E	Vemurafenib	6.4	diploid
O-0477	metastasis	85	V600E	Vemurafenib	5.4	gain
O-0480	metastasis	80	V600E	Vemurafenib	1.5	diploid
O-0481	metastasis	100	V600E	Vemurafenib	5.6	diploid
O-0482	primary	95	V600E	Vemurafenib	5.5	gain
O-0483_a*	metastasis	95	V600E	Dabrafenib	3.4	gain
O-0483_b*	metastasis	70	V600E			gain
O-0550_a	metastasis	95	V600E	Combo	15.8	gain
O-0550_b	metastasis	100	V600E			gain
O-0557_a	metastasis	95	V600E	Combo	22.2	gain
O-0557_b	metastasis	85	V600E			gain
O-0559	metastasis	80	V600E	Vemurafenib	12.9	gain
O-0592	metastasis	95	V600E	Vemurafenib	1.7	NA <sup>§</sup>
O-0864	primary	70	V600E	Combo	2.5	diploid
O-1230	metastasis	88	V600E	Vemurafenib	4.4	diploid
O-1361	metastasis	95	V600E	Combo	18.8	gain
O-1570	metastasis	90	V600E	Dabrafenib	7	gain
O-1614	metastasis	95	V600E	Dabrafenib	36.7	gain
O-1681	primary	88	V600E	Vemurafenib	11.2	NA
O-1684	metastasis	70	V600E	Combo	10.5	gain
O-1716	metastasis	95	V600R	Dabrafenib	11.5	gain
O-1787	primary	100	V600E	Dabrafenib	15.2	gain
O-1977	metastasis	95	V600E	Vemurafenib	5.5	gain
O-199	metastasis	80	V600E	Vemurafenib	3.6	gain
O-2087	metastasis	95	V600E	Dabrafenib	43.2	gain
O-2259_a	primary	80	V600K	Vemurafenib	5.4	gain
O-2259_b	metastasis	100	V600K			gain
O-2287	metastasis	100	V600E	Combo	43.2	gain
O-2386	metastasis	90	V600E	Vemurafenib	2.1	gain
O-2513	metastasis	95	V600_K601E	Dabrafenib	2	gain
O-2792	metastasis	85	V600E	Dabrafenib	1.4	diploid
O-2977	metastasis	88	V600E	Vemurafenib	5.6	gain
O-3020	metastasis	88	V600E	Vemurafenib	16.6	diploid
O-3321	primary	90	V600E	Combo	12.8	gain
O-3848	metastasis	70	V600K	Vemurafenib	3.2	gain
O-3854	metastasis	88	V600E	Combo	15.7	gain
O-4229	metastasis	88	V600E	Dabrafenib	5.1	diploid
O-4246	metastasis	80	V600E	Vemurafenib	4.2	diploid
O-4337	metastasis	100	V600E	Combo	8.2	diploid
O-4519	metastasis	90	V600K	Combo	12.1	gain
O-4568	primary	95	V600K	Vemurafenib	7.5	gain
O-4758	metastasis	90	V600K	Vemurafenib	24.2	gain
O-4769	metastasis	88	V600E	Vemurafenib	33.6	gain
O-4871	metastasis	88	V600E	Combo	26	diploid
O-5158	metastasis	88	V600E	Dabrafenib	4	diploid
O-5213	metastasis	100	V600E	Dabrafenib	7.5	gain
O-5554	metastasis	90	V600E	Combo	33.6	diploid
O-5646_a	metastasis	75	V600E	Vemurafenib	17.5	gain
O-5646_b	metastasis	70	V600E			gain
O-6576	primary	88	V600K	Dabrafenib	21.7	gain
O-6635	metastasis	90	V600E	Vemurafenib	2.8	diploid

\*\_a/\_b: specimens from the same patient; <sup>§</sup>Not Assigned

**Table 3. Univariate and multivariate survival analyses.**

	Median PFS months (95% CI)	Univariate analysis			Multivariate analysis		
		HR	95% CI	<i>p-value</i>	HR	95% CI	<i>p-value</i>
<b>Gender</b>							
M	8.2 (5.5-15.7)	1.55	0.82-2.94	0.179			
F	7.2 (3.4-12.8)	1					
<b>Age (years)</b>							
		1.03	1.00-1.05	0.033			
<b>ECOG PS</b>							
0	12.1 (6.4-15.8)	1					
1-3	5.5 (2.0-7.0)	2.36	1.13-4.90	0.021			
<b>BRAF</b>							
V600E	7.5 (5.5-15.2)	1					
V600K	9.8 (3.2-24.2)	1.16	0.48-2.79	0.747			
<b>Stage</b>							
IIIB	-	1			1		
IIIC-IV	7.0 (5.4-11.5)	4.80	1.13-20.32	0.033	6.78	1.51-30.50	0.013
<b>Therapy</b>							
Combo	15.7 (8.2--)	1			1		
Mono	5.6 (4.4-7.5)	2.51	1.15-5.50	0.021	2.46	1.05-5.78	0.039
<b>BRAF copy number</b>							
Diploid	4.7 (2.5-8.2)	1.92	0.97-3.82	0.062	2.86	1.29-6.35	0.01
Gain	12.1 (5.6-15.8)	1			1		
<b>BRAF mut allele %</b>							
Heterozygous	12.0 (5.6-15.8)	1			1		
High	7.5 (2.1-21.7)	1.28	0.59-2.78	0.530	2.16	0.86-5.47	0.102
Low	3.0 (1.4-5.5)	7.37	2.41-22.50	<0.001	4.54	1.33-15.53	0.016
<b>BRAF mut allele %</b>							
Heterozygous		0.78	0.36-1.69	0.530	0.46	0.18-1.17	0.102
High		1			1		
Low		5.75	1.69-19.56	0.005	2.10	0.53-8.28	0.290

**Supplementary table 1**  
Nucleotide sequences of primers and probes used in the qPCR analyses.

Target	Forward primer	Reverse primer	Probe
Albumin	5'-GCTGTCATCTCTGTGGCT-3'	5'-GGGAGCTGCTGGTTCCTTT-3'	5'-VIC-CAAAACCTGTCATGCCACACA-MGB-3'
BRAF wt/mut alleles	5'-ATAGGTGATTTTGGTCTAGCTACA-3'	5'-GTAACTCAGCAGCATCTCAGGG-3'	5'-FAM-GGAGTGGGTCCCATCAGTTT-MGB-3'
BRAF wt_allele	5'-TAGGTGATTTTGGTCTAGCTAGCAGT-3'	5'-GTAACTCAGCAGCATCTCAGGG-3'	5'-FAM-GGAGTGGGTCCCATCAGTTT-MGB-3'
BRAF V600E_allele	5'-TAGGTGATTTTGGTCTAGCTAGCAGA-3'	5'-GTAACTCAGCAGCATCTCAGGG-3'	5'-FAM-GGAGTGGGTCCCATCAGTTT-MGB-3'
BRAF V600K_allele	5'-AGGTGATTTTGGTCTAGCTAAA-3'	5'-GTAACTCAGCAGCATCTCAGGG-3'	5'-FAM-GGAGTGGGTCCCATCAGTTT-MGB-3'

**Supplementary Table 2**

Detailed description of BRAF copy number (CN) and mutant-allele specific quantification results.

ID sample	qPCR analysis		CNV Analysis				FISH analysis		merged BRAF-CN category	mutant-allele specific analysis		integrated CN/mut_allele category	
	CN	category	CN BRAF	CN chr.7p11-q21 (centromere)	CN ALB	overall ploidy	category	CN BRAF		CN chr.7 centromere	category		% BRAFmut allele
O-0433	2.0	diploid	2.0	2.0	2.3	aneuploid	diploid/disomy	3.2	2.9	gain/polysomy	diploid	heterozygous	diploid/heterozygous
O-0477	2.2	diploid	4.0	4.0	4.0	aneuploid	gain/polysomy				gain	heterozygous	gain/heterozygous
O-0480	2.0	diploid	2.3	2.3	2.0	aneuploid	diploid/disomy	2.3	2.3	diploid/disomy	diploid	low	diploid/low
O-0482	2.3	diploid	2.7	2.3	2.0	aneuploid	gain/disomy	2.7	2.5	gain/polysomy	gain	heterozygous	diploid/heterozygous
O-0550_a*	1.9	diploid	4.0	4.0	4.0	aneuploid	gain/polysomy	5.1	4.0	gain/polysomy	gain	heterozygous	gain/heterozygous
O-0550_b*	2.2	diploid	3.0	2.0	2.0	diploid	gain/disomy	4.1	3.5	gain/polysomy	gain	heterozygous	gain/heterozygous
O-0557_a	3.0	gain	3.0	2.0	2.0	diploid	gain/disomy	2.9	1.9	gain/disomy	gain	heterozygous	gain/heterozygous
O-0557_b	1.9	diploid	2.4	2.7	2.0	aneuploid	gain/polysomy	2.8	2.4	gain/polysomy	gain	low	NA/low
O-0559	2.0	diploid	2.3	2.0	2.0	aneuploid	diploid/disomy				NA ^	heterozygous	diploid/heterozygous
O-0592	2.2	diploid	2.3	2.0	2.0	aneuploid	diploid/disomy				diploid	low	diploid/low
O-0864	2.0	diploid	2.0	2.0	2.0	aneuploid	diploid/disomy				diploid	low	diploid/low
O-1230	2.2	diploid	2.0	2.0	2.0	aneuploid	diploid/disomy				NA	heterozygous	NA/heterozygous
O-1681	2.2	diploid	3.0	3.0	2.0	diploid	gain/polysomy	2.6	2.5	gain/polysomy	gain	low	gain/low
O-1977	2.1	diploid	3.3	3.3	3.0	aneuploid	gain/polysomy	4.3	4.1	gain/polysomy	gain	high	gain/high
O-2386	2.2	diploid	2.0	2.0	2.0	diploid	diploid/disomy				diploid	low	diploid/low
O-2792	2.2	diploid	2.3	2.3	2.0	aneuploid	diploid/disomy				diploid	heterozygous	diploid/heterozygous
O-3020	2.1	diploid	2.3	2.3	2.0	aneuploid	diploid/disomy				diploid	heterozygous	diploid/heterozygous
O-3854	1.9	diploid	3.0	3.0	3.0	aneuploid	gain/polysomy				gain	heterozygous	gain/heterozygous
O-4229	2.3	diploid	2.3	2.3	2.0	aneuploid	diploid/disomy				diploid	heterozygous	diploid/heterozygous
O-4246	2.3	diploid	2.3	2.3	2.0	aneuploid	diploid/disomy				diploid	heterozygous	diploid/heterozygous
O-4337	2.2	diploid	2.0	2.0	2.0	diploid	diploid/disomy	1.6	1.6	diploid/disomy	diploid	high	diploid/heterozygous
O-4871	2.2	diploid	2.0	2.0	2.0	diploid	diploid/disomy				diploid	high	diploid/heterozygous
O-5158	2.3	diploid	2.0	2.0	2.0	aneuploid	diploid/disomy				diploid	heterozygous	diploid/heterozygous
O-5554	2.3	diploid	2.3	2.3	2.3	aneuploid	diploid/disomy				diploid	heterozygous	diploid/heterozygous
O-6635	2.3	diploid	2.3	2.3	2.0	aneuploid	diploid/disomy				diploid	heterozygous	diploid/heterozygous
O-0483_a	3.0	gain	3.0	3.0	2.0	aneuploid	gain/polysomy	2.5	2.5	gain/polysomy	gain	high	gain/high
O-0483_b	2.4	gain	2.7	2.7	2.0	aneuploid	gain/polysomy	3.5	3.2	gain/polysomy	gain	NA	NA/NA
O-1361	2.7	gain	2.7	2.3	2.0	aneuploid	gain/disomy				gain	heterozygous	gain/heterozygous
O-1570	3.0	gain	4.0	4.0	2.0	diploid	gain/polysomy	3.1	3.0	gain/polysomy	gain	heterozygous	gain/heterozygous
O-1614	3.2	gain	4.0	4.0	3.0	aneuploid	gain/polysomy				gain	NA	NA/NA
O-1684	3.2	gain	3.0	3.0	2.0	diploid	gain/polysomy				gain	heterozygous	gain/heterozygous
O-1716	2.7	gain	5.0	5.0	4.0	aneuploid	gain/polysomy	4.1	4.2	gain/polysomy	gain	heterozygous	gain/heterozygous
O-1787	2.4	gain	3.0	3.0	2.0	aneuploid	gain/polysomy				gain	NA	NA/NA
O-199	3.0	gain	2.7	2.7	2.0	aneuploid	gain/polysomy				gain	heterozygous	gain/heterozygous
O-2087	2.8	gain	2.7	2.3	2.0	aneuploid	gain/disomy				gain	low	gain/low
O-2259_a	4.0	gain	3.7	4.0	2.0	aneuploid	gain/polysomy	3.7	3.0	gain/polysomy	gain	high	gain/high
O-2259_b	3.5	gain	4.3	4.3	2.0	aneuploid	gain/polysomy				gain	high	gain/high
O-2287	3.0	gain	5.0	5.0	4.0	aneuploid	gain/polysomy				gain	high	gain/high
O-2513	3.3	gain	3.0	2.0	2.0	diploid	gain/disomy				gain	heterozygous	gain/heterozygous
O-2977	2.7	gain	3.0	3.0	2.7	aneuploid	gain/polysomy				gain	NA	NA/NA
O-3321	2.6	gain	3.0	3.0	2.0	diploid	gain/polysomy				gain	heterozygous	gain/heterozygous
O-3848	2.6	gain	7.0	6.0	4.0	aneuploid	gain/polysomy	5.9	4.3	gain/polysomy	gain	high	gain/high
O-4519	3.0	gain	3.0	3.0	2.0	diploid	gain/polysomy				gain	high	gain/high
O-4568	2.5	gain	6.0	6.0	2.0	aneuploid	gain/polysomy				gain	high	gain/high
O-4758	3.5	gain	6.0	2.0	2.0	diploid	gain/disomy				gain	high	gain/high
O-4769	3.7	gain	7.0	7.0	3.0	aneuploid	gain/polysomy				gain	heterozygous	gain/heterozygous
O-5213	2.8	gain	2.7	2.3	2.0	aneuploid	gain/disomy				gain	high	gain/high
O-5646_a	3.0	gain	3.0	3.0	2.0	diploid	gain/polysomy	2.9	2.5	gain/polysomy	gain	heterozygous	gain/heterozygous
O-5646_b	3.2	gain				diploid	gain/polysomy	2.7	2.5	gain/polysomy	gain	high	gain/high
O-6576	2.7	gain				diploid	gain/polysomy				gain	high	gain/high

\*\_a/\_b: specimens from the same patient; ^Not Assigned